Metal-inducible promoters of *Synechocystis* sp. PCC 6803 and their use for whole-cell bioreporter development

PhD Thesis by
Loredana Peca

Under the supervision of
Dr. Imre Vass and Dr. Péter B. Kós

Institute of Plant Biology
Biological Research Center
Hungarian Academy of Sciences

University of Szeged
2009

«*We must not forget that when radium was discovered no one knew that it would prove useful in hospitals. The work was one of pure science. And this is a proof that scientific work must not be considered from the point of view of the direct usefulness of it. It must be done for itself, for the beauty of science, and then there is always the chance that a scientific discovery may become like the radium a benefit for humanity.*»

Marie Curie

Lecture at Vassar College, May 14, 1921

Table of contents

List of Abbreviations

AAS – atomic absorption spectrometry

AsO_2^- (arsenite anion) – As^{3+}

AsO_4^{3-} (arsenate anion) – As^{5+}

bp – base pairs

$Cr_2O_7^{2-}$ (chromite anion) – Cr^{3+}

CrO_4^{2-}(chromate anion) – Cr^{6+}

IC_{min} – metal salt concentration that produces a slight growth retardation, during 2-4 days of growth

IC_{max} – metal salt concentration that produces complete growth Inhibition

IC_{50} – half maximal inhibitory concentration

O/P – the operator-promoter region of a specific gene

ORF – open reading frame

PBP – phycobiliprotein

PBS – pycobilisome

qRT-PCR – quantitative real-time PCR

Tris – tris(hydroxymethyl)aminomethane

WT – wild type

Note: For simplicity, throughout this study, the term metal refers to both metal and semimetal

1. Introduction

Metal pollution is a quickly growing problem for the aquatic and terrestrial ecosystems. Organisms must tightly control intracellular metal ion levels to avoid toxicity. Toxicity is a result of excessive accumulation of essential metal ions, or an effect of over-accumulation of metal ions with no biological function. All organisms possess resistance mechanisms for protection against the excess of metal ions, encoded on plasmid or chromosomal genes. They are believed to have arisen soon after life began, in a biosphere polluted by volcanic activities and other natural geological sources (Silver and Phung 1996). The main mechanisms of resistance are: efflux 'pumping' of the toxic ions that enter the cell, enzymatic detoxification that converts more toxic to less toxic or less available metal ion species, and intracellular sequestration of the toxic metal ions. These processes are usually regulated by metalloregulatory proteins of either the MerR or ArsR/SmtB families.

Analysis of the fully sequenced *Synechocystis* genome (Kaneko et al. 1996) led to the identification of 11 clustered chromosomal ORFs that encode homologs of metal transport proteins. The region is organized into six putative transcriptional units: *(i*) the *nrsBACD* operon induced by Ni^{2+} and Co^{2+} and regulated by the upstream *nrsSR* operon products (García-Dominguez et al. 2000, López-Maury et al. 2002), (ii) *ziaA,* induced by Zn^{2+}, encoding a putative Zn^{2+} efflux P_1-type ATPases and regulated by the product of the preceding ORF, *ziaR* (Thelwell et al. 1998), and (iii) *coaT*, induced by Co^{2+} and Zn^{2+}, encoding a putative Co^{2+} translocating P_1-type ATPase under the regulation of the upstream *coaR* product (Rutherford et al. 1999, García-Dominguez et al. 2000). The resistance to arsenic salts in *Synechocystis* is encoded by the *arsBHC* operon. The operon is induced by $As^{5+}/As^{3+}/Sb^{3+}$ and its expression is under the regulation of the ArsR repressor protein. Besides CoaT and ZiaA, *Synechocystis* has two more P_1-type ATPases, CtaA and PacS that are putative copper cation transporters localized in the plasma membrane and thylakoid membrane, respectively [Tottey et al. 2001). Atx1 is a metallochaperone which interacts with the amino-terminal domains of CtaA and PacS and might play a role in chaperoning Cu^{2+} en route to the thylakoid (Borrelly et al. 2004b, Tottey et al. 2002).

In the *Synechocystis* genome there are two ORFs that encode members of the chromate ion transporter (CHR) superfamily (Díaz-Pérez et al. 2007): *slr5038*, located on the pSYSM plasmid, and the chromosomally encoded *chrA*. The function has been elucidated only for two members of this superfamily. They are membrane proteins that pump out chromate from the cytoplasm using the proton motive force, conferring in this way chromate

resistance (Alvarez et al. 1999, Pimentel 2002). Another member of this superfamily, SrpC from *Synechococcus* sp. PCC 7942, is encoded on the plasmid pANL that was shown to be involved in cell adaptation to sulfur starvation. The *srpC* disruption mutant showed an increase, rather than a decrease, in chromate resistance, when grown in low sulfate medium (Nicholson and Laudenbach 1995). A hypothesis was formulated that CHR proteins perform chromate/sulfate antiport: they change the intracellular accumulated chromate for sulfate from the growth environment; when the sulfate concentration in the growth environment is occasionally lower than the chromate concentration, the antiporter works as a chromate uptake system, therefore explaining the chromate resistance phenotype of the *srpC* disruption mutant (Nies 1998).

In the last two decades, bacterial resistance mechanisms against various metal ions have been used to construct whole-cell bioreporters. These are genetically modified living bacteria, which express molecular fusions of regulatory circuits operated by metal ions with reporter genes encoding easily detectable proteins. Hence, they are able to sense the metal ions in their environment, representing an alternative to traditional analytical chemical methods. Their greatest advantage is the ability to detect the bioavailable fraction (rather than total concentration) of an analyte, allowing for more accurate assessment of polluted sites. Photoautotrophic cyanobacteria represent an advantage over the use of heterotrophic microorganisms because they can grow on low-cost media and require little maintenance. Because *Synechocystis* is naturally transformable and its full genomic sequence is available, it represents a suitable organism for whole-cell bioreporter construction.

2. Research Background

2.1. Bioinorganic chemistry and metallomics

At about the same time of the discovery of DNA structure and function, in the early 1950s, increased attention started to be paid to the inorganic content of cells and its biological role. Until that time, traditional biochemistry focused mainly on organic biomolecules like DNA and proteins, and many metal ions were disregarded as irrelevant "trace elements". Since then, scientists have realized that several metal ions have a very important function in the metabolism of all organisms (Fraústo da Silva and Williams 2001). Bioinorganic chemistry emerged as a dynamic research domain situated at the interface between inorganic chemistry and biochemistry, combining knowledge of metal ions chemistry with knowledge about biomolecules in an effort towards understanding the chemistry of metal-containing molecules of life processes. Specific areas of interest in bioinorganic chemistry include metal transport and storage, electron transfer metalloproteins, toxicity and detoxification mechanisms of metal ions used by different organisms, as well as processes associated with the introduction of metal probes or metal-based drugs into biological systems (Lippard and Berg 1994).

The last decade saw the emergence of different "-omics'', the disciplines aiming at the complete analysis of a particular class of components of an organism. As more systems requiring metal ions have been discovered and characterised, a critical mass of knowledge has accumulated to legitimate the emergence of "metallomics" as a new frontier of bioinorganic research that aims at comprehending the molecular mechanisms of metal (Szpunar 2005)-dependent biological processes (Mounicou et al. 2009) and is predicted to develop as an interdisciplinary science complementary to genomics and proteomics. "Metallome" is the entire complement of metal-containing biomolecules from a cell, tissue or organism, expressed at a given time under certain conditions. "*Since the identification of metallomes and the elucidation of their biological or physiological functions in the biological systems is the main research target of metallomics, chemical speciation for specific identification of bioactive metallomes is one of the most important analytical technologies to establish metallomics as the integrated bio-metal science"* (Haraguchi 2004).

2.2. The biological roles of transition metals

Eleven elements are absolutely required for biological processes (see bulk elements in Fig. 1). Another thirteen elements are essential in varied amounts in most, but not necessarily all organisms: iron and zinc (in relatively large amounts), copper, cobalt, manganese, nickel, chromium, vanadium, boron, silicon, selenium, fluorine, iodine, and yet 7 elements are thought to be required by certain species: tin, cadmium, strontium, barium, arsenic, bromine, and tungsten (Frausto da Silva and and Williams 2001). The lack of knowledge regarding the "essentiality" of some elements is due to insufficient investigations and to the limits of the quantitative analytical methods.

Transition metals are found in the cell in ionic forms, with variable oxidation states. Their ions are small, charged entities that are generally found as directely bound to the side-group of proteins, or inserted in chelating rings, as cofactors (Fig. 2). They participate in redox processes (especially the ions of transition metals like Cu, Fe and Ni), help stabilizing protein folds (e.g. Zn^{2+} in zinc fingers, see Krishna et al. 2003), and seem to contribute to the structure of active sites of proteins (e.g., Zn^{2+} and Cu^{2+} in the Cu-Zn superoxide dismutases, see Cioni et al. 2003). Transition metals, and especially zinc, most commonly catalyze the intra- or intermolecular rearrangement of electrons (Theil and Raymond 1994). A substantial part of the transition metal ions are included in tetrahedral preformed complexes such as metalloporphyrin or -corrin rings that are termodinamically very stable. These chelating units provide bioinorganic functional groups of widespread occurrence and utility in biology, being found in complexes, such as chlorophylls (Mg), cytochromes, sirohaem (Fe), factor F430 (Ni), vitamin B12 (Co) (Fig. 2).

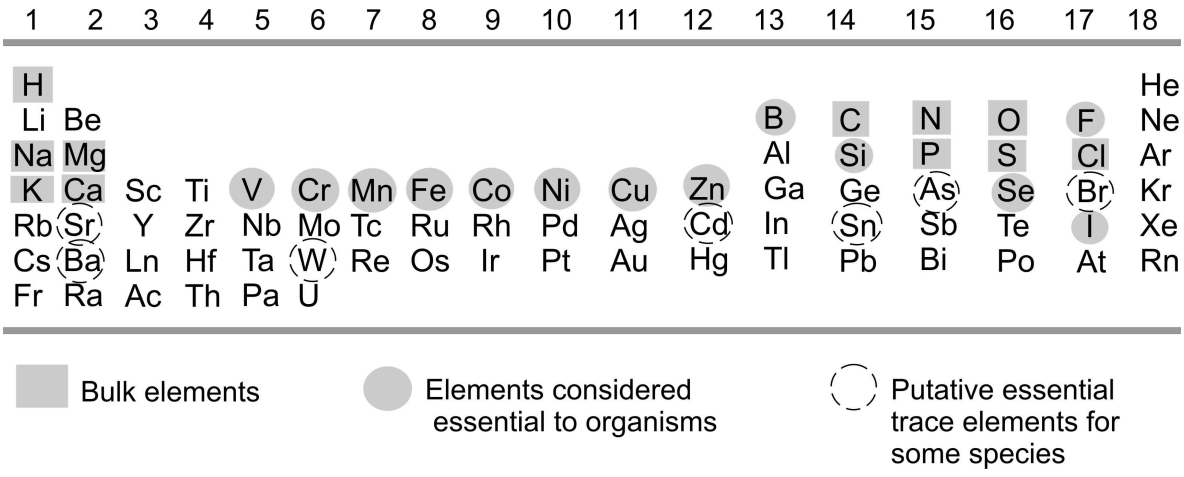

Figure 1. The distribution of elements essential for life in the periodic table (redrawn after Williams 2007)

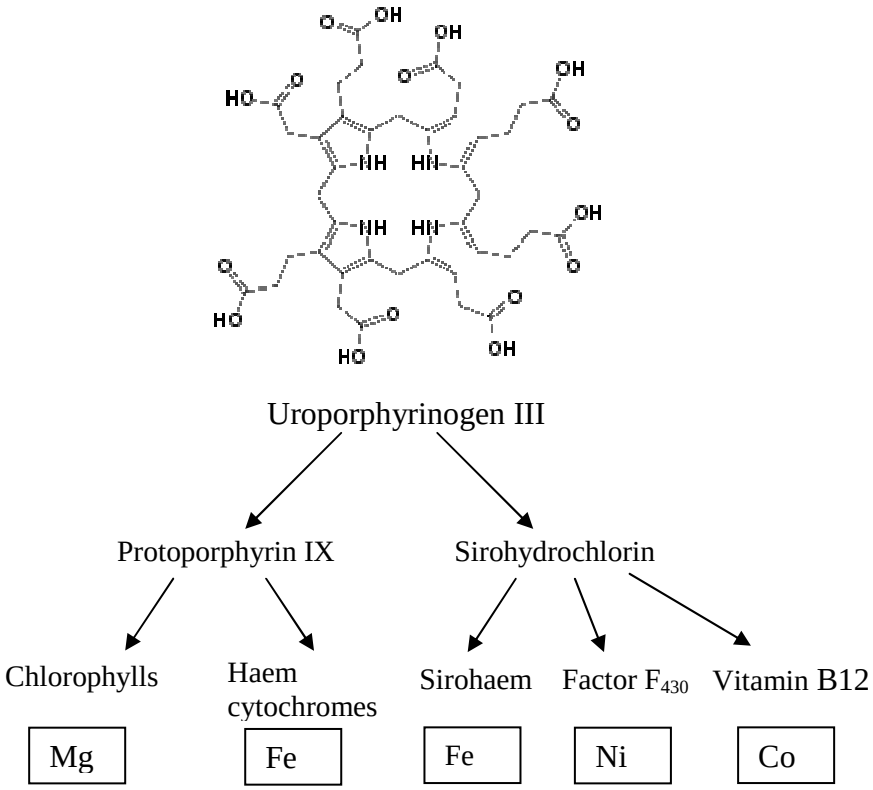

Figure 2. The common precursor of diverse polypyrrole chelates that contain different metal ions (from Fraústo da Silva and Williams 2001).

2.3. Metal toxicity

Toxicity is a result of over-accumulation of essential metal ions, or a consequence of exposure to metals with no biological function (e.g., lead and mercury). Unlike organic pollutants that can be degraded into relatively nontoxic products, the metal pollutants cannot be degraded. The toxic effects of metals are basically determined by the inorganic and bioinorganic chemistry of their ions and depend on environmental factors that affect metal ion bioavailability: such as pH (e.g. copper is poorly available in highly alkaline lakes; Robinson et al. 1999), redox potential of the environment, temperature, presence of inorganic anions and cations (e.g., the presence of calcium and phosphate notably reduces zinc toxicity to cyanobacteria; Shehata and Whitton 1982), clay and organic substances, and water hardness (presence of dissolved Ca^{2+} and Mg^{2+} with HCO_3^{1-} and CO_3^{2-}) (Hobman et al. 2007). An important factor in metal toxicity is the ability to enter the cell (see section 2.5.) and to interact with ligands, or to participate in harmful cellular reactions. There will be primary effects caused by interactions between the toxic metal and the cellular components, but there will also be secondary effects arising from the displacement of metals from

biological molecules or metal ion-mediated oxidative stress resulting in widespread damage to membranes, proteins and DNA and impairment of enzyme function.

A generally accepted theory for predicting metal toxicity states that the interaction between a metal ion and a complex cellular ligand (e.g., nucleic acids, protein side chains, and organic cofactors) depends on the polarizing power (charge/radius ratio) of the metal ion. Therefore, the higher the polarizing power of a metal cation, the stronger the interaction with cellular ligands, and the "softer" the metal ion (Hughes and Poole 1989). The polarizing power of metal ions increases from left to right across the periodic table. On that account, the binding preference of an individual metal cation for a certain ligand usually follows the Irving–Williams series, which for the first row transition metals is $Ca^{2+} < Mg^{2+} < Mn^{2+} < Fe^{2+} < Co^{2+} < Ni^{2+} < Cu^{2+} > Zn^{2+}$ (Lippard and Berg 1994). Many of the most toxic metals are soft Lewis acids (see Duffus 2002 for Lewis acids classification for metal ions), like Cd^{2+}, Hg^{2+}, Pb^{2+}, Ag^{+} and Au^{+}. These metals prefer coordinating S and N groups (soft Lewis bases), such as cysteine thyol (SH) groups that serve an important structural role in the protein tertiary structure, and also coordinate essential metals in the active sites of many metalloproteins (Petsko and Ringe 2004). Other "soft" metals attack histidine nitrogens, thioether groups of methionine side chains and oxygen groups in biological molecules. As a consequence of these actions, the toxic thiophilic metals entering the cell will displace essential metals (hard Lewis acids) with a lower affinity for their ligands from enzymes and will alter the protein structure by cross-linking the sulfur-containing side chains of their cysteine and methionine residues.

Experiments performed mainly in eukaryots have shown that the redox-active metals (e.g. Fe and Cu), as well as some redox-inactive metals, such as Pb, Cd, Hg, Ni, and As, are involved in oxidative stress damage in a variety of different model organisms (for review see Leonard et al. 2004). In addition to Fe and Cu, metals like Cr, Co (Kasprzak 2002), Ti, and V (Stohs and Bagchi 1995) are reported to be redox-active. The redox active metals contain unpaired electrons in their d-orbital, and are capable of generating free radical species via redox cycling mechanisms with biological reductants (Frank and Mudway 2007). The reaction between certain redox-active metals, the superoxide ion and hydrogen peroxide results in hydroxyl free radical (OH·) production by Fenton chemistry (reaction 1). The thiophilic metal-induced oxidative stress might be produced through the binding of the thiols (– SH) of glutathione or thioredoxin which are essential to redox regulation (Hansen et al. 2006, Imlay 2006).

$$Mn^{n+} + H_2O_2 \rightarrow M^{(n+1)+} + OH^- + OH^{\cdot} \qquad (1)$$

The problem of balancing redox metal homeostasis and oxidative stress is most acute in photosynthetic organisms, in which metals like iron, manganese, magnesium, and copper are involved in many redox reactions in the two photosystems, providing multiple sites at which reactive oxygen species can be generated (Shcolnick and Keren 2006). When interacting with H_2O_2, metals also produce other strong oxidants, such as metallo-oxo and peroxo species (reactions 2 and 3) (Kasprzak 2002).

$$M^{n+}+H_2O_2 \rightarrow [MO]^{n+}+H_2O \qquad (2)$$

$$M^{n+}+H_2O_2 \rightarrow [MO_2]^{(n-2)+}+2H^+ \qquad (3)$$

2.4. Bacterial uptake of metal ions

The cellular import and export of metal are in kinetic equilibrium (Nies, 2007). The cyanobacterial envelope has a fine structure similar to the one found in gram-negative bacteria, consisting of an outer membrane and a plasma membrane, separated by a periplasmic space that contains a peptidoglycan layer (Allen 1968, Golecki 1977). Bacteria have developed sophisticated uptake mechanisms for aquiring their essential metal ions from the environment. Acquisition of iron is especially challenging under normal physiological conditions because Fe^{3+}, although plentiful in nature, has extremely low solubility at neutral pH (10^{-18} M). To aquire the necessary intracellular Fe^{3+} (at least 10^{-6} M), microorganisms secrete very high affinity iron chelators (siderophores) to transport iron into the cell (Braun and Killmann 1999). It is believed that the metal ions diffuse across the outer membrane into the periplasm through porins (Nies 2007, Waldron and Robinson 2009), orthologs of *Escherichia coli* OmpF and OmpC (Nikaido and Vaara 1985) or, in the case of iron-siderophores, through active transport (Braun and Hantke 2007). The uptake systems that import the metal ions into the cytoplasm can be grouped in two general types: (i) fast and rather unspecific secondary transport systems that transport a wide range of metal ions, and (ii) slow, highly substrate-specific, inducible primary transport systems that are produced when a specific metal ion is lacking in the cell (Nies 2007). Bacteria also have inducible, membrane-potential-dependent systems that are highly specific, such as NiCoT proteins involved in uptake of Ni^{2+} and Co^{2+} (Rodionov et al. 2006).

The primary uptake systems are ABC-type ATPase transporters and P-type ATPases. The ABC (ATP-binding cassette)-type ATPases have periplasmic substrate-binding proteins and selectively import manganese, zinc, nickel, cobalt-containing cobalamin derivatives, iron, as well as sulfate, molybdate, tungstate, and phosphate across the plasma membranes of

gram-negative bacteria (Ferguson and Deisenhofer 2004). P-type ATPases are uptake or efflux systems, depending on the individual protein. The members of the P_1-type ATPase subclass are mostly metal cation exporters, but a few of them act as importers for cations, such as Mg^{2+}, K^+, Zn^{2+}, and Cu^{2+}. They generally possess a cytosolic metal-binding domain that contains a pair of cysteine residues within a ferredoxin-like fold (Banci et al. 2002). In the case of several putative P_1-type ATPases, importers for Cu^{2+}, these domains interact with specific cytosolic copper-binding proteins, known as metallochaperones, and presumably pass the copper cations to them (Harrison et al. 2000).

Unspecific uniporters, or proton symporters, are responsible for a general supply of a range of metals. Examples are: (i) the MntH, the broad spectrum H^+-coupled transition metal divalent cation (Fe^{2+}, Mn^{2+}, and Zn^{2+}) antiporter (Papp-Wallace et al. 2007), (ii) ZIP transport proteins, like *E. coli* ZupT that transport Zn^{2+}, Fe^{2+} and possibly Mn^{2+}, and other non-physiological divalent metals (Grass et al. 2005), (iii) permeases for sulfate that also transport chromate (Cervantes et al. 2001), and (iv) inorganic phosphate transporters that also carry arsenate.

Silver and co-workers (1996) rised the following common sense question: “Why it is easier to spend metabolic energy bringing in toxic ions and then more energy pumping them out than to exclude them totally”? A possible reason the authors found was that the metabolic expenses for maintaining highly specific uptake pumps is greater than the genetic expenses of having plasmid genes in the population that can spread when necessary.

2.5. Bacterial metal ion resistance

Metal resistance systems are believed to have arisen soon after life began, in a biosphere polluted by volcanic activities and other natural geological sources (Silver and Phung 1996). The industrial biotopes rich in toxic metals created over the last two centuries may have increased the selective pressure on resistance-encoding genes. Baterial plasmids contain genes for resistance systems to various toxic metal ions, including Ag^+, As^{3+}, As^{5+}, Cd^{2+}, Co^{2+}, Cr^{6+}, Cu^{2+}, Hg^{2+}, Ni^{2+}, Sb^{3+}, TeO_3^{2-}, and Zn^{2+}. Such systems have been found on plasmids of almost all tested bacterial groups. They are generally plasmid-encoded, but some of them are encoded by chromosomal genes (Silver and Phung 1996). The main mechanisms of resistance are: (i) efflux ‘pumping’ of the toxic ions that enter the cell, (ii) enzymatic detoxification that converts more toxic metal ion species to less toxic or less available ones, and (iii) intracellular sequestration of metal ions by binding to metallothioneins and phytochelatins. These processes are usually regulated by metalloregulatory proteins of either the MerR or ArsR families (Helmann et al. 2007). The combination of fast and unspecific

uptake systems with inducible and highly specific uptake systems efficiently supplies the required metal ions in the cells, but has the disadvantage of importing toxic ions like arsenate, chromate, and Cd^{2+}. Cells address this problem by inducible efflux systems that decrease the cytoplasmic concentration of metal cations (Nies 2007). These efflux systems can be either ATPases or secondary membrane potential-coupled transporters. The energy-coupled exporters of metal ions are mostly PIB-type ATPases, an old phylogenetic branch of the P-type ATPase superfamily. They have eight membrane-spanning helices (Kühlbrandt 2004) and generally possess one (or more) cytosolic metal binding domains that contain a pair of metal-coordinating cysteine residues within a ferredoxin fold (Waldron and Robinson 2009). The metal ion transported and the direction of transport cannot be predicted from the sequence of a PIB-type ATPase (Tottey et al. 2001). The specificity must reside in the precise geometry of the side chains in the ion-binding sites (Kühlbrandt 2004). Their export activity is induced by thiol compounds (Rensing et al. 1999, Sharma et al. 2000), therefore P_{IB}-type ATPases might be able to remove metal ions out of glutathione complexes for export outside the cell (Nies 2007). Examples of such metal resistance proteins include ZntA and CadA (Okkeri et al. 1999, Rosen 2002) that remove toxic ions, such as Zn^{2+}, Cd^{2+} Ag^{+}, or Pb^{2+}, from the cell. The most widely distributed secondary efflux systems for transition metal cations are the proteins that belong to the cation diffusion facilitators (CDF) family (Paulsen and Saier 1997, Nies 2003), which probably function as cation/proton antiporters (Chao 2004). Chromate resistance (CHR) efflux proteins export chromate and probably other substrates also (Díaz-Pérez et al. 2007), as outlined in section 1.9.3. ArsB proteins efflux arsenite and can associate with the primary efflux ATPases ArsA to form an efficient export system for arsenite (section 1.9.2.).

An example of detoxification mechanism is the reduction of inorganic As^{5+} to As^{3+}, which is the substrate of the arsenic efflux pumps. The reaction is performed by ArsC cytosolic arsenate reductases. In prokaryotes two different families of arsenate reductases can be found: tioredoxin-coupled (e.g. *Staphylococcus aureus* ArsC pI258 and *Bacillus subtilis* ArsC) and glutaredoxin-coupled (e.g. ArsC from plasmid R773 in *E. coli*) (Páez-Espino et al. 2009). The mechanism of As^{5+} reduction is similar for both families and involves three different thiolate nucleophiles that function as a redox cascade (Messens and Silver 2006). It is worth mentioning that microbial reduction of As^{5+} to As^{3+} can facilitate the release and transport of this toxic form of arsenic into aquatic environments and into drinking water (Islam et al. 2004).

The functioning of the metallothionein SmtA from *Synechococcus* is an example of intracellular metal ion sequestration (Fig. 3). The *smtA* gene is induced in response to surplus

Zn^{2+} and Cd^{2+}, and is controlled by the DNA-binding repressor SmtB, encoded by the neighbouring upstream gene, (Huckle et al. 1993). SmtB is similar in sequence to ArsR, which is required for arsenite-responsive regulation of the *ars* operator-promoter (Wu and Rosen 1991), and to CadC, which is required for cadmium-responsive expression of *cadA*, encoding a Cd^{2+}-efflux ATPase (Endo and Silver 1995). These proteins are included in the ArsR-SmtB family of sensor proteins (Busenlehner et al. 2003). SmtB was the first sensor for metal ions to be structurally characterized, revealing a winged helix-turn-helix repressor with two predicted pairs of metal binding sites per dimer (Cook et al. 1998). Metallochaperones also play a role in protecting the cells from excess amounts of metal ions by sequestering them for delivery to protein targets (Rosenzweig 2002). In bacteria, metallochaperones are only known for copper (Tottey et al. 2001), and have recently been discovered for arsenic (Lin et al. 2006). Exploration of metabolic pathways involved in resistance to metal ions offers potential applications in pollution monitoring (Harms 2007) and bioremediation studies (Lovley 2003).

2.6. *Synechocystis* sp. PCC 6803 as a model organism

Cyanobacteria are the only prokaryotes which possess the capability to carry out oxygen-producing photosynthesis. Cyanobacteria contribute significantly to global photosynthetic productivity, thus making it relevant to study how the different environmental stress factors can alter their physiological states (Castielli et al. 2009). The general assembly of photosynthetic membranes in cyanobacteria is similar to that from eukaryotic algae and plants. Therefore, the lessons learned from the study of cyanobacteria could be applied to higher plants that are of higher interest due to their economical value. The unicellular cyanobacterium *Synechocystis* is naturally transformable at high efficiency (Kufryk et al. 2002), and after uptake, the foreign DNA can be integrated into the organism's genome by homologous recombination. (Vermaas 1996). The genome of *Synechocystis* was sequenced in 1996 by the Kazusa DNA Research Institute in Japan (Kaneko et al. 1996), becaming the first sequenced photosynthetic prokaryot and the fourth sequenced genome in the world. Its chromosome has 3.573.470 bp and contains 3267 ORFs (Furumichi et al. 2002). The function of nearly half of the genes has been deduced using similarity searches (Ikeuchi and Tabata 2001). The four plasmids harboured by *Synechocystis* (pSYSM, pSYSX, pSYSA and pSYSG) were sequenced in 2003 (Kaneko et al. 2003) and contain a total of 397 putative ORFs, most of them (77%) of unknown function. Three genome databases, that act as central repositories for information on gene structure and function, have been established: CyanoBase, CyanoMutants (Ikeuchi and Tabata 2001) and CYORF (Furumichi et al. 2002). A DNA microarray covering 3079 chromosomal ORFs of *Synechocystis* became commercially available at TaKaRa (Japan) about a decade ago, and another full-genome version was developed by Postier and co-workers (2003). These are powerful tools for systematic analysis of genome-wide expression profiles. Therefore, *Synechocystis* is a good choice to address fundamental and applied research problems, and it has been increasingly used, especially in the last decade, as a model system for the study of metabolic pathways and regulatory networks, as well as the mechanisms of photosynthesis and stress responses (Glatz et al. 1999). Still, when compared to well-studied bacteria, such as *E. coli*, *Synechocystis* has a larger proportion of unknown genes, because cyanobacteria and their genes have not been well studied, despite their importance in the evolution of life and the maintenance of biosphere.

2.7. *Synechocystis* response to general and metal ion stress

Although several DNA microarrays studies brought important contributions to our general understanding of the molecular mechanisms of stress responses in cyanobacteria (recently reviewed by Los et al. 2008), the metal ion stress, resulting from excess or limited metal availability, is not yet in the spotlight of the cyanobacteriologist community's attention. Still, some attempts were done to elucidate the response of *Synechocystis* to excess Cd^{2+}, Fe^{2+} and Zn^{2+} at the genome level (Houot et al. 2007). Stress-induced genes can be categorized as specific stress genes, induced in response to a particular type of stress and general stress genes, induced by a multitude of stress factors. We may distinguish many genes for shock proteins and proteases that belong to the latter category, their expression being induced by oxidative, hyperosmotic, heat, salt, UV-B, and light, but not by cold stress. For example, the small heat shock protein *hspA* was shown to be induced by oxidative (Li 2004, Yu et al. 2007), hyperosmotic (Paithoonrangsarid et al. 2004), heat (Lee et al. 1998, Suzuki et al. 2006), salt (the second highest expressed gene; Kanesaki et al. 2002), cadmium (Houot et al. 2007), UV-B and light stress (Huang et al. 2002) and sorbitol (Fang and Barnum 2004). In addition to the small shock proteins, furhter major chaperones are induced by various stress factors belong to the DnaK system, that include the *dnaJ* gene that was shown to respond to various stress conditions, such as H_2O_2 (Li 2004), high light (Mary et al. 2004), and iron deficiency (Singh et al. 2003).

A major task of contemporary biology is to understand and predict the functioning of regulatory networks (Lemeille et al. 2005). We summarize the main regulatory mechanisms employed by *Synechocystis* for coping with stress conditions. The *Synechocystis* genome contains nine putative sigma factors-encoding ORFs (Kaneko et al. 1996) that belong to the σ^{70} family. Sequence homology suggests that the *sigA* gene encodes the primary sigma factor, essential for cell viability. The *sigB*, *sigC*, *sigD* and *sigE* genes encode group 2 sigma factors that show significant sequence similarity with the SigA factor but are nonessential. And finally, the *sigF*, *sigG*, *sigH* and *sigI* genes encode group 3 sigma factors. Attemps to characterize the functional role of each sigma factor have recently been made. All group 2 sigma factors were found to be involved in acclimation to salt- or sorbitol-induced osmotic stress (Pollari 2008). The *sigD* gene is induced by various kinds of stress conditions: cold, osmotic, and salt stress (Los et al. 2008), high light (Hihara et al. 2001), inorganic carbon limitation (Wang et al. 2004) and H_2O_2 (Li 2004, Yu et al. 2007). All group 2 sigma factors were found to be involved in acclimation to salt- or sorbitol-induced osmotic stress. The

transcription factor *sigD* is a primary-like sigma factor that is similar to the primary sigma factor but not essential (Pollari and Tyystjärvi 2007).

In prokaryotes the stress-inducible regulation of gene expression is frequently associated with two-component systems for signal perception and transduction (described in section 1.9). A collection of fully segregated *Synechocystis* knockout mutants for 44 out of the 47 histidine kinases and 42 out of the 45 response regulators was screened by genome-wide DNA microarray analysis and by slot-blot hybridization analysis under diverse stress conditions (Murata et al. 2006, Los et al. 2008). This type of regulation in *Synechocystis* was shown to be involved in the response to various stress factors: excess of Ni^{2+} (López-Maury et al. 2002), manganese limitation (Ogawa et al. 2002, Yamaguchi et al. 2002), phosphate deprivation (Hirani et al. 2001, Suzuki et al. 2004), high salt stress (Marin at al. 2003), high osmolarity (Mikami et al. 2002, Painthoorangsarid et al. 2004) and low temperature stress (Suzuki et al. 2001). Some of the two-component systems can perceive and transduce more than one kind of environmental signal. For example, Hik33 is involved in the sensing of cold stress, hyperosmotic stress and salt stress. These findings cannot be explained by the current model of two-component system. The model states that a given histidine kinase senses and transduces a specific stress factor and regulates the expression of a particular set of genes via the phosphorylation of its cognate response regulator. Therefore, it is possible that the specificity of the responses to individual types of stress is attributable to additional as yet unidentified components of two-component systems (Murata et al. 2006). The histidine kinase NrsS and its cognate response regulator NrsR (Hik33-Rre31) were shown to regulate transcription of the Ni^{2+}-resistance operon *nrsBACD* in *Synechocystis* (López-Maury et al. 2002). Other genes that fall under its regulation when the cells are exposed to high concentrations of Ni^{2+} ions await discovery. Hik 33 regulates the expression of *nblA1* and *nblA2*, involved in phycobilisome (PBS) degradation upon nitrogen starvation (Baier et al. 2001). It is known that cyanobacteria can adapt their phycobilisome content and composition to changes in nutrient availability, light wavelength and intensity, and temperature (Prassana et al. 2004). The change of cyanobacterial cell coloration to chlorotic yellow in cells deprived of an essential macronutrient (e.g. sulfur or phosphorus) is known as bleaching and is mainly caused by repression of phycobiliprotein synthesis coupled with the rapid degradation of the pre-existing phycobiliproteins (reviewed by Schwarz et al. 2005). Non-bleaching phenotypes were discovered and their molecular analysis led to the discovery of several genes, including *nblA*, that are considered essential for phycobilisome degradation (Collier and Grossman 1994). However, the specific role of NblA in phycobilisome degradation is subject to speculation (Schwarz et al. 2005). A recent study indicates that exposure of *Anabaena*

NCCU-9 cells to Pb^{2+}, Cr^{6+}, Cu^{2+}, Zn^{2+}, Ni^{2+} and Cd^{2+} resulted in phycobiliprotein reduction (Fatma H and T 2009). Another study performed in *Microcystis aeruginosa* 854, concluded that the decrease of phycobiliproteins might be an adaptive mechanism of this organism under high Cd^{2+} conditions (Zhou et al. 2006). The *nblA* genes in *Synechocystis* were found to be upregulated by H_2O_2 (Li et al. 2004, Yu et al. 2007).

Several redox-sensitive transcriptional regulators have been reported in *Synechocystis*. PerR is an oxidant-responsive transcriptional regulator. PerR proteins function as the central regulators of the inducible peroxide stress response in certain gram-positive and gram-negative bacteria (Mongkolsuk and Helmann 2002). PerR regulation was first described in *B. subtilis*, in which it functions as a peroxide-sensitive repressor and is regulated by both peroxide and metal ions (manganese or iron) (Herbig and Helmann 2001, Fuangthong et al. 2002). The protein encoded by *perR* has recently been shown to play a central role in the protection against cadmium stress as a Cd^{2+}-specific transcriptional regulator of photosynthetic machinery breakdown, downregulation of the ribosomal genes concomitant with the upregulation of the arsenate reductase-encoding *arsC* gene and *suf* genes (Houot et al. 2007). Adjacent to *perR* and transcribed in opposite direction is the *ahpC* gene. PerR is thought to regulate the expression of *ahpC* and possibly its own gene (Kobayashi et al. 2004). Addition of H_2O_2 was shown to induce both genes and abolish the binding of PerR protein to the intergenic region of *ahpC* and *perR* (Kobayashi et al. 2004).

The *ahpC* gene encodes a type 2 peroxiredoxin with glutathione-dependent peroxidase activity (Kobayashi et al. 2004, Hosoya-Matsuda et al. 2005). Peroxiredoxins exert their protective antioxidant role in cells through their peroxidase activity, through wich hydrogen peroxide and various organic hydroperoxides (ROOH) are reduced and detoxified (reviewed by Hoffman et al. 2002). The protein encoded by *ahpC* is annotated as AhpC/TSA family protein in CyanoBase. Based on sequence homology analysis, AhpC is categorized as a member of type II peroxiredoxins, which belong to the peroxiredoxin superfamily (reviewed by Dietz et al. 2002, Wood et al. 2003), and shows remarkable glutathione-dependent peroxidase activity (Hosoya-Matsuda et al. 2005). Genetic disruption of the *ahpC* gene had a dramatic effect on the viability of the cyanobacterial cells under both low or high light conditions (Kobayashi et al. 2004, Hosoya-Matsuda et al. 2005), suggesting that this peroxiredoxin has an essential role in this cyanobacterium.

As shown in chapter 1.5., one of the frequent factors limiting cyanobacterial growth in aquatic ecosystems is iron limitation. It represents the best studied case of metal stress response in cyanobacteria and leads to the induction of a set of proteins, one of the most prominent one being IsiA (or CP43') (Straus 1994). The expression of IsiA was observed

only in the PBS –containing cyanobacteria (DeRuyter and Fromme 2008). The 2D reconstruction based on electron microscopy of liquid crystals in *Synechocystis* revealed transient, iron stress-induced complexes consisting of an 18-mer ring of chlorophyll-binding IsiA molecules around a PSI trimer (Bibby et al. 2001, Boekema et al. 2001). Two hypotheses have been made regarding IsiA function: protection against photodamage (Sandström 2001) or light harvesting for PSI (Melkozernov et al. 2003). Among the investigated conditions, the expression of *isiA* gene is highest under iron deficiency (Singh et al. 2003, DeRuyter and Fromme 2008), but has also been observed under various stress conditions, such as salt, heat (Geiss et al. 2001) and oxidative stress (Li 2004, Yu et al. 2007). Another stress-responsive gene is *lilA*, that is cotranscribed with *scpD* (small CAB-like protein; Suzuki et al. 2001) and the corresponding gene products belong to the extended family of light harvesting-like (Lil) proteins (Kufryk et al. 2008). Both transcripts were found to be responsive to H_2O_2 (Li et al. 2004, Yu et al. 2007), low temperature (Suzuki et al. 2001), osmotic (Mikami et al. 2002) and salt stress (Marin et al. 2003).

2.8. Metal ion resistance genes and their functions in *Synechocystis*

2.8.1. A gene cluster involved in resistance to Zn^{2+}, Co^{2+}, and Ni^{2+}

Analysis of the fully sequenced *Synechocystis* genome (Kaneko et al. 1996) led to the identification of 11 ORFs clustered in a 12 kb region of the chromosome that encode homologs of metal transport proteins (Fig. 4, upper part). The region is organized into 3 functional units: *(i*) the *nrsBACD* operon involved in Ni^{2+} and Co^{2+} tolerance and regulated by the upstream *nrsSR* operon (García-Dominguez et al. 2000, López-Maury et al. 2002), (ii) *ziaA* encoding a putative Zn^{2+} efflux P-type ATPases and regulated by the product of the preceding ORF, *ziaR* (Thelwell et al. 1998), and (iii) *coaT* encoding a putative Co^{2+} translocating P-type ATPase under the regulation of the upstream *corR* product (Rutherford et al. 1999, García-Dominguez et al. 2000). The current knowledge about the function of the genes in this locus is summarized below.

The *nrsBACD* operon is strongly induced by Ni^{2+} and, to a lower extent, by Co^{2+} (García-Dominguez et al. 2000, López-Maury et al. 2002). However, the *nrsA* and *nrsD* disruption mutants showed reduced resistance to Ni^{2+}, but not to Co^{2+}. It has been hypothesized that *nrsA* and *nrsB* products form a Ni^{2+} efflux system, based on the homology of their deduced amino acid sequence with two subunits of the *Cupriavidus metallidurans*

CH34 CzcCB$_2$A cation-proton antiporter for Co^{2+}, Zn^{2+}, and Cd^{2+} (Nies 1989). The *nrsD* product showed high homology to the proteins encoded by the *nreB* genes from *Alcaligenes xylosoxidans* 31A (Schmidt and Schlegel 1994) and *Achromobacter xylosoxidans* (Grass et al. 2001), components of low-level Ni^{2+} resistance systems. NrsD has12 predicted transmembrane segments and also shows high homology with members of the major facilitator superfamily of permeases (MSF; Pao et al. 1998), a large group of secondary transporters. It is not homologous to members of any of the two categories of permeases known to be involved in nickel uptake: neither single-component carriers including NixA, UreH, HoxN, and HupN (Rodionov et al. 2006) nor multicomponent ATP-binding cassette nickel permeases including Nik or Ynt complexes (Navarro et al. 1993, Sebbane et al. 2002). Nevertheless, due to the decreased Ni^{2+} resistance phenotype resulting from *nrsD* interruption, it was hypothesized that NrsD is a member of the MFS permeases involved in Ni^{2+} export. The C-terminal part of NrsD contains 14 His residues that were shown to bind Ni^{2+}, as well as Co^{2+}, Cu^{2+} and, to a lower extent, Zn^{2+}, when fused with GST (García-Domínguez et al. 2000). The *nrsBACD* operon is thought to have two promoters, one constitutive and the other inducible by the *nrsRS* system in the presence of Ni^{2+} (López-Maury et al. 2002). The protein encoded by *nrsC* shows no homology to proteins encoded by *czc* or to proteins involved in other metal ion resistance systems, but the two thirds of its C-terminal part show high homology to bacteriophage-encoded lysozymes and *Neisseria gonorrhoeae* autolysin A, and it has two putative transmembrane helices in the N-terminal region (García-Domínguez et al. 2000).

Upstream of *nrsBACD* there is a transcription unit formed by the *nrsR* and *nrsS* genes. While the C-terminal part of the NrsS protein shares homology with members of the PhoR subfamily of histidine kinases, the NrsR is a response regulator of the OmpR/PhoB subfamily. The operon is transcribed from a single promoter and shows a similar pattern of induction as that of *nrsBACD* after 1h incubation with 17 µM Ni^{2+} or Co^{2+}, and the induction was abolished in a Δ*nrsRS* deletion mutant. Therefore, it was hypothesized that *nrsRS* encodes an autoregulated two-component signal transduction system (Stock et al. 2000) controlling the nickel-dependent expression of the *nrsBACD* operon (López-Maury et al. 2002).

In prokaryotes, global regulation of the cell response to environmental changes is largely achieved via two-component regulatory systems. Generally, the first component is a membrane-bound sensor kinase that is phosphorylated on a conserved His residue in response to an environmental signal. The second component is a response regulator whose N-terminal receiver domain accepts the phosphate group from the kinase and most often induces a

change in gene expression through its C-terminal transactivation domain that binds DNA (Rhee et al. 2008). Upon phosphorylation of the receiver domain, several PhoB-like factors were shown to dimerize and bind to the DNA (Fiedler and Weiss 1995, Da Re et al. 1999). The full length NrsR protein expressed in *E. coli* was unable to bind to the *nrsBACD-nrsRS* intergenic region. However, an N-terminal truncated form of NrsR bound specifically to this region (López-Maury et al. 2002), in agreement with the finding that deletion of the N-terminal receiver domain can lead to a constitutive DNA binding activity (Ellison et al. 2000). An earlier work postulated a redox sensing role for this two-component system, based on the pleiotropic phenotype of a Δ*nrsR* (*rppA*) deletion mutant with altered levels of chlorophyll and PBP, up-regulated PSII gene transcripts and down-regulated phycobilisome-related genes. A notably higher induction in D1 protein- encoding *psbA* and PBS degradation protein-encoding *nblA* genes was found in Δ*nrsR,* relative to the WT. Surprisingly, in the same study, the Δ*nrsS* (*rppB*) deletion mutant had no detectable phenotype (Li and Sherman 2000). The authors supposed that a different histidine kinase might be responsible for NrsR phosphorilation. These data are in contradiction with the phenotype of the double mutant Δ*nrsRS* created by López-Maury and co-workers (2002), in which no change in chlorophyll and PBP content or in *psbA* and *nblA* expression was detected, relative to the WT. Therefore, it is possible that the phenotype observed by Li and Sherman (2000) in the Δ*rppA* mutant was not caused by the lack of NrsR, but by the activity of the NrsS kinase in the absence of NrsR, its natural phosphorilation substrate (López-Maury et al. 2002). The N-terminal half of NrsS shows significant sequence similarity with the α subunit of the methyl-coenzyme M reductase (MCR), the last enzyme in methane formation pathway from several methanobacteria. The active site in MCR contains a tetrapyrrole ring of a Ni-F^{430} cofactor (Ermler et al. 1997, Sarangi et al. 2009) and a Gln residue from the region of the MCR α subunit that aligns with one of the NrsS periplasmic domains, coordinates Ni^{2+}, raising the hypothesis that the Ni^{2+} sensing domain of NrsS and MCR α subunit are phylogenetically related (López-Maury et al. 2002). Therefore, the model developed by López-Maury et al. (2002) states that the presence of Ni^{2+} in the medium activates the NrsS kinase which transfers a phosphate to the N-terminal receiver domain of the response regulator (NrsR). The C-terminal transactivation domain of the phosphorylated NrsR binds to the *nrsRS-nrsBACD* intergenic region, activating the transcription of the *nrsBACD* genes and positively autoregulating its own synthesis. The molecular bases of Ni^{2+} sensing and signal transduction are not elucidated.

Adjacently to *nrs* operons there are two oppositely oriented genes: *coaT* and *coaR*. The *coaT* gene is induced by both Co^{2+} and, to a lesser extent, by Zn^{2+}, and its protein product shows a clear homology with cation-transporting P-type ATPases. The gene-disrupted mutant

showed a decreased resistance to Co^{2+} (García-Dominguez et al. 2000) and an increased accumulation of ^{57}Co in the cytoplasm (Rutherford et al. 1999), indicating that CoaT is a Co^{2+} efflux P-type ATPase. The fact that *coaT* is also induced by Zn^{2+} (García-Dominguez et al. 2000) suggests that, this ATPase might be involved in Zn^{2+} tolerance. Anyhow, the *Synechocystis* Δ*zia*Δ*coa* double mutant displayed similar sensitivity to Zn^{2+} as Δ*zia* single mutants, indicating that there is no residual transport of Zn^{2+} by CoaT (Borrelly et al. 2004a). The *coaR* gene encodes a polypeptide composed of two different domains. The N-terminal part is similar to the DNA binding domain of MerR family members (Hobman et al. 2005), and the C-terminal part show a very high similarity to precorrin isomerases (PCI) of diverse origins. PCIs catalyze the final step in the synthesis of the corrin ring of cobalamin (vitamin B12) by transferring a methyl group from C-11 to C-12 of the substrate, precorrin-8x, yielding hydrogenobyrinate (HGB). PCI was shown to bind tightly to its product, HGB. The structure of *Pseudomonas denitrificans* PCI complexed with HGB was solved by Shipman in 2001. All these data suggested that intermediates of vitamin B12 biosynthesis can act as effectors by interacting with the PCI-like domain of CoaR. Expression from the *coaT* operator-promoter was enhanced in a *cbiE* interruption mutant (encoding precorrin-6 methyltransferase, a vitamin B12 precursor), revealing that the cobalamin synthesis pathway "inhibits" *coaT* expression. It seems that when the intracellular requirements of Co^{2+} for cobalamin biosynthesis are fullfiled, the CoaT exporter is activated and Co^{2+} is pumped out of the cell (cobalamin is the only known Co^{2+}-containing metalloprotein in *Synechocystis*). When the C-terminal Cys-His-Cys (CHC) motif in CoaR was replaced with Ser-Asn-Ser, the recombinant CoaR still bound to the O/P_{coaT} but did not activate transcription after exposure to Co^{2+}, indicating a role for the CHC motif in Co^{2+} binding, probably through thiolate and/or imidazole ligands (Rutherford et al. 1999). Thus, it was hypothesized that CoaR plays a central role in Co^{2+} homeostasis via responses to two effectors: Co^{2+}, as a positive effector, and intermediates in the vitamin B12 pathway as negative effectors. The currently accepted model of MerR metalloregulator action mechanism of involves transcriptional activation by realignment of irregularly spaced consensus RNA polymerase recognition sequences (19 or 20 bp rather than the canonical 16-18 bp found in consensus σ-70 recognition sites) (Summers 1992). O/P_{coaT} has 20 bp between the -35 and -10 elements, and a deletion of 1 to 2 nucleotides was shown to induce an enhanced constitutive expression. It is inferred that Co^{2+} binding triggers a transition in CoaR that underwinds the O/P_{coaT} region to realign promoter elements (Rutherford et al. 1999).

The *ziaA* gene encodes a polypeptide with sequence features of heavy metal transporting P_{IB}-type ATPases. Transcription of *ziaA* was shown to be induced by Zn^{2+} under

the control of the Zn^{2+}-responsive repressor ZiaR (Thelwell et al. 1998). A mutant strain with disrupted *ziaA* sequence showed reduced tolerance to Zn^{2+}, as well as reduced export of Zn^{2+} to the periplasm (Thelwell et al. 1998). The transcription of *ziaA* is under the regulation of the transcriptional repressor ZiaR (Fig. 3) that belongs to the ArsR/SmtB family (López-Maury et al. 2003). Gel-retardation assays detected ZiaR-dependent complexes formed with the O/P_{zia}, and ZiaR–DNA binding was enhanced by treatment with a metal chelator *in vitro* (Thelwell et al. 1998).

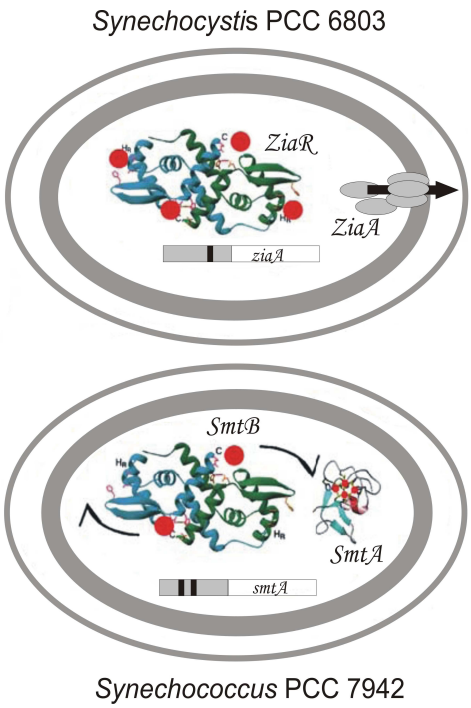

Figure 3. Two different mechanisms for coping with elevated concentrations of Zn^{2+}
Elevated cytosolic Zn^{2+} triggers the dissociation of the *Synechocystis* ZiaR (modeled structure) and the *Synechococcus* SmtB (resolved structure) zinc-responsive repressor proteins from the O/P_{ziaA} and O/P_{smtA}, respectively. Dissociation of the repressor proteins leads to the expression of structurally different proteins with distinct consequences for the cellular distribution of zinc (red circles): export into the periplasm by ZiaA (ovals) or intracellular sequestration by SmtA (resolved structure). The *ziaA* and *smtA* genes and their associated O/P regions are represented by white and gray rectangles, respectively. The O/P_{smt} contains two copies of the SmtB-binding site, the O/P_{zia} only one copy of a similar hyphenated inverted repeat (thick black lines) (from Cavet et al. 2003).

2.8.2 Resistance to arsenic salts

The resistance to arsenic salts in *Synechocystis* is encoded by the *arsBHC* operon. The *arsB* encodes a putative arsenite carrier homologous to the *Saccharaomyces cerevisiae* ARR3 (35% amino acid identity) and *Bacillus subtilis* ArsB (26% amino acid identity) proteins that are the prototypes of the ArsB/ARR3 family of arsenite transporters (López-Maury et al. 2003). This family contains membrane proteins with 10 predicted membrane-spanning segments. A better characterized group of bacterial arsenite carriers are the ArsB proteins with 12 transmembrane segments like those encoded by the *E. coli* plasmid R773 and present in *S. aureus* pI258 (Liu et al. 2003). They are most likely uniporters that can use the membrane potential to extrude arsenite. Some organisms are more resistant to arsenite because they encode an additional protein, ArsA, that can form an ATP-coupled pump with

ArsB (Dey and Rosen 1995). The disruption of *arsB* in *Synechocystis* leads to As^{5+}- and As^{3+}-hypersensitive phenotype, supporting the role of ArsB in arsenite export (López-Maury et al. 2003). The second gene of the operon, *arsH*, encodes a protein of unknown function, related to the *Yersinia enterocolitica arsH* gene that is required for resistance to arsenite and arsenate (Neyt et al. 1997). Its disruption showed no phenotype in *Synechocystis* (López-Maury et al. 2003). The last gene of the operon, *arsC*, encodes an arsenate reductase homologous to ArsC pI258 from *S. aureus* plasmid. The recombinant ArsC protein encoded by the *Synechocystis* showed strong arsenate reductase activity, as well as weak (and possibly vestigial) phosphatase activity. Although related to thioredoxin-dependent arsenate reductases, it uses the GSH/glutaredoxin system for reduction (Li et al. 2003). The ArsC protein of *Synechocystis* contains the Cys-X_5-Arg-Ser/Thr-X_{85-105}-Asp-Pro sequence that is conserved among the members of the low molecular weight protein-tyrosine phosphatase family and their homologs, indicative of a phosphohydrolytic ancestry (Li et al. 2003). It is worth mentioning here that a recently discovered *Oscillatoria*-like strain of cyanobacteria, living in anoxic arsenite- and sulfide-rich hot springs, was able to grow photoautotrophically when arsenite was used as the only photosynthetic electron donor. This strain contained genes encoding a putative As^{5+} reductase, but no detectable homologs of the chemolitotrophic As^{3+} oxidase genes, suggesting a reverse functionality for the reductase (Kulp et al. 2008). In addition to the chromosomal *arsC* gene, *Synechocystis* contains two plasmid genes that encode identical proteins belonging to the *E. coli* family of arsenate reductases (Kaneko et al. 2003). The genes were designated *arsI1* and *arsI2* and are located on the plasmids pSYSM and pSYSX, respectively. Both ArsI enzymes are active arsenate reductases that belong to the glutaredoxin-dependent family, but their roles in arsenate resistance are essential only in the absence of ArsC (López-Maury et al. 2009).

The *arsBHC* operon was induced by oxyanions of trivalent arsenic and antimony salts and, to a lesser extent, by trivalent bismuth and pentavalent arsenic salts. The operon expression is under the regulation of a protein that belongs to ArsR/SmtB family and is encoded by an unlinked gene termed *arsR* (López-Maury et al. 2003; Fig. 5). The *arsR* deletion mutants showed constitutive derepression of the *arsBHC* operon and the recombinant ArsR protein bound to the O/P_{arsBHC} in the absence of metals and dissociates from the DNA in the presence of Sb^{III} or As^{3+}, but not in the presence of As^{5+}, suggesting that trivalent metalloids are the true inducers of the system (López-Maury et al. 2003).

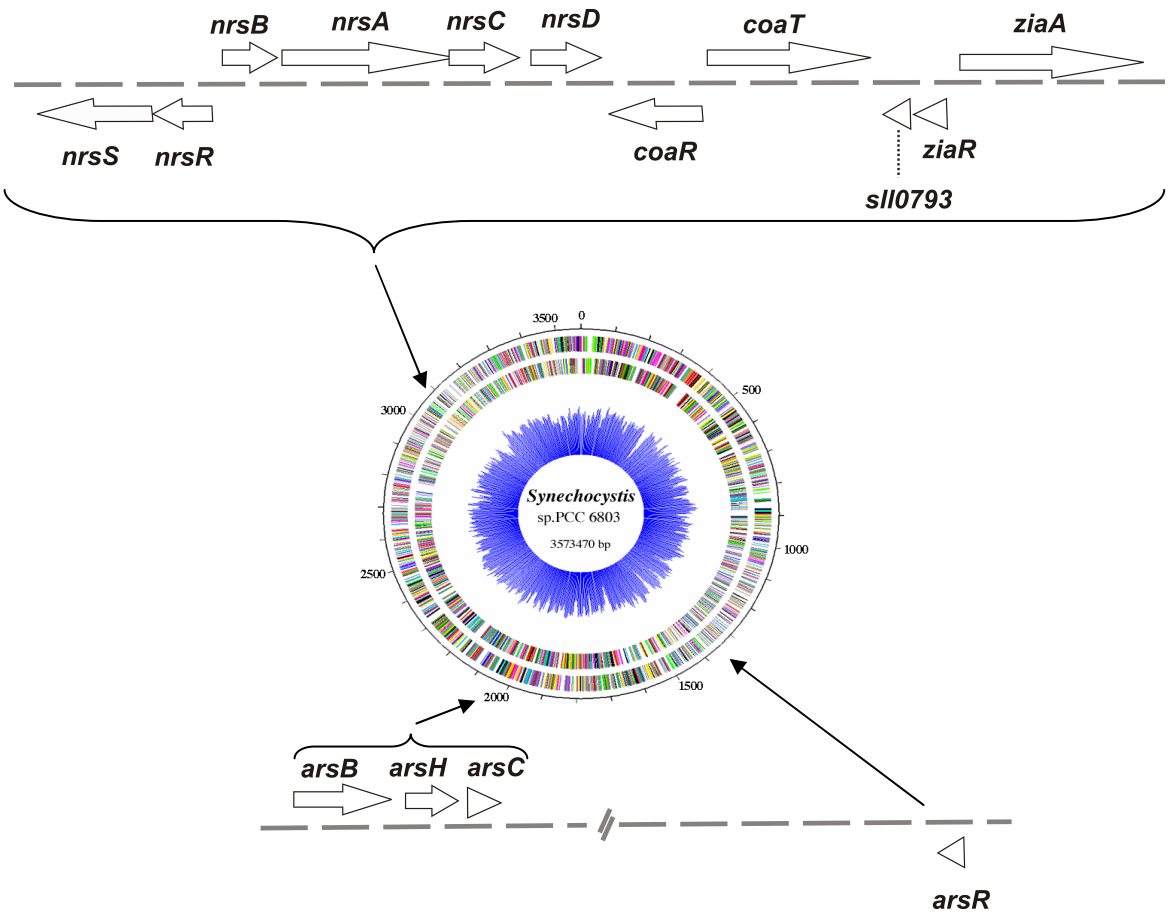

Figure 4. Localization of metal-regulated genes in the chromosome of *Synechocystis*. The arrows represent ORFs and indicate the direction of transcription (drawn to scale). The upper part of the figure shows a 12 kb gene cluster that confers resistance to Ni^{2+}, Co^{2+} and Zn^{2+}. The lower part of the figure shows genes involved in resistance to As^{5+} and As^{3+}.

2.8.3 Genes encoding putative chromate ion transporters

In the *Synechocystis* genome there are two ORFs: *slr5038* and *slr1457* (*chrA*), that encode members of the chromate ion transporter (CHR) superfamily (Díaz-Pérez et al. 2007, Nies et al. 1998). None of these genes were previously investigated and the encoded putative chromate transporters were not identified by large-scale proteomic approaches (Wang et al. 2009). The CHR superfamily contains about 135 nonredundant protein sequences with broad phyletic distribution (from archaea to eukaryotes) that contain either one or two conserved CHR domains. The superfamily is divided in the SCHR and LCHR families and 10 subfamilies (Díaz-Pérez et al. 2007). SCHR contains short-chain sequences with a single CHR domain, whereas LCHR contains long-chain sequences with two membrane CHR domains separated by a hydrophilic loop. With few exceptions, monodomain *chrA* genes are always present as a tandem gene pair in each organism. Phylogentic analysis has shown that

the N-terminal domains of LCHR proteins cluster together, as well as their carboxy-terminal domains (Díaz-Pérez et al. 2007), supporting the hypothesis raised by Nies and co-workers (1998), that the origin of bidomain LCHR proteins was an ancient duplication, followed by a gene fusion of two ancestral monodomain CHRs. The similarity of the amino and carboxyl domains of LCHR proteins to two different clusters suggests that the two CHR domains cannot interchange, and therefore might perform different functions. The function has been elucidated only for two members of the CHR superfamily: ChrA encoded by plasmid pUM505 of *Pseudomonas aeruginosa* (Cervantes et al. 1990), and the protein with the same name encoded by plasmid pMOL28 from *Cupriavidus metallidurans* (previously *Alcaligenes eutrophus, Ralstonia eutrophus* and *Ralstonia metallidurans*; Nies et al. 1989 and 1990). These two proteins belong to the LCHR5 and LCHR2 subfamilies, respectively (Díaz-Pérez et al. 2007). They are membrane proteins that pump out chromate from the cytoplasm using the proton motive force, conferring in this way chromate resistance (Alvarez et al. 1999, Pimentel et al. 2002). The putative protein products ChrA and Slr5038 of *Synechocystis* belong to the LCHR3 and LCHR4 subfamilies, respectively, none of wich have members known to be associated with chromate transport (Díaz-Pérez et al. 2007). SrpC, a member of the LCHR2 subfamily, is a sulfur-regulated protein encoded by plasmid pANL of *Synechococcus* sp. PCC 7942 (hereafter referred to as *Synechococcus*) that may function in sulfate uptake instead of chromate ion extrusion. A *srpC* disruption mutant showed an increase, rather than the expected decrease, in chromate resistance (Nicholson and Laudenbach 1995). Nies and co-workers (1990) proposed the hypothesis that CHR superfamily proteins perform chromate/sulfate antiport, thereby exporting the erroneously accumulated chromate by exchanged for sulfate that is usually high in the extracellular medium compared to the chromate concentration. At low sulfate and high chromate concentrations in the growth medium, the antiporter is expected to work as a chromate uptake system, therefore explaining the chromate resistance phenotype of the *srpC* interruption mutant (Nies et al. 1998). The genomic context suggests that CHR proteins also possess other physiological functions, in addition to chromate transport (Díaz-Pérez et al. 2007).

2.8.4. Copper transport

In addition to CoaT and ZiaA, *Synechocystis* has two more P1-type ATPases, CtaA and PacS, that are putative copper cation transporters localized in the plasma membrane and thylakoid membrane, respectively (Tottey et al. 2001). Some cyanobacteria, including *Synechocystis*, can use copper-containing plastocyanin, instead of iron-containing cytochrome

c6, in photosynthetic electron transport. The availability of copper in the growth media controls which protein is synthesized: plastocyanin when the amount of copper is adequate, or cytochrome c_6 under copper deprivation (Zhang et al. 1992). Both plastocyanin and cytochrome c_6 are located in the thylakoid lumen. Upon disruption of *ctaA*, the cells showed unaltered metal tolerance and accumulated less Cu^{2+} within the cell. Both Δ*ctaA* and Δ*pacS* showed an increase in photooxidation of cytochrome *c*6 at 0.2 mM copper, consistent with their supposed role in copper cation uptake. However, the *pacS*-disrupted mutant was hypersensitive to Cu^{2+}. A possible explanation offered by Tottey et al. was that copper toxicity may be lower in the thylakoid than in other compartments of the cell because of sequestration by plastocyanin and the abundance of anti-oxidant systems (Tottey et al. 2001). The current view is that PacS and CtaA supply copper for photosynthetic electron transport in *Synechocystis* and are required for efficient switching to the use of copper in plastocyanin, rather than heme iron, in cytochrome c6 for photosynthetic electron transport (Tottey et al. 2001). Atx1 is a metallochaperone (related to *Bacillus subtilis* CopZ, human Atox1 and *Saccharomyces cerevisiae* ATX1; Borrelly et al. 2004b) which interacts with the amino-terminal domains of CtaA and PacS (Tottey et al. 2002) and might play a role in chaperoning Cu^{2+} en route to the thylakoid. *Synechocystis* mutants with a disrupted *atx1* gene showed cytochrome oxidase and plastocyanin deficiencies, although the phenotype was milder than that of Δ*ctaA*, but was additive in the double mutant Δ*atx1*Δ*ctaA* (Tottey et al. 2002). An NMR-generated structural model of Atx1 in complex with the amino-terminal domain of PacS has been generated (Banci et al. 2006). Neither metallothionein nor Cu^{2+} exporter have been found in *Synechocystis* to date. Transgenic strains, expressing human liver metallothionein showed higher Cu^{2+}-resistance than the WT and accumulated an appreciable amount of Cu^{2+} from the medium (Song et al. 2001).

2.9. Whole-cell bioreporters for metal ion detection

The whole-cell bioreporter technology started with the development in 1990 of the first whole-cell bioluminescent bioreporter for naphthene detection (King et al. 1990), created by a transposon insertion of the *lux* gene cassette from *Vibrio fischeri* into a naphtene catabolic plasmid in *Pseudomonas fluorescens*. The authors have anticipated the development of additional reporter strains for different chemical agents with valuable applications in mixed culture biological applications, such as waste treatment, and in environmental systems, such as ground water, where bioluminescent reporters can act as specific sensors of chemical

agents. Indeed, in the next two decades, construction and testing of various genetically modified bioreporter bacteria was performed for the detection of a wide range of polluting and toxic chemicals. The advances made in understanding bacterial resistance mechanisms against various metal ions have been used to construct living whole-cell bioreporters or bioreporters (for the principle, see Virta et al. 1998; for an extensive review, see Harms 2007). The whole-cell bioreporters are genetically modified organisms that make use of natural regulatory circuits (transcriptional regulators and O/Ps) artificially fused with promoterless reporter genes (GFP, β-galactosidase, insect or bacterial luciferases) coding for easily detectable proteins. The chemical compounds activate O/Ps via transcriptional regulators or multi-step signaling pathways and trigger the expression of the reporter genes that yield a detectable output signal. Figure 5 shows a schematic representation of a whole-cell bioreporter based on the bacterial *lux* reporter system, derived from bioluminescent bacteria, such as *Vibrio fischeri* or *Photorhabdus luminescens*. The *luxAB*-encoded luciferase enzyme catalyzes the oxidation of a reduced flavin and a long-chain aldehyde, producing oxidized flavin and the corresponding long chain fatty acid, accompanied by light emission. A fatty acid reductase complex encoded by *luxCDE* is responsible for the recycling of the fatty acid to the aldehyde (Engebrecht et al. 1983). The intensity of the bioluminescent response correlates (within a certain range) with the bioavailability of the investigated analyte, defined as the analyte fraction "which is freely available to cross an organism's cellular membrane from the medium that the organism inhabits at a given time" (Semple et al. 2004). The ability of whole-cell bioreporters to specifically asses the bioavailable metal ions represents their main advantage over traditional chemical analytical methods, which

$$RCHO + FMNH_2 + O_2 \xrightarrow{\text{luciferase}} RCOOH + FMN + H_2O + \text{bioluminescence}$$

typically quantify total concentration, disregarding their metal speciation and availability to organisms. However, bioavailability is subjective and the bioavailability of a certain metal fraction to the bioreporter is not necessarily representative for its bioavailability to humans or other organisms of interest (Harms 2007).

Several cyanobacterial reporters for the detection of metal availability have been constructed: for Fe^{3+} in *Synechocystis* (Kunert et al. 2000) and *Synechococcus* (Durham et al. 2002, Hassler et al. 2006, Boyanapalli et al. 2007), for Zn^{2+}, Co^{2+}, Cd^{2+} in *Synechococcus* (Erbe et al. 1996). The general use of cyanobacteria as bioreporters was reviewed by Bachmann (2003). In a recent review, Harms and co-workers (2006) are questioning the value of whole-cell bioreporters for large scale environmental applications outside of academia. Examples of such applications are scarce, but an encouraging one is the successful

use of a luminescent As^{3+}/As^{5+} bioreporter bacterium (Stocker et al. 2003) to about 200 groundwater well samples from arsenic-contaminated regions in Vietnam, resulting in more than 90% correct bioreporter measurements (Trang et al. 2005). Arsenic is nowadays considered as one of the greatest environmental hazards, endangering the lives of several hundred million people (Ravenscroft et al. 2009) in countries like Bangladesh, India and Vietnam.

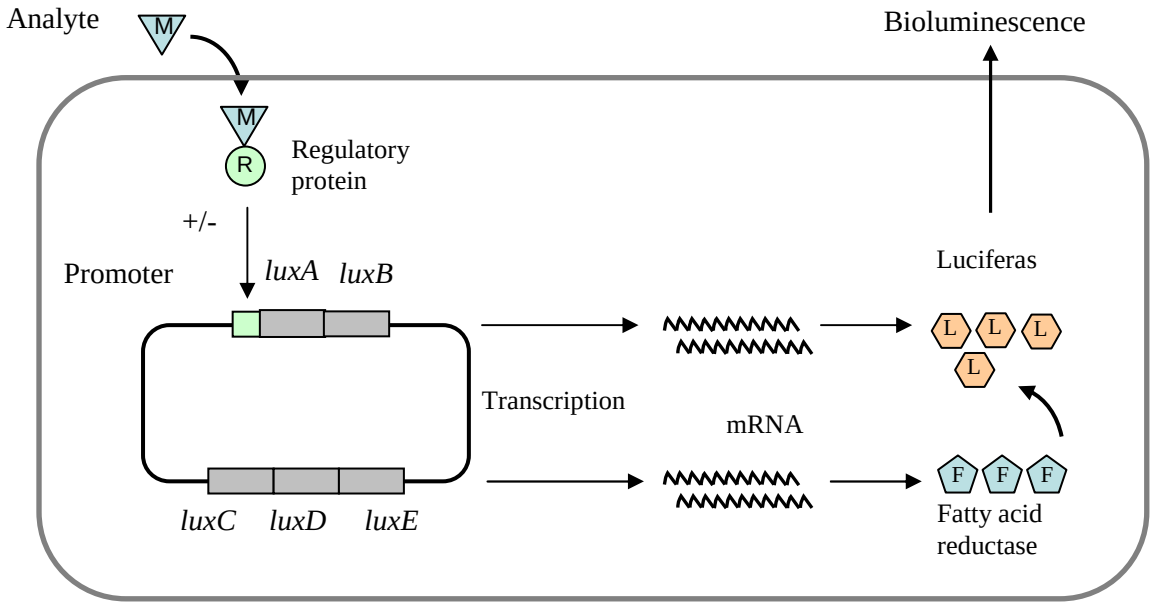

Figure 5. Diagram of a class I (van der Meer 2004) wholle-cell luminescence bioreporter for based on the bacterial *lux* reporter system. Upon entering the cell the metal (M) induces the transcription of *luxAB* operon, through a positive or negative regulatory protein (R). The accumulated luciferase interacts with its *luxCDE*-encoded fatty acid substrate and produces a blue/green light signal (bioluminescence).

3. Aims of the study

The main goals of our studies were to

- Investigate the changes in transcript level for genes that were demonstrated, or suggested to be involved in metal ion transport in the cyanobacterium *Synechocystis*, following a short exposure to concentrations close to IC_{min} of the following metal ions: Co^{2+}, Zn^{2+}, Ni^{2+}, Cd^{2+}, Cr^{3+}, Cr^{6+}, As^{3+} and As^{5+};

- Characterize the activity of two whole-cell bioluminescent reporters that were previously generated in our laboratory by fusing the Co^{2+}/Zn^{2+} inducible $O/P_{\boldsymbol{coaT}}$ (the operator-promoter region of the *coaT*) or the Ni^{2+}/Co^{2+} inducible $O/P_{\boldsymbol{nrsBACD}}$, with the promotorless *luxAB* reporter genes, and to test their application to environmental samples. Generate an arsenic bioreporter on the same principle using the $As^{3+}/As^{5+}/Sb^{3+}$-inducible $O/P_{\boldsymbol{arsBHC}}$;

- Investigate the function and regulation of the *slr5038* gene that encodes a putative chromate transporter, and was shown by us to be induced by As^{3+}, and also by Cr^{6+} when the cells were grown in low sulfate medium;

- Find the concentration ranges for Cd^{2+}, Ni^{2+}, As^{3+}, Zn^{2+}, Co^{2+}, and Cu^{2+} in which *Synechocystis* cells respond specifically to the ion excess, as well as the concentration ranges in which general and oxidative stress responses occur.

4. Materials and Methods

4.1. Growth conditions and metal salt treatment

The Synechocystis sp. PCC 6803 wild-type and its mutant derivatives were grown photoautotrophically at 40 µmol photons m^{-2} s^{-1} and 30 °C in BG-11 medium (Rippka et al. 1979) in a 3% CO_2-enriched atmosphere. Cultures of the mutant strains were grown in the presence of 25 µg mL^{-1} spectinomycin, 5 µg mL^{-1} chloramphenicol or 80 µg mL^{-1} kanamycin. Metal salt treatments were carried out in microtiter plates in BG-11 supplemented with $ZnSO_4$, $CdCl_2$, $NiCl_2$, $CoCl_2$, $NaAsO_2$, KH_2AsO_4, $CuSO_4$, $Cr_2(SO_4)_3$ or Na_2CrO_4. The cultures of *Anabaena sp.* PCC 7120 and *Synechococcus* sp. PCC 7942 were manipulated in the same way.

4.2. Growth inhibition caused by excess metal ions

The growth of cyanobacterial cultures was quantified by measuring the optical density at 720 nm for a period of 3 to 4 days. Two inhibition parameters were determined for each metal ion: minimal inhibitory concentration (IC_{min}) and maximal inhibitory concentration (IC_{max}). The IC_{min} refers to the lowest tested concentration leading to growth inhibition and IC_{max} refers to the highest tested concentration where no further growth was observed.

4.3. RNA extraction and qRT-PCR analysis

Total RNA was isolated from 20 ml samples of mid-log phase *Synechocystis* culture by the method of (Mohamed and Janson 1989) with the following modifications: the cultures were immediately mixed with an equal volume of cell stop solution containing 5% (v/v) H_2O-saturated phenol in absolute ethanol and the 3-step hot phenol extraction was followed by a single-step chloroform extraction. Samples of 5 µg total RNA were further purified using deoxyribonuclease I (Fermentas) and NucleoSpin RNA II (Macherey-Nagel). First-strand cDNA was synthesized from 0.4 -1 µg total RNA using RevertAid H Minus M-MuLV Reverse Transcriptase (Fermentas) and random hexamer primers. The reverse transcription was carried out at 42 °C for 60 min. The resulting cDNA was used as template for SYBR Green quantitative real-time PCR with Power SYBR Green PCR Master Mix (Applied Biosystems). Oligonucleotides were designed using Primer Express 2.0 software (Applied Biosystems). The amplification was performed by incubating the reaction mixture at 94 °C for 2 min, followed by 40 PCR cycles (95°C for 15 s and 60°C for 1 min). Gene expression

was calculated using delta-delta C_T method and was normalized to the expression of the RNase P subunit B-encoding *rnpB* gene as internal standard. We have used as a control for gene expression studies cells grown in BG-11 medium that contains 0.77 µM Zn^{2+}, 0.32 µM Cu^{2+}, and 0.14 µM Co^{2+}.

4.4. Extraction of genomic DNA

Genomic DNA isolation was performed according to the following protocol: 2 ml *Synechocystis* cell suspension of OD_{720} ~1 was mixed with an equal volume of ethanol containing 5% phenol (v/v), freeze-thawed at -80°C and 65°C and centrifuged (1300 g, 5 min, 4°C). The obtained pellet was resuspended in 50 µl STET buffer (8% sucrose, 5% Triton X-100, 50 mM Tris-Cl, pH 8.0, 50 mM EDTA), freeze-thawed two times as above, mixed with 50 µl acid washed sand and 60 µl TE-saturated phenol: chloroform (1:1) and vortexed vigorously for 1 min. An additional volume of 60 µl STET buffer was added followed by 1 min vortexing. The mix was centrifuged as above and the supernatant was saved, mixed with 60 µl chloroform, vortexed, and centrifuged as above. The DNA in the supernatant was precipitated overnight at -20°C with 10 µl 3M NaOAc and 250 µl ethanol. The precipitated DNA was collected by centrifugation (13000 g, 30 min, 4°C). The pellet was washed with 70% ethanol, dried, and resuspended in 100 µl 0.1 x TE buffer (10 mM Tris-Cl, pH 8.0; 1 mM EDTA).

4.5. Construction of reporter strains

Two bioreporter strains, *nrsLux* and *coaLux,* were previously generated in our laboratory. Here we briefly describe the principle. A sequence from upstream of the *coaT* coding region containing the O/P_{coaT} and *coaR* regulator gene, was amplified from the genomic DNA using the primers displayed in Figure 6, introducing a *Sal*I recognition site at the 5'-end of the amplicon. Similarly, the upstream region of the *nrsB* coding region, containing the $O/P_{nrsBACD}$ and the sequence of the *nrsR* regulator gene (Fig. 6) was amplified. The amplicons were ligated upstream of the promoterless *luxAB* luciferase genes from *Vibrio harveyi*, in the *Sal*I+*Sma*I-digested pND6luxAB vector (Fig. 6). The construct was used for transformation of a *Synechocystis* strain harboring the fatty acid reductase complex genes *luxCDE* from *V. harveyi*, producing the aldehyde substrate for luciferase. The constructs were integrated into the *Synechocystis* genome, along with a chloramphenicol resistance cassette, via homologous recombination at a neutral site (Aoki et al. 1995), using the corresponding homologous

Table 1. PCR oligonucleotide primers used in this work

Gene symbol	Oligonucleotide sequence	Gene symbol	Oligonucleotide sequence
nrsB-F	5’ CTTTCTGGCACTGGGTTTGAC	*artC-R1*	5’ CAATCTCCTTTGCCTGGGC
nrsB-R	5’ TGGGCTGTTACGAGATTGGG	*artT-F1*	5’ TGATCGCCCTGATGGAAGAA
coaT-F	5’ TGCTCAACAGGTGGGAGTCA	*artT-R1*	5’ GAGCCGTATTTACCGGAAAAGA
coaT-R	5’ TCTTCGGGCAAAAGTTCTGC	*artT-F2*	5’ AAATGGCACCCTGCCATTAG
ziaA-F	5’ TTGGTAAAGCCGGGTGAAAA	*artT-R2*	5’ TGCAATCCCTGTCATTGCAC
ziaA-R	5’ TCCCCCTAAAATCTCGCCAT	*lilA-F*	5’ GTCTTCCGCAAAGACTTCAACC
arsB-F	5’ TCCTTTACGCACCTTTGGGT	*lilA-R*	5’ AATGGCGAAGAGAGTATTGGTG
arsB-R	5’ CTGTCAAGTTACTGGCCGCC	*nblA1-F*	5’ ACCTGAATCCTTCGATCTCACC
chrA-F	5’ CCGGTGGACTATGGCACTTTA	*nblA1-R*	5’ CCGGATGACGTTGGATTTAATC
chrA-R	5’ CCTGCAATCGTTGCCATTTT	*isiA-F*	5’ ATGGCGGACAAATTGTGGAT
pacS-F	5’ TCCCAGCAAACCGAGGATAG	*isiA-R*	5’ TTTTGCCCTGGCCCTTAAG
pacS-R	5’ CGTTACCAATTTGGCCGAAA	*perR-F*	5’ ACAGTTCCCTCAAGGCTTTGC
ctaA-F	5’ TCGCTCGCAATCAGCAATTA	*perR-R*	5’ AACTCCTCCCAATCCACATCC
ctaA-R	5’ GGAGAGTATCCCGCAAGGC	*sigD-F*	5’ GCTTTGGCCTCAATGATGG
atx1-F	5’ TGTGAAGCCTGTGCCGAAG	*sigD-R*	5’ GATCATGGACTTGCGTTTGC
atx1-R	5’ GGCATCCTCATTTTGCACG	*hspA-F*	5’ AGAATTACCTGGCATGGACCC
artR-F	5’ TCTGCAAATATTGCGGATGG	*hspA-R*	5’ AACTGCCATAGCGGAACTCTG
artR-R	5’ CGCATAAATTCAGGTACTTCGG	*dnaJ-F*	5’ AGCGCTTGAATGAGGCTTATGC
artS-F	5’ TCCTGAACCCTACATTGGCC	*dnaJ-R*	5’ TGATGCGGCCGAATTTTG
artS-R	5’ TCTGAGCATTGGTTAACGTGG	*ahpC-F*	5’ CGCTATTCCATGTTTGTCAACG
artC-F1	5’ AATGTGGTGGTGCAGGAACA	*ahpC-R*	5’ AGCACCTTTGAGGTAGGCCAAC

sequences HS1–HS2 in the pND6luxAB integration vector (Fig. 6). The growth rates in BG-11 of the obtained *coaLux* and *nrsLux* reporter strains were comparable with that of the wild type (data not shown).

For the generation of the *arsLux* strain, we have amplified a sequence of 373 bp from upstream of the *arsBHC* coding region containing the O/P_{arsBHC} and the 5’ end of *sll0914* using the primers displayed in Figure 7, by introducing a *Xho*I site at the 5’ end of the amplicon and a *Hind*III site at the 3’ end of the amplicon. Similarly, the upstream region of the *ziaA* gene, containing the O/P_{ziaA} and the 5’ end sequence of the *ziaR* regulator gene was

amplified (Fig. 7). The two amplicons were ligated upstream of the promoterless luciferase genes *luxAB* from *Vibrio harveyi*, into the *Xho*I+*Hind*III digested vector pND6luxAB (Fig. 7). The construct was used for transformation of the same 'substrate' strain. The reason why the *ziaLux*$_T$ reporter strain we created contained a truncated version of the repressor-encoding *ziaR*, was that the previously constructed strain, *ziaLux*, with the entire sequence of *ziaR*, proved nonfunctional.

4.6. Bioluminescence assay

Metal salt treatments were carried out in 96-well black microtiter plates with low autofluorescence in 300 µL-per-well volume (200 µL culture and 100 µL salt per well of microtiter plate). The plates were covered with needle-punctured transparent foil and incubated for 3 h, or 18 h in the case of *arsLux* reporter strain, in light (40 photons µmol m^{-2} s^{-1}) or darkness in 3% CO_2-enriched atmosphere. Assays were performed with four parallel measurements at 25 °C. Luminescence intensity was determined with a Top Count NXT luminometer (Packard Instruments) and was expressed as counts per second. The relative luminescence induction was calculated by dividing the mean luminescence signal of a treated sample by the mean luminescence signal of the untreated sample. The half maximal inhibitory concentration (IC_{50}) refers to the concentration of an interfering metal ion that produce 50% inhibition of the bioluminescent response.

4.7. Acidic extraction of environmental sample

The soil-like material analyzed in this study consists of a mixture of different chemical and oil industry wastes from Almásfüzitő bauxite residue disposal area in NE Hungary. Its heavy metal content considerably exceeds the threshold limits allowed for soils by Hungarian environmental regulations. Samples collected in triplicate from the composting piles were dried, ground, then the coarse material was removed and the remaining material was passed through a 2-mm sieve. To assess the exchangeable, acid-soluble fractions of Ni^{2+}, Co^{2+} and Zn^{2+}, one-step acetic acid extraction of the material was carried out according to the method of Bódog and Polyák (1996). Aliquots of 1.0 g soil were mixed with 40 mL 0.11 M CH_3COOH. The suspension was shaken for 16 h at room temperature and then centrifuged for 15 min at 1500 *g*. A volume of 0.04 mL HNO_3 was added to the supernatant and made up to 50 mL. The metal content was determined by atomic absorption spectrometery (AAS; Perkin-Elmer model 3110). Each soil sample was analyzed in triplicate. For the bioluminescence measurements, the pH of the CH_3COOH-extracted sample was adjusted to 7.5 with 1M Tris-HCl pH 8.0.

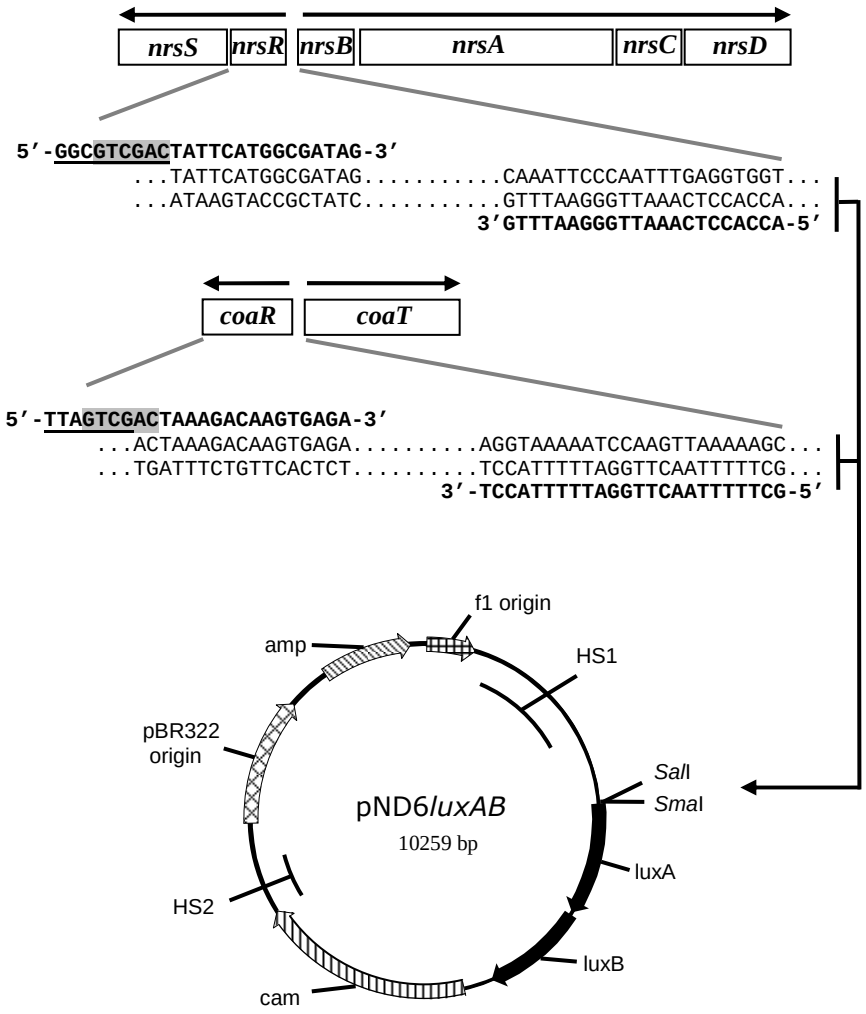

Figure 6. Cloning strategy used for construction of *nrsLux* and *coaLux* reporters. The upper part of the figure shows the structure of the chromosomal *nrs* and *coa* operons and the sequences of PCR primers (shown in bold) used to amplify the *nrsBACD* and *coaT* promoters, along with their regulator gene sequences. Arrows above the ORFs indicate the directions of transcription. The non-complementary bases of the primers are underlined and *Sal*I recognition sites are highlighted. The lower part of the figure shows the map of the pND6luxAB plasmid. HS1 and HS2 represent the flanking sequences required for double homologous recombination. The HS1 sequence spans from 155889 to 156981 and HS2 sequence spans from 156978 to 157478 in the *Synechocystis* genome according to conventional numbering in the database CyanoBase. Cloning of *Sal*I-digested PCR products into the *Sal*I+*Sma*I-digested pND6lux-AB allowed the construction of *nrs-luxAB* and *coa-luxAB* transcriptional fusions. Symbols amp and cam refer to genes conferring resistance to ampicillin and chloramphenicol.

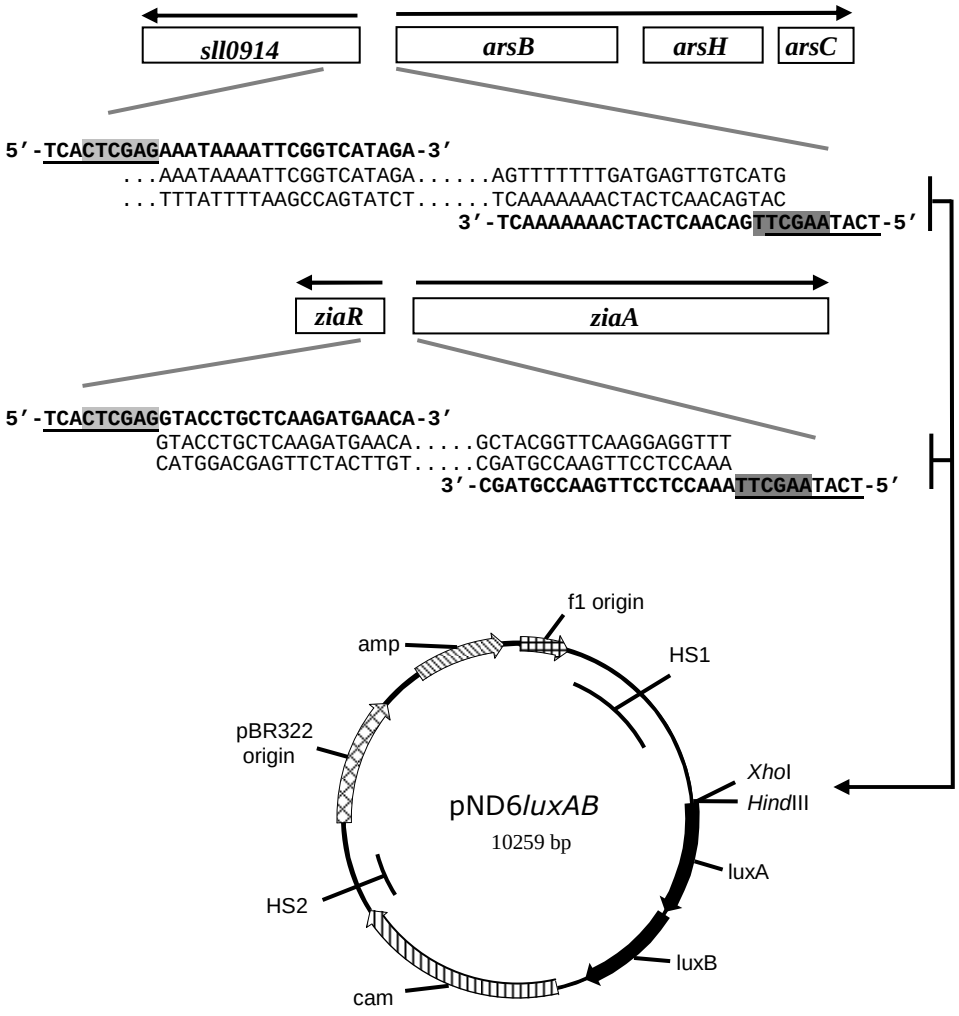

Figure 7. Cloning strategy used for construction of *arsLux* and *ziaLux*$_T$ reporters. The upper part of the figure shows the structure of the chromosomal *ars* and *zia* operons and the sequences of PCR primers (shown in bold) used to amplify a region of 373 bp upstream of *arsBHC* operon and *ziaA* promoter togheter with the first 26 bp of the regulator gene *ziaR*. The non-complementary bases of the primers are underlined. *Xho*I and *Hind*III recognition sites are highlighted in light gray and dark gray. The lower part of the figure shows the map of pND6luxAB. HS1 and HS2 represent the flanking sequences required for double homologous recombination. Cloning of *Xho*I+*Hind*III-digested PCR products into the *Xho*I+*Hind*III -digested pND6lux-AB vector allowed the construction of *ars-luxAB* and *zia-luxAB* transcriptional fusions. The meaning of the symbols amp, cam, HS1, HS2, the arrows above the ORFs and the underlined bases are the same as in Figure 6.

4.8. Measurement of the chlorophyll fluorescence induction transients

Chlorophyll fluorescence induction transients (OJIP) were measured by a double-modulation fluorometer (FL-3000, Photon System Instruments, Brno). Red (639 nm) actinic illumination intensity was adjusted to the instruments maximal value of 1000 µmol photons $m^{-2}s^{-1}$. The timing of a measurement was defined in the experimental protocol of the FluorWin software (Photon System Instruments, Brno) and executed by a microprocessor in the control unit of the fluorometer. Fluorescence was detected at every 10 µs in the first 0.2 ms, then every 100 µs up to 2 ms, and so on, finally every 100 ms. F_0 was taken at 10 µs and F_{max} between 200 ms and 1 s.

5. Results and discussion

5.1. Effect of metal ions on cell growth

With the aim of finding candidate genes for constructing bioreporters, as a first step of our study, we investigated specific metal ion-induced gene expression changes for a selected set of genes. To this end we chose a concentration for each metal salt that is high enough for inducing the specific metal homeostatic genes but not as high as to cause pleiotropic effects with the activation of other non-specific genes of *Synechocystis*, since it is known that metal ions may trigger a wide range of transcriptomic responses (Hobman et al. 2007). We investigated the concentration dependence of growth inhibition by Co^{2+}, Zn^{2+}, Ni^{2+}, Cd^{2+}, Cu^{2+}, Cr^{3+}, Cr^{6+}, As^{3+}, and As^{5+} ions for a period of 2 to 5 days, as a simple marker of their cytotoxicity. Representative growth curves are shown in Figure 8. These data were used to establish IC_{min} and IC_{max} for each metal, as described in the Materials and Methods. We found about an order of magnitude difference between IC_{min}, with only slight retardation in growth, and IC_{max}, with complete growth inhibition. These concentrations and their ratios were specific to each metal ion (Table 2). We found that Co^{2+}, Cu^{2+} and Cd^{2+} were the most toxic among the tested metals, causing slight growth inhibition at concentrations as low as 2

Table 2. IC_{min} and IC_{max} values for the studied metal ions
IC_{min} refers to the lowest tested concentrations where growth inhibition of *Synechocystis* cells could be observed and IC_{max}, to the highest concentration where no further growth could be observed.

Metal ion	IC_{min}	IC_{max}
Cu^{2+}	1.25 µM	5 µM
Cd^{2+}	1.5 µM	>10 µM
Co^{2+}	2 µM	>32 µM
Zn^{2+}	5 µM	32 µM
Ni^{2+}	3 µM	50 µM
Cr^{6+}	7 µM	> 40 µM
Cr^{3+}	80 µM	> 320 µM
As^{3+}	1.9 mM	3.5 mM
As^{5+}	37.5 mM	400 mM

µM. No severe growth inhibition was observed up to 1.9 mM As^{3+}, although 3.5 mM totally inhibited cell growth during an incubation period of 3 days. Therefore, for As^{3+} the ratio of IC_{max} to IC_{min} was twofold, while for the other metal ions was about tenfold, with the exception of Cu^{2+} that showed a ratio of about fourfold.

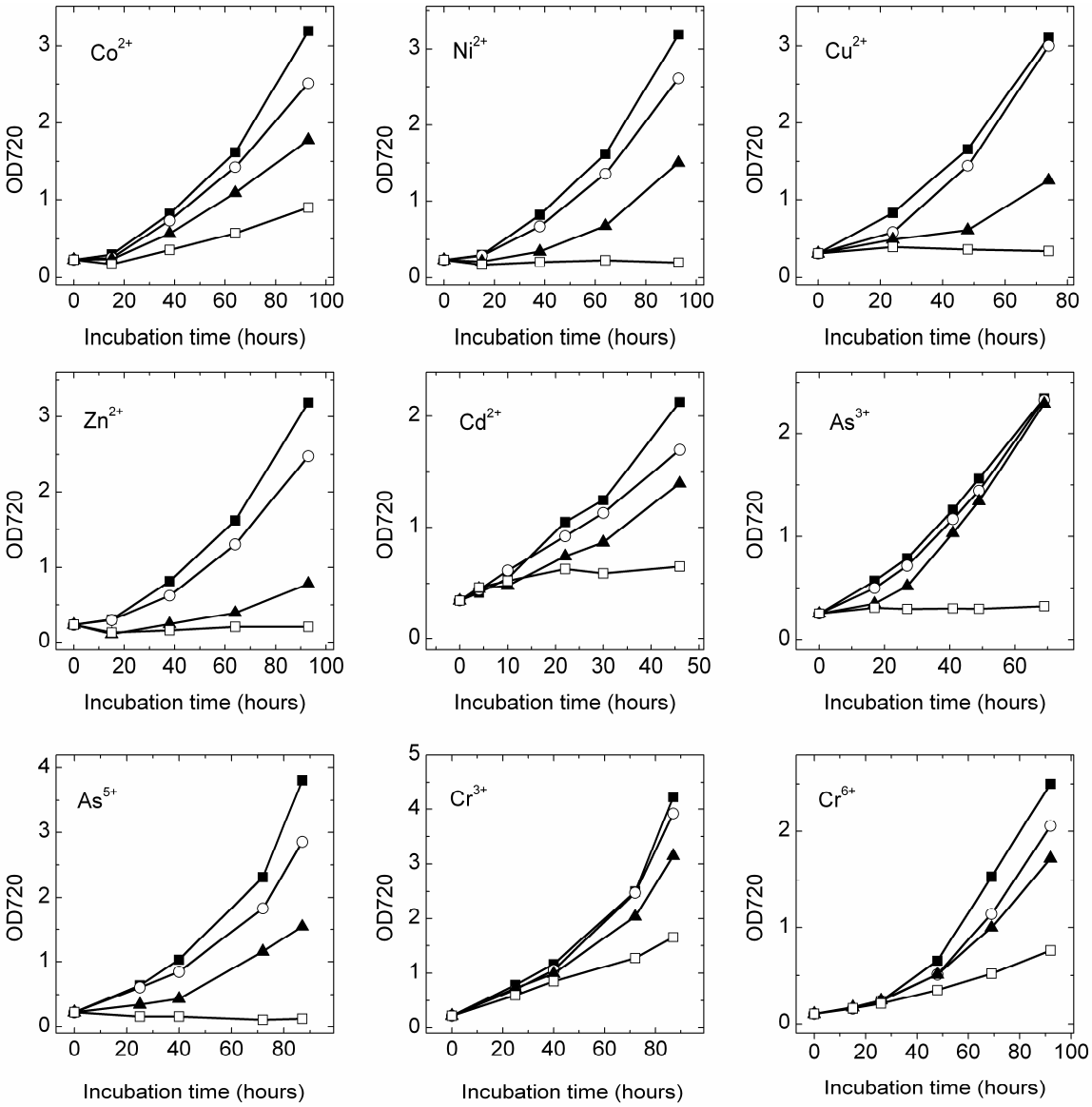

Figure 8.The effect of metal ions on cell growth. *Synechocystis* cells grown in BG-11 medium were supplemented with different metal ions, as indicated below, and growth was monitored by measuring OD_{720}. Co^{2+} at 0 (■), 2 (○), 8 (▲), and 32 µM (□); Ni^{2+} at 0 (■), 9 (○), 27 (▲), and 50 µM (□); Cu^{2+} at 0 (■), 1.25 (○), 2.5 (▲), and 5 µM (□); Zn^{2+} at 0 (■), 8 (○), 16 (▲), and 32 µM (□); Cd^{2+} at 0 (■), 2.6 (○), 6.5 (▲), and 10 µM (□); As^{3+} at 0 (■), 0.33 (○), 1.9 mM (▲), and 3.5 mM (□); As^{5+} at 0 (■), 100 (○), 300 (▲), and 400 mM (□);Cr^{3+} at 0 (■), 80 µM (○), 160 µM (▲), and 320 µM (□); Cr^{6+} at 0 (■), 10 (○), 20 (▲), and 40 µM (□).

5.2. Metal-induced changes in the transcript level of a selected set of genes

5.2.1. Identificiation of culturing conditions for gene expression experiments

We used qRT-PCR to investigate the expression of selected metal-inducible genes in *Synechocystis*. To clarify if the expression pattern depends on the growth stage of the cell culture, we have collected total RNA at four different stages of the exponential phase of culture growth, either after 15 min, or 1 h incubation in BG-11 medium supplemented with 5 µM Zn^{2+}, and looked at the *ziaA* and *coaT* transcript levels. We found a similar expression pattern for *ziaA* and *coaT* at 6.2 (OD_{580} = 1.06), 10.2 (OD_{580} = 1.74) and 14.7 (OD_{580} = 2.5) µg chlorophyll mL^{-1} either after 15 min or 1 h incubation, respectively (Fig. 9). Gene transcripts were fast accumulated over a period of 15 min following $ZnSO_4$ addition and the transcript level did not increase further in the next 45 min. We have taken this result as an indication that expression of other metal inducible genes is also largely independent of the age of the culture. Therefore, gene expression experiments were carried out with *Syechocystis* cultures in mid-log growth phase (chlorophyll concentration ~6 µg ml^{-1}; OD_{720} ~0.9), and the incubation periods with metal salts were 15 min, 1 h or 2 h.

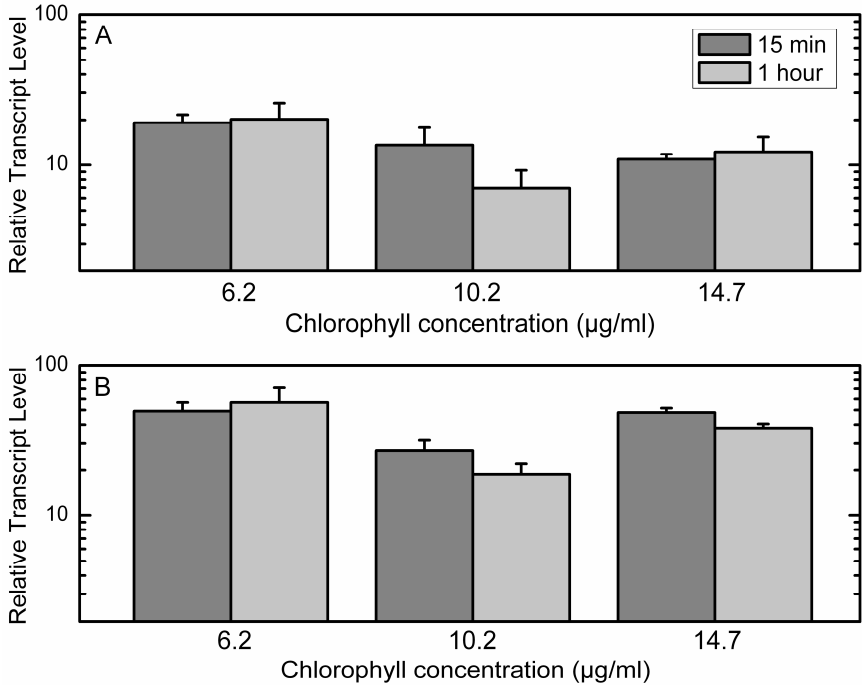

Figure 9. The dependence of gene expression on the age of the cell culture. Cells at different growth stages were incubated in 5 µM Zn^{2+}-supplemented BG-11 for 15 min or 1 h, and *coaT* (A) and *ziaA* (B) expression was assessed by qRT-PCR.

5.2.2. Identification of candidate genes for bioreporter development

Our aim was to find candidate genes that are specifically induced by single, or related species of, metal ions and could be suitable for the development of metal-specific bioreporters. To this end we have chosen the following ORFs, encoding already characterized putative metal ion transporters: *chrA, artT, arsB, pacS, atx1, ctaA, ziaA, coaT, nrsB* (see Table 3. for ORF IDs), and investigated their expression pattern upon incubation with several metal salts. The BG-11 medium was supplemented with metal concentrations falling between IC_{min} and IC_{max}, as follows: 3 µM Co^{2+}, 5 µM Zn^{2+}, 15 µM Ni^{2+}, 1.5 µM Cd^{2}, 50 µM Cr^{6+}, 50 µM Cr^{3+}, 1 mM As^{3+} and 1 mM As^{5+}, and 0.68 µM Cu^{2+}. As previously mentioned, we found that a pronounced gene induction generally occurred within 15 min of exposure, and the expression pattern did not change significantly for the next 45 min (Fig. 9), with the exception of As^{3+} and As^{5+}-triggered *arsB* transcript level that decreased about 10-fold (data not shown). In the following we will discuss only those genes which were observed on different occasions to be induced more than 3-fold.

5.2.2.1. Inducibility of the O/P_{ziaA}

The *ziaA* gene showed a marked induction following cell incubation in BG-11 supplemented with various concentrations of Zn^{2+} for 2 h. A concentration of 2 µM Zn^{2+} is enough for full induction of *ziaA* gene and the level of gene transcript remains constant up to about 42-fold induction up to 32 µM Zn^{2+}. We found that besides the known Zn^{2+}-triggered induction of the *ziaA* gene, Cd^{2+} is a potent inducer of this gene. The *ziaA* transcript increased about 24-fold after 1 h incubation with Zn^{2+} or Cd^{2+} (Fig. 11). Upon 2 h incubation with 2 µM Cd^{2+} the *ziaA* transcript level increased 10-fold , and further to 24-fold when the BG-11 medium was supplemented with 4 µM Cd^{2+}. Incubation with higher Cd^{2+} concentrations (8 and 16 µM) resulted in ~12 fold induction of *ziaA* (Fig. 12, panel A). This result is in contradiction with the data of García Domínguez and co-workers (2000), who found no increase in the transcript level of *ziaA* in *Synechocystis* upon 1 h treatment with 15 µM Cd^{2+}.

Table 3. *Synechocystis* genes assayed in this study			
ORF ID	Gene symbol	ORF ID	Gene symbol
sll0798	*nrsS, rppB, hik30*	*slr5038*	*artT**
sll0797	*nrsR, rppA*	*slr0944*	*arsB*
slr0793	*nrsB*	*slr0946*	*arsC*
slr0794	*nrsA*	*sll1957*	*arsR*
slr0795	*nrsC*	*sll1920*	*pacS*
slr0796	*nrsD*	*slr1950*	*ctaA*
sll0794	*coaR, corR*	*ssr2857*	*atx1*
slr0797	*coaT, corT*	*sll0247*	*isiA*
sll0793	–	*slr1738*	*perR*
sll0792	*ziaR*	*sll2012*	*sigD*
slr0798	*ziaA*	*sll1514*	*hspA*
slr1457	*chrA*	*sll1666*	*dnaJ*
sll5035	*artR**	*sll1621*	*ahpC*
sll5036	*artS**	*slr1544*	*lilA*
slr5037	*artC**	*ssl0452*	*nblA1*
Note: Where more than one gene symbols are found in the literature, the one used in this study is underlined. The gene designations introduced by us are indicated by (*)			

It also contradicts the results of Thelwell and co-workers (1998) who found no Cd^{2+}-induced β-galactosidase activity in *Synechococcus* strain R2-PIM8 (*smt*) that carries a *ziaR-O/*P_{ziaA}*-lacZ* transcriptional fusion after ~20 h incubation with 1.5 μM Cd^{2+}. But similar results, namely *ziaA* upregulation by Cd^{2+}, were shown by Houot and co-workers (2007) at short time after us, attesting the reliability of our qRT-PCR data.

Since P_1-type ATP-ases commonly have high specificity for metal ions which they transport (Liu et al. 2002), we think it is not likely that Cd^{2+} is a gratuitous inducer, but, rather, it is transported by the ZiaA ATP-ase of *Synechocystis.* The *ziaA* expression is regulated by the ZiaR (Fig. 5) that belongs to the ArsR/SmtB family of metalloregulatory proteins. The proposed mechanism is that ZiaR homodimer binds to the *O/*P_{ziaA} and represses transcription of the *ziaA* gene. When ZiaR binds Zn^{2+}, it dissociates from the DNA, allowing transcription of *ziaA* (Thelwell et al. 1998). Two other members of the ArsR/SmtB family, SmtB (*Synechococcus*) and CadC (*S. aureus*) were shown to trigger the derepression of P_1-ATPases upon binding of both Zn^{2+} and Cd^{2+}. Recent crystallographic studies found that

CadC has two metal-binding sites, both able to bind both Zn^{2+} and Cd^{2+} (Kandegedara et al. 2009). Regulatory site 1 is composed of four cysteine residues C7, C11, C58, and C60 (Sun et al. 2001). Regulatory site 2 is formed at the dimerization interface and is composed of D^{101} and H^{103} from one monomer and H^{114} and E^{117} from the other monomer (Ye et al. 2005). All 4 amino acid residues of site 2 are conserved in *Synechocystis*, together with 3 out of 4 cysteine residues from site 1 (Fig. 10), making it likely that ZiaR also binds Cd^{2+}, in addition to Zn^{2+}. It is worth noting that there are other P_1-ATPases described in the literature that transport multiple metal ions, including Cd^{2+} and Zn^{2+}, like Bxa1 from *Oscillatoria brevis*, induced by both monovalent (Cu^+ and Ag^+) and divalent (Zn^{2+} and Cd^{2+}) cations (Liu et al. 2002). Therefore, it is possible that, besides Zn^{2+}, ZiaA also exports Cd^{2+}. No cadmium resistance system was discovered in *Synechocystis* to date.

```
ZiaR 1 MSKSSLSKSQS--CQNEEMPLCDQPLVHLEQVRQVQPEVMSLDQAQQMAEFFSALADPSRLRLMSALARQE-LCVCDLAA 77
SmtB 1 MTKPVLQDGETVVCQGTHAAIASE-------LQAIAPEV-----AQSLAEFFAVLADPNRLRLLSLLARSE-LCVGDLAQ 67
CadC 1 MKK---KDTCEIFCYDEE------------KVNRIQGDLQTVD-ISGVSQILKAIADENRAKITYALCQDEELCVCDIAN 64

ZiaR 78 AMKVSESAVSHQLRILRSQRLVKYRRVGRNVYYSLADNHVMNLYREVADHLQESD--- 132
SmtB 68 AIGVSESAVSHQLRSLRNLRLVSYRKQGRHVYYQLQDHHIVALYQNALDHLQECR--- 122
CadC 65 ILGVTIANASHHLRTLYKQGVVNFRKEGKLALYSLGDEHIRQIMMIALAHKKEVKVNV 122
```

Figure 10. Alignment of the translated sequences of *ziaR* (*Synechocystis*), *smtB* (*Synechococcus*) and *cadC* (*Staphylochoccus aureus*). The amino acid residues of metal binding site 1 and 2 from CadC and their conserved metal-coordinating residues from ZiaR and SmtB are highlighted.

5.2.2.2. Inducibility of the $O/P_{nrsBACD}$

We found that *nrsB,* the first ORF of the *nrsBACD* operon, is very highly induced by Ni^{2+} and, to a lower extent by Co^{2+} in accordance with previous studies (García-Domínguez et al. 2000, López-Maury et al. 2002). Upon 1 h incubation with 15 µM Ni^{2+} or *3* µM Co^{2+}, the transcript level of *nrsB* increased 333-fold and 4.7-fold, respectively (Fig. 11). The *nrsB* transcript level increased up to 800 fold upon exposure to 0.8 µM Ni^{2+} for 2 h and a high level of transcript (between 425 and 790 fold induction) was maintained in the cells up to at least 27 µM Ni^{2+}. The level of the Co^{2+}-triggered *nrsB* transcript was about 70-fold lower than the Ni^{2+} induced one. We found that upon 2 h incubation with 4 µM Co^{2+}, the maximal transcript level (about 6-fold induction) was reached and it was kept until at least 16 µM Co^{2+}, with a small decrease at 32 µM Co^{2+} (to four-fold induction) (Fig. 12, panel B). All these findings indicated that $O/P_{nrsBACD}$ could be a very good candidate for bioreporter development, especially due to the lack of a nickel bioreporter in the literature.

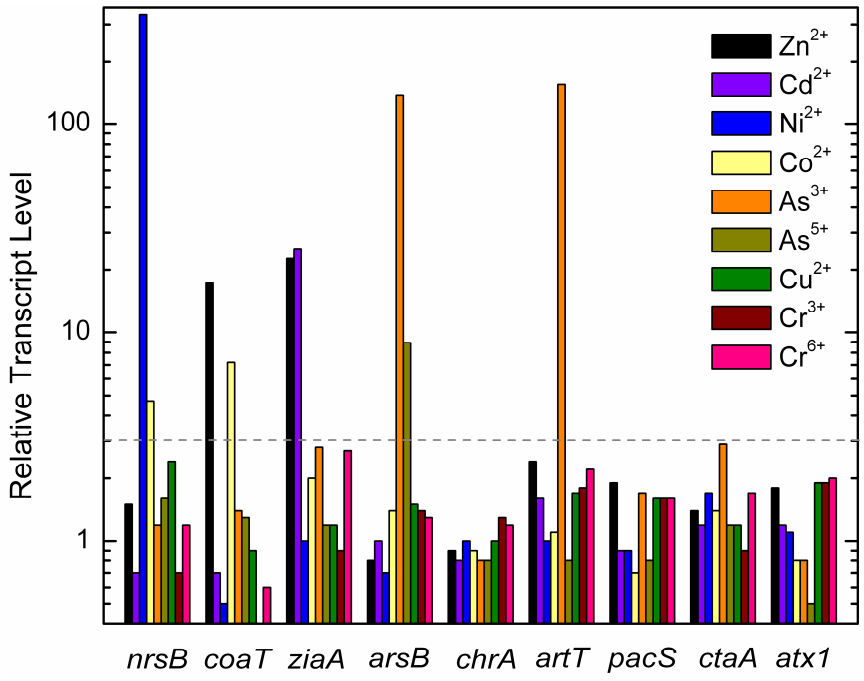

Figure 11. Metal-dependent expression of selected Synechocystis genes. Total RNA was isolated from mid-log-phase Synechocystis cells exposed for 1 h to 3 µM Co^{2+}, 5 µM Zn^{2+}, 15 µM Ni^{2+}, 1.5 µM Cd^{2+}, 50 µM Cr^{6+}, 50 µM Cr^{3+}, 1 mM As^{3+}, 1 mM As^{5+}, and 0.7 µM Cu^{2+}. Control cells were not exposed to metal salts. One µg of total RNA was reverse-transcribed and used as template for qRT-PCR with gene-specific primers (Table 1). The gene expression fold-change threshold of 3 is indicated by a dotted line.

The data available in the literature about *coaT* inducibility are contradictory. One study showed that O/P_{coaT} was induced only by 1 µM Co^{2+} (and not by 2 µM Zn^{2+}) after ~20 h incubation period in a *coaR-*O/P_{coaT}*-lacZ* transcriptional fusion (Rutherford et al. 1999). García-Domínguez and co-workers (2000) found that *coaT* transcript level was highly increased upon exposure to *15* µM Co^{2+} for 1 h, and to a lower extent, 15 µM Zn^{2+} for the same period of time. Our results indicated that upon 2 h of Co^{2+} treatment, the *coaT* transcript accumulates at higher levels than following exposure to Zn^{2+} at concentrations up to ~8 µM. The level of induction becomes equal at 16 µM, and at the concentration of 32 µM, Zn^{2+} becomes a more potent inducer than Co^{2+} (Fig. 29, panel E). A shorter, 1 h exposure to 3 µM Co^{2+} and 5 µM Zn^{2+} resulted in comparable accumulation of the *coaT* transcript (Fig. 11).

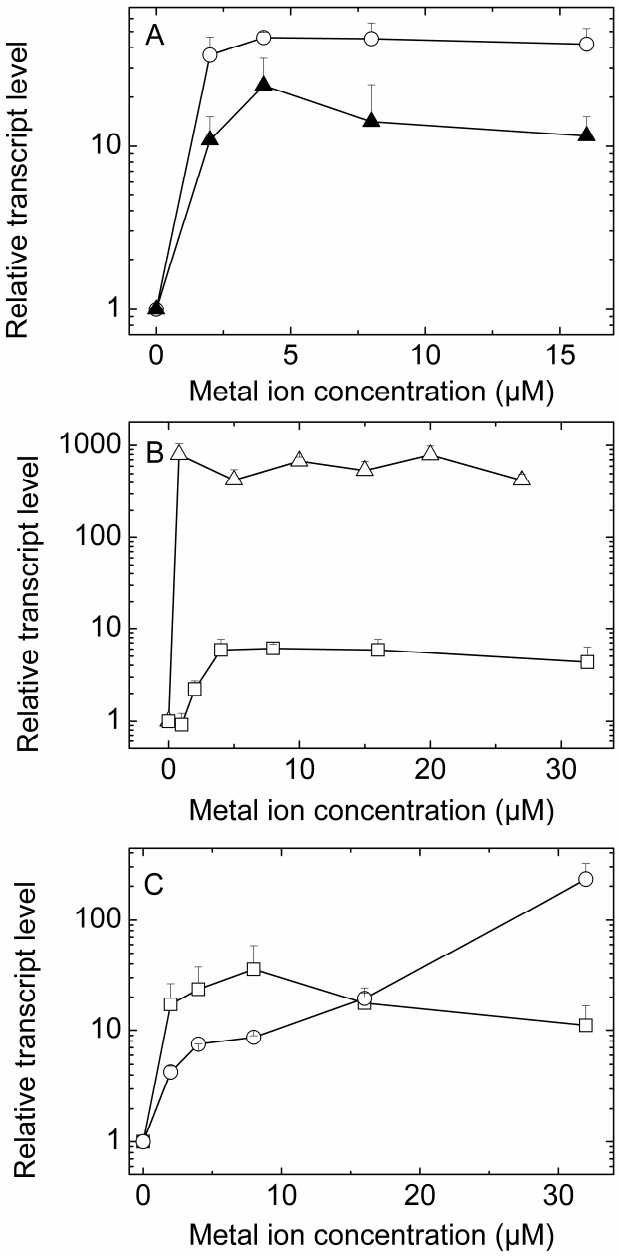

Figure 12. Concentration-dependent accucmulation of metal ion-inducible transcript. *Synechocystis* cells were grown in BG-11 and supplemented with the indicated concentrations of Zn^{2+}(○), Co^{2+}(□),Cd^{2+}(▲), and Ni^{2+}(Δ). Total RNA was isolated from the cultures after 2 h of exposure and the expression level of *ziaA* (A), *nrsB* (B) and *coaT* (C) was determined by qRT-PCR.

5.2.2.3. Inducibility of the O/P_{artT}

The *slr5038* gene (designated by us *artT*) gene encodes a putative chromate transporter that belongs to the LCHR4 family (Díaz-Pérez et al. 2007). During the general screen for potential candidates for bioreporter development we have not found a Cr-triggered induction of *artT*, but we noticed a very high (420-fold) induction after one hour exposure to

1 mM As^{3+} (Fig. 11). In a concentration dependence assay we observed that, following 15 min incubation, the *artT* gene was induced 8-fold by 73 µM As^{3+}, further increased to 615-fold induction when treated with 610 µM As^{3+}, and subsequently decreased to about 360-fold induction for the interval 936 µM to 2.2 mM As^{3+}, and to 212 fold induction when exposed to 3.48 mM As^{3+} (Fig. 13, panel A). As^{5+} in the 0.7 µM to 37.5 mM range did not induce the *artT* gene (Fig. 13, panel B). Therefore, the expression of the *artT* gene expression is regulated by arsenite, but not by arsenate. This is a novel finding, since this is the first report of an arsenite induced member of the CHR superfamily (Díaz-Pérez et al. 2007). Therefore, unlike *arsB* that is induced by both As^{3+} and As^{5+} (Fig. 11 and 13), the expression of the *artT* gene is regulated only by As^{3+} and not by As^{5+}, suggesting that the transcription of these genes is controlled by different types of regulators.

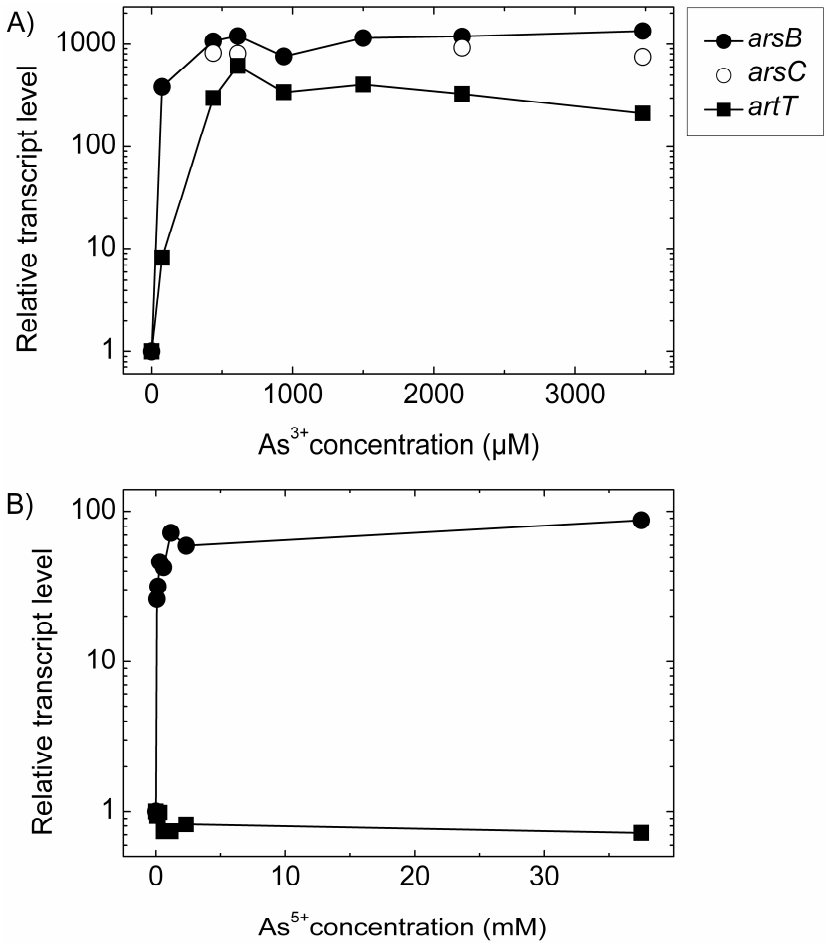

Figure 13. Arsenite- and arsenate- induced expression of the *arsB*, *arsC* and *artT* genes. *Synechocystis* cells were grown in BG-11 and supplemented with the indicated concentrations of As^{3+} or As^{5+}. Total RNA was isolated from the cultures after 15 min (A) or 2 h (B) of exposure and the expression levels of *arsB* (●), *arsC* (○) and *artT* (■) were determined by qRT-PCR.

5.2.2.4. Inducibility of the O/P_{ctaA}, O/P_{pacS} and O/P_{atx1}

The transcripts of the *ctaA*, *pacS* and *atx1* genes did not significantly increase during 1 h incubation in BG-11 supplemented with 0.7 µM Cu^{2+} (Fig. 11), or 2 h incubation with 0.5, 1.25, 2.5 or 5 µM Cu^{2+} (data not shown). Therefore, the *pacS* seems to be regulated in a different way than its homolog in *Synechococcus* whose transcript and protein product levels were specifically increased upon addition of copper to the growth medium (Kanamaru 1994).

5.3. New metal bioreporters

5.3.1. Bioreporter strai0s based on the O/P_{coa}, O/P_{nrs}, and O/P_{zia}

5.3.1.1. Selectivity and sensitivity of bioreporter strains

Three bioreporter strains were previously constructed in our laboratory, as described in the Materials and Methods, using the O/P_{coa}, O/P_{nrs}, and O/P_{zia} promoters. We will refer to these bioreporter stains as *coaLux*, *nrsLux* and *ziaLux1*, respectively. The *coaLux* and *nrsLux* constructs were functional as bioreporters, and we characterized them during this work. The *ziaLux1* construct, containing a full version of the repressor-encoding *ziaR*, was not functional in the tested conditions. We have designed a second version of the *ziaR-O/PziaA-luxAB* fusion ($ziaLux_T$) that contains a truncated *ziaR* gene, lacking 308 bp from the 3' end. This construct also did not show luminescence activity upon incubation with Zn^{2+} (data not shown).

Luminescence measurements were optimized to detect the presence of metal ions with a simple protocol. Mid-log phase *Synechocystis coaLux* and *nrsLux* cultures were incubated in light with metal salts in black microtiter plates with low autofluorescence signal. We found that the optimal induction time was 3 h. Longer incubation time did not significantly increase the relative induction. The specificity of the bioluminescent response in the *coaLux* and *nrsLux* strains was investigated in BG-11 medium containing different metal salts for which the IC_{min} and IC_{max} concentrations were previously established (section 4.1.). Two concentrations in these ranges where chosen for each of Co^{2+}, Zn^{2+}, Ni^{2+}, Cd^{2+}, Cr^{6+}, and As^{3+} as indicated in Fig. 14. From the tested metal salts, only Zn^{2+} and Co^{2+} induced significant bioluminescent response in the *coaLux* strain (Fig. 14, panel A), whereas the response of the *nrsLux* strain was specific to Ni^{2+} (Fig. 14, panel B).

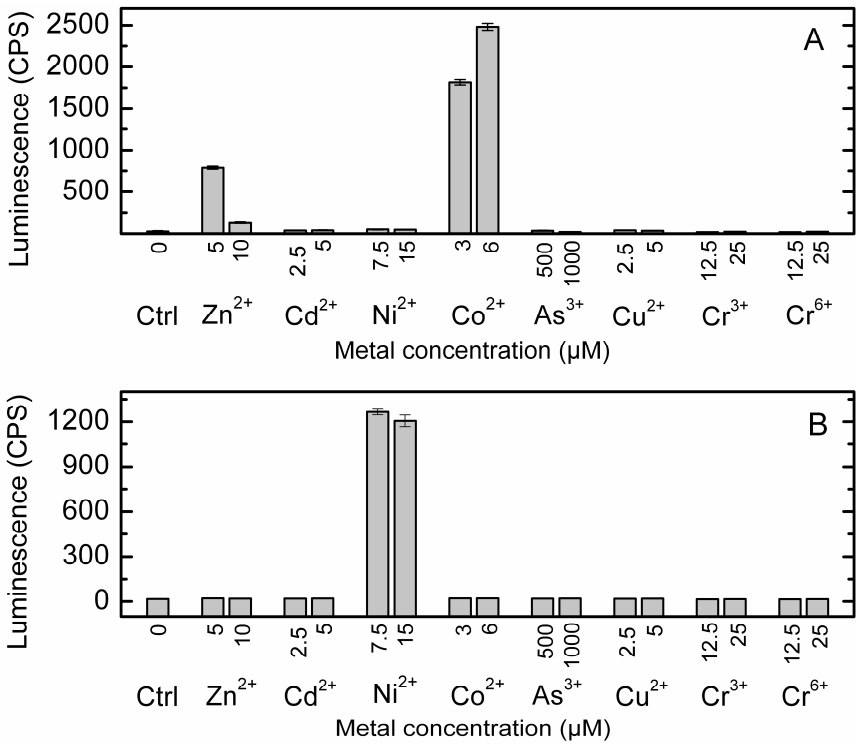

Figure 14. Specificity of the bioluminescent response of the *coaLux* and *nrsLux* bioreporter strains to different metal salts. Cells were incubated in light for 3 h in BG-11 medium supplemented with known concentrations of selected metal salts. Assays were performed with four parallel measurements. Standard errors are indicated.

Both the *coaLux* and *nrsLux* strains showed dose-dependent responses to the metal salts added into the culture medium. When incubated in light, the *coaLux* sensor responded to Co^{2+} and Zn^{2+} in the 0.3 to15 µM (Fig. 15, panel B) and 1 to 15 µM (Fig. 15, panel A) concentration ranges, respectively. The luminescence increased gradually with increasing concentrations of Co^{2+} and Zn^{2+} up to 6.4 µM (relative luminescence induction ~70-fold) and 3.2 µM (relative luminescence induction ~25-fold), respectively, followed by a decline at higher concentrations. In mixed samples of Co^{2+} and Zn^{2+}, the *coaLux* reporter strain responded in an additive manner up to ~2 µM, after which the luminescence response to the Co^{2+} and Zn^{2+} mixture became higher than the sum of the individual responses (Fig. 16). The *nrsLux* sensor responded to Ni^{2+} in the 0.2 to 50 µM concentration range. The maximum response was about 50-fold induction of luminescence intensity at about 6.4 µM Ni^{2+} in the medium (Fig. 15, panel C). At higher Ni^{2+} concentrations the luminescence signal gradually decreased. We observed a background luminescence emission for the *coaLux* reporter strain (2-3 times higher than the wild type luminescence emission), presumably due to the low but constant expression of the uninduced *coaT* gene, indicating the leaky nature of its promoter (data not shown).

The luminescence response of the *coaLux* and *nrsLux* reporter strains was also evaluated in darkness. Under this condition the luminescence peak was shifted to higher concentrations of Co^{2+} and Zn^{2+} in the *coaLux* reporter, accompanied by a reduction of the maximal extent of luminescence value to approximately 65% and 50% of the respective values obtained in the light. Due to these changes in the shape of the luminescence response curves the detection range increased about 4-fold: up to 26 µM Co^{2+} (relative luminescence induction ~25-fold) (Fig. 15, panel B) and up to about 13 µM Zn^{2+} (relative luminescence induction ~12-fold) (Fig. 15, panel A). On the contrary, the *nrsLux* reporter strain did not show any luminescence when incubated in darkness with the tested concentrations of Ni^{2+} (Fig. 15, panel C). The cause remained elusive. Due to the lack of *nrsLux* activity in darkness, all the bioluminescence assays with this strain were carried out in light.

Therefore, the detection range of *coaT* is 0.3 to 6.4 µM for Co^{2+} and 1 to 3.2 µM for Zn^{2+} when incubated in light. The shape of the concentration-dependent luminescence response for Zn^{2+} and the detection range are similar to those obtained with the cyanobacterial sensor based on *Synechococcus smt-luxCDABE* transcriptional fusion (Erbe 1996). Incubation in darkness, in case of the *coaLux* reporter strain, has the advantage of extending the detection range up to 25.6 µM Co^{2+}, and up to about 12.8 µM Zn^{2+}. The application of the *coaLux* bioreporter for Zn^{2+} detection has been tested using a polluted soil-like sample collected from a composted mixture of different chemical and oil industry wastes (see paragraph 4.3.1.3 below).

The increasing utilization of nickel in modern technologies leads to an accumulation of nickel compounds in the environment that may represent a serious hazard to human health. Among the known health risks of nickel exposure are skin allergies, kidney and cardiovascular system poisoning, lung fibrosis and stimulation of neoplastic transformation (Denkhausa and Salnikowb 2002). Therefore, a cheap and effective detection method for environmental monitoring of nickel would be very useful. We present here the first Ni^{2+}-specific whole-cell reporter with a clear dose dependent response. The detection range of *nrsB*, from 0.2 to 8 µM Ni^{2+}, matches the upper nickel concentration limit admitted in the drinking water, as specified by WHO's Guidelines for Drinking-water Quality (0.07 mg/L = 1.19 µM). Therefore, the *nrsLux* reporter presented here is potentially useful in the development of a bioreporter for Ni^{2+} detection in drinking water. Cyanobacteria are photoautotrophic organisms that can grow on low-cost media and require little maintenance. Therefore, using cyanobacteria for biosensing purposes represents an advantage over the use of heterotrophic microorganisms (Bachmann 2003, Erbe et al. 1996). We brought our contribution to the field of whole-cell bioreporters, in general, and cyanobacterial

bioreporters, in particular, by demonstrating the potential for development of rapid, simple and economical field assay for nickel, cobalt and zinc detection.

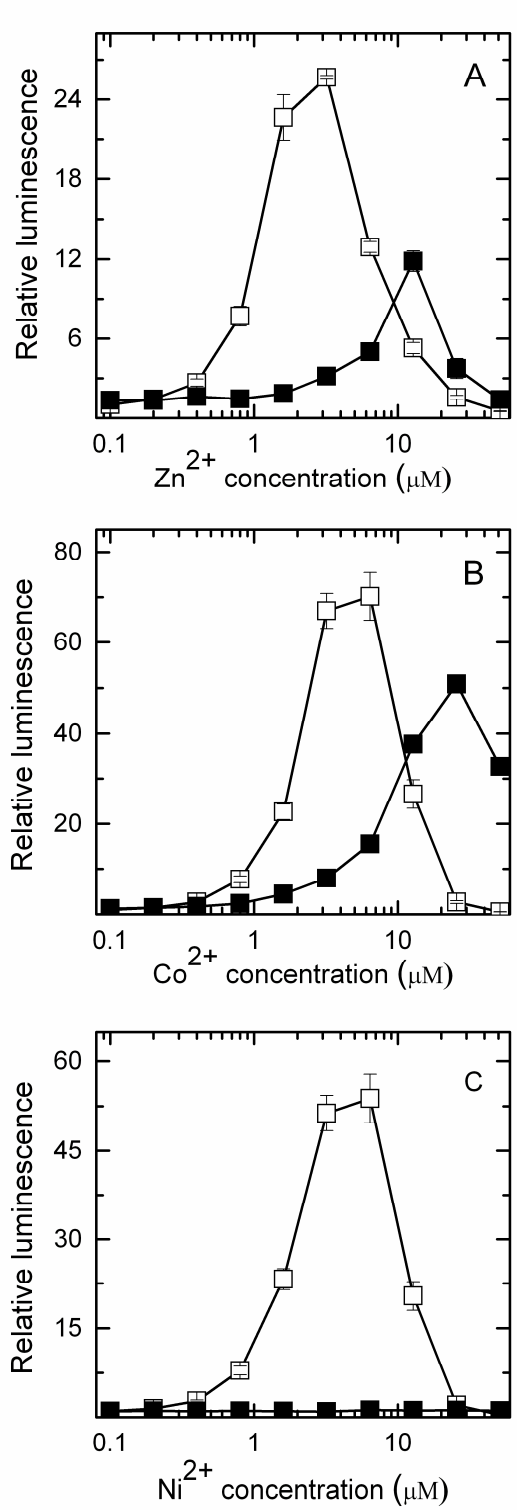

Figure 15. The bioluminescent responses of *coaLux* (A and B) and *nrsLux* (C). Cells were incubated for 3 h in BG-11 medium supplemented with Zn^{2+}, Co^{2+} or Ni^{2+} salts, in light (open symbols) and darkness (closed symbols) and the bioluminescence was measured as described in Materials and Methods. Each point represents the mean of four parallel measurements. Standard errors are indicated.

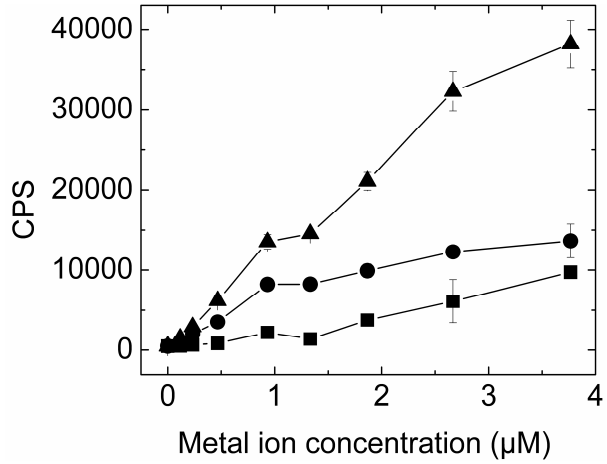

Figure 16. The bioluminescent response of *coaLux* reporter following incubation with Zn^{2+}, Co^{2+} and a mixture of Zn^{2+} and Co^{2+}. Cells were incubated for 3 h in BG-11 medium supplemented with Zn^{2+}(■), Co^{2+}(●) and a mixture of Zn^{2+} and Co^{2+}(▲), and the bioluminescence was measured as described in the Materials and Methods. Each point represents the mean of two parallel measurements. Standard errors are indicated.

5.3.1.2. Effect of Zn^{2+} on Ni^{2+}-induced response in the *nrsLux* strain

Since zinc and nickel pollution often coexist, the performance of the *nrsLux* reporter strain was tested in mixed samples using Ni^{2+} and Zn^{2+} salt standards. Incubation was carried out in light for 3 h after the addition of metal salts. The Ni^{2+} concentration was maintained at constant 8 µM level that produces the maximum luminescence signal in the *nrsLux* reporter strain, while Zn^{2+} concentration was varied from 0 to 16 µM, and the luminescence production was monitored. Interestingly, the Ni^{2+}-specific response was markedly reduced in the presence of increasing Zn^{2+} concentrations from 2 µM that produces about 20% inhibition, to 16 µM that reduced the Ni^{2+}-induced luminescence signal with 90% (Fig. 17). The half maximal inhibitory concentration of Zn^{2+} (IC_{50}) on the Ni^{2+}-induced bioluminescence response was about 6 µM.

5.3.1.3. Quantification of the bioavailable zinc in soil samples

In order to asses the performance of the constructed *coaLux* and *nrsLux* reporter strains, the acetic acid extracts of contaminated soil, containing an average of 1.88 µM Ni^{2+}, 0.72 µM Co^{2+} and 188.7 µM Zn^{2+} as determined by AAS, were used. Cells were incubated with 1.11-fold serial dilutions of the acetic acid extracts for 3 h in light, than the bioluminescence was assayed. For calibration purposes, the bioreporter cells were incubated with 1.11-fold serial dilutions of a $ZnSO_4$ standard solution. The response curve obtained with the standard samples could be fitted using a linear function with good correlation

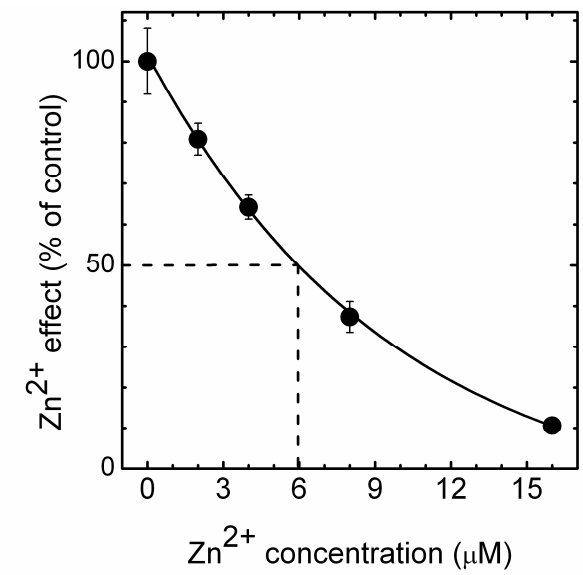

Figure 17. Concentration-response curve for the inhibition of Ni^{2+}-induced luminescence response in *nrsLux* bioreporter by Zn^{2+}. Data are expressed as percentage of the response in the presence of 8 µM Ni^{2+} alone. Each point represents the mean of data obtained in 4 wells for each concentration with the indicated standard error. The solid line represents a formal fitting of the experimental data with an exponential function. The dotted lines indicate the IC_{50} value of Zn^{2+}.

(R^2 = 0.95) in the 1.6 to 2.5 µM range (Fig. 18). Calculation of Zn^{2+} concentrations in the environmental sample dilutions were performed using a linear calibration curve (y = 1118.2 x - 1813.6, where y represents the luminescence signal and x stands for Zn^{2+} concentration). The results obtained by AAS and the luminescence-based detection technique show good correlation (Table 4). The concentration of Zn^{2+} calculated from the luminescence response of the *coaLux* reporter strain represent an average of 91.5 (± 1.4 SD) % of the AAS-determined zinc concentration, that can be interpreted as the bioavailable zinc fraction, or the amount of zinc "freely available to cross an organism's cellular membrane from the medium the organism inhabits at a given time" (Semple et al. 2004). The Co^{2+} content of the environmental sample was not taken into account since its value was negligible when compared with the Zn^{2+} concentration. The soil samples were also incubated with the *nrsLux* reporter strain, since it contained 1.88 µM Ni^{2+}, which is in the detection range of the *nrsLux* strain. However, no luminescence signal was detected upon incubation with the undiluted acetic acid extract of the contaminated soil, presumably due to the inhibitory level of zinc content, exceeding about 17 times the IC_{50} value.

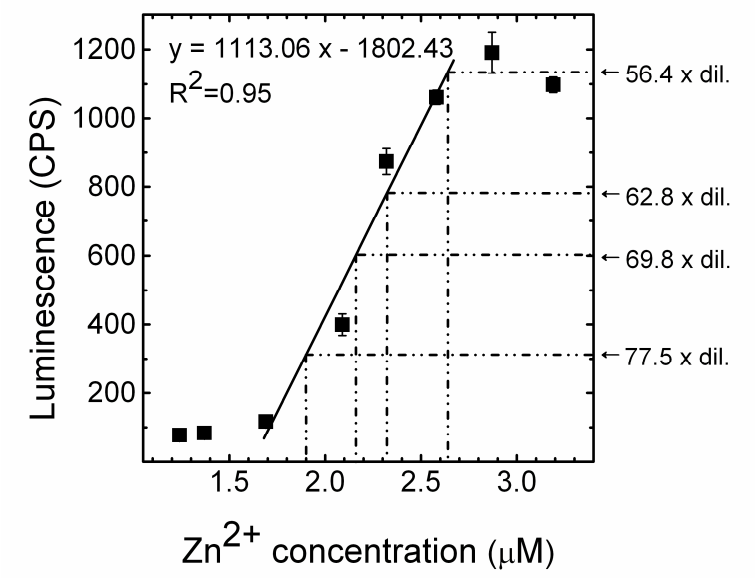

Figure 18. The bioluminescence response of the *coaLux* reporter strain to a zinc-containing environmental sample. The reporter strain was incubated with 1.11-fold serial dilutions of $ZnSO_4$ and acetic acid-extract from a polluted soil sample for 3h in light, then the bioluminescence was assayed. Linear range of coaLux response to the standard sample dilutions and the equation of linear regression are presented. The extent of luminescence response to the different dilutions of the environmental sample extract is shown by the horizontal lines, whereas the Zn^{2+} concentrations calculated from the regression equation are shown by the vertical lines (see the values in Table 4). The experiment was performed with four parallel measurements. Standard errors are indicated.

Table 4. Comparison of zinc content determined by AAS and by *coaLux* reporter strain in the acetic acid-extractable fraction of an environmental sample. Liquid suspensions of the reporter strain were incubated with different dilutions of the acetic acid extract of environmental sample, the bioluminescence induction was determined and the corresponding Zn^{2+} concentration was calculated from the equation of the standard curve displayed in Figure 18.

Fold dilution[a]	*Zinc concentration (μM)*	
	AAS[b]	*biosensing (coaLux reporter)*[c]
56.4	*2.87*	*2.64*
62.8	*2.58*	*2.32*
69.8	*2.32*	*2.16*
77.5	*2.09*	*1.9*

[a]Fold dilution of the acetic acid-extractable fraction of an environmental sample with a content of 162 μM zinc, as determined by AAS
[b] Zinc concentration measured by AAS
[c] Zinc concentration calculated from the standard curve

5.3.2 A bioreporter strain based on the O/P$_{ars}$

In the case of the *arsLux* bioreporter strain a longer incubation with the arsenic salts is required prior to the bioluminescence measurement. We found that relatively high induction was obtained upon overnight incubation. The specificity of the bioluminescent response was investigated in BG-11 medium containing different metal salts. From the tested metal salts, only As^{3+} and As^{5+} induced significant bioluminescent response in the *arsLux* strain (Fig. 19). The *arsLux* bioreporter responded to As^{3+} and As^{5+} in very different concentration ranges. The detection limit for As^{3+} is ~8 µM, which produces a 4.4-fold induction in luminescence. From 8 µM to about 500 µM the luminescence signal shows a linear increase (Fig. 20, panel A). The response was similar for 500 µM and 1000 µM As^{3+} (40 fold induction), after which the signal decreased to the initial level, at 2000 µM As^{3+}. The detection limit for As^{5+} is two orders of magnitude higher than for As^{3+} (~2.3 mM) (Fig. 20, panel B). The bioluminescent signal increased slowly up to 10 mM As^{5+} and then, at a higher rate, up to 150 mM As^{5+} (the highest concentration tested).

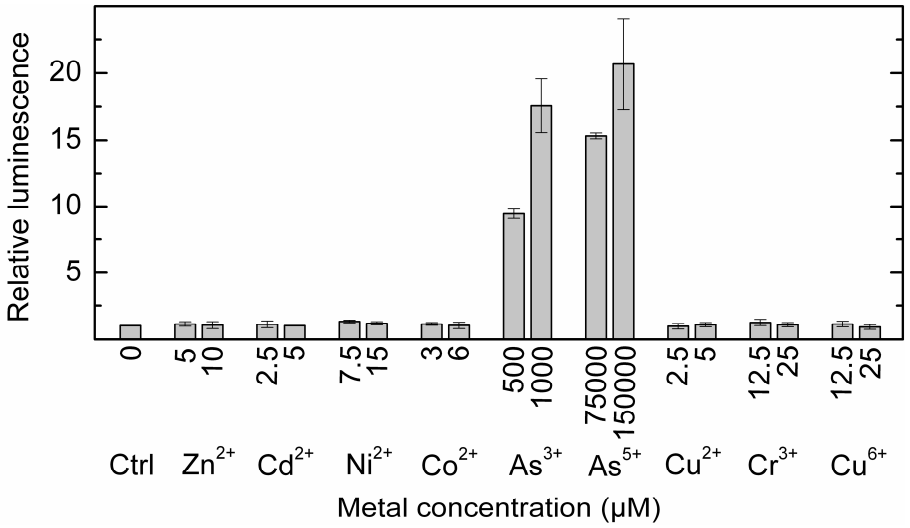

Figure 19. The bioluminescent response of the *arsLux* bioreporter strain to different metal salts. Cells were incubated in light for 18 h in BG-11 medium supplemented with known concentrations of selected metals. The assays were performed with three parallel measurements. Standard errors are indicated.

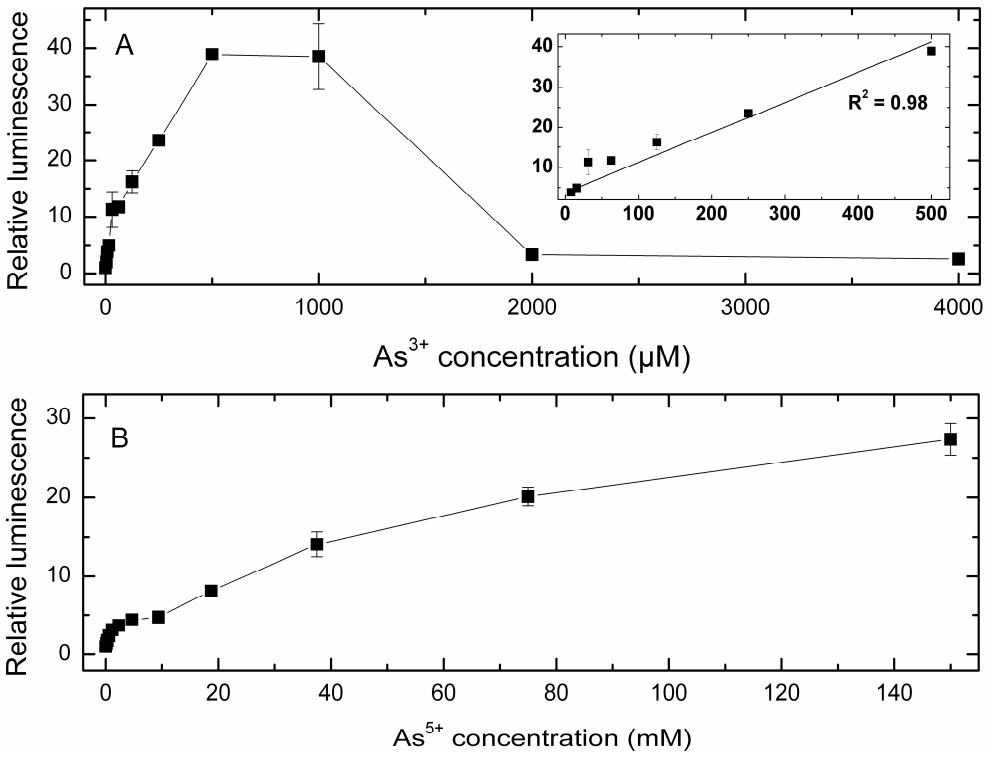

Figure 20. The bioluminescent response of *arsLux* to As^{3+} and As^{5+}. Cells were incubated for 3 h in BG-11 medium supplemented with As^{3+} (A) and As^{5+} (B), and bioluminescence was measured as described in the Materials and Methods. The inset graph in panel A shows the linear response range of the bioreporter to As^{3+}. Each point represents the mean of four parallel measurements. Standard errors are indicated.

The highest numbers of bioreporters were constructed to target either mercury ions or inorganic arsenic species. The extant arsenic bioreporters rely on the *ars* genes from *E. coli* and *S. aureus* and different reporter genes*: lacZ* (Diario 1995, Ramanathan 1998, Stocker 2003), *luxAB* (Cai and DuBow 1996, Ramanathan et al. 1997, Stocker et al. 2003), and *gfp* (Liao and Ou 2005, Stocker et al. 2005). The reported sensitivities and ranges of detected concentrations (Fig. 21) have to be regarded with great caution due to the use of different calibration schemes (Harms 2007). Here we report the first whole-cell arsenic bioreporter generated in a cyanobacterial strain. Future plans include increasing the sensitivity of *arsLux* reporter strain. In some cases small variations in the protocol of the bioluminescent assay, such as dilution of the bioreporter cells, have led to greatly increased sensitivities (Rasmussen et al. 1997).

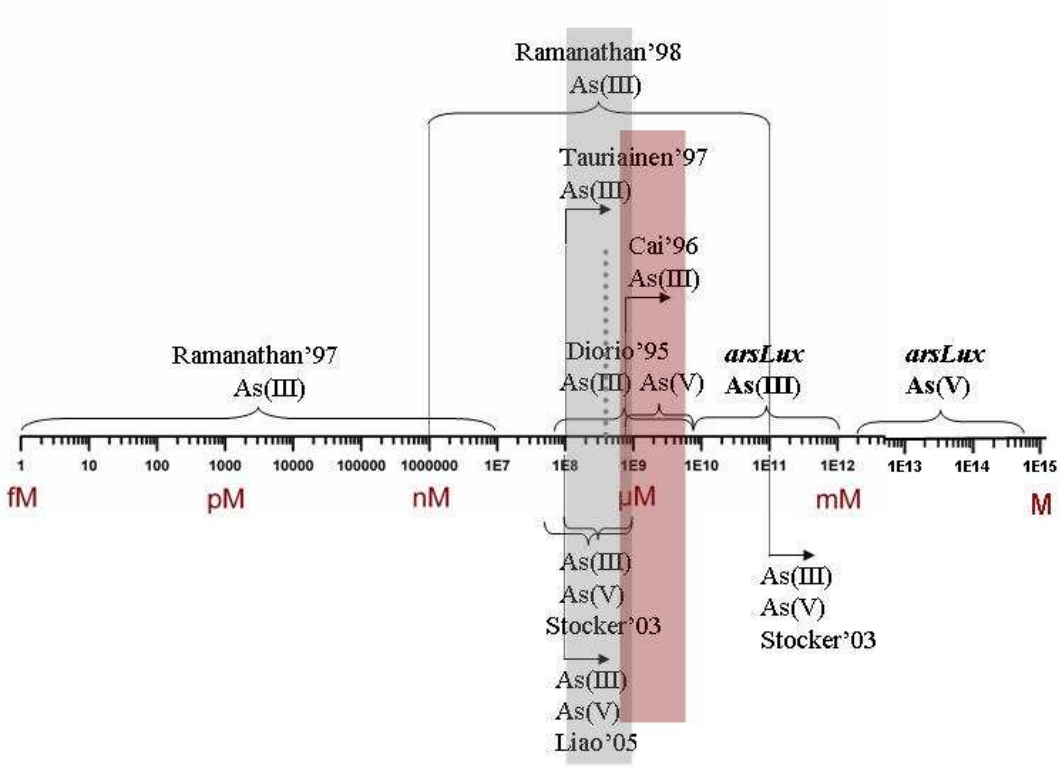

Figure 21. Detection ranges for As^{3+} and As^{5+} of *arsLux* and other arsenic bioreporters found in literature. The WHO drinking water quality limit for arsenic ions (10 µg/l = 0.13 µM) is indicated as a dotted line. The concentration range of general interest for arsenic biosensing applications is highlighted in gray. The water from about 11 Hungarian settlements with a total population of about 24000 contains arsenic levels higher than 0.65 µM (Jones et al. 2008) with a peak value of 7.3 µM (Csalagovits 1999) - highlighted in red colour.

5.4. A putative chromate/sulfate transporter

5.4.1. Inducibility of putative chromate transporter genes

We found that neither *artT,* nor *chrA* transcript levels are changed considerably after 15 min incubation in BG-11 medium supplemented with 7, 20 or 50 µM bichromate ($Cr_2O_7^{2-}$) (qRT-PCR data not shown). It has been demonstrated in a variety of bacteria that chromate is actively transported across membranes via the sulfate uptake system (Cervantes et al. 2001, Cervantes and Campos-García 2007), and also that sulfur deprivation increases the rate of sulfate transport in *Synechococcus* (Green and Grossman 1988). Therefore, we looked at the expression of the *artT* and *chrA* genes after addition of bichromate to cells that were grown in low sulfate medium for a short time. The cells were grown in normal BG-11 medium that

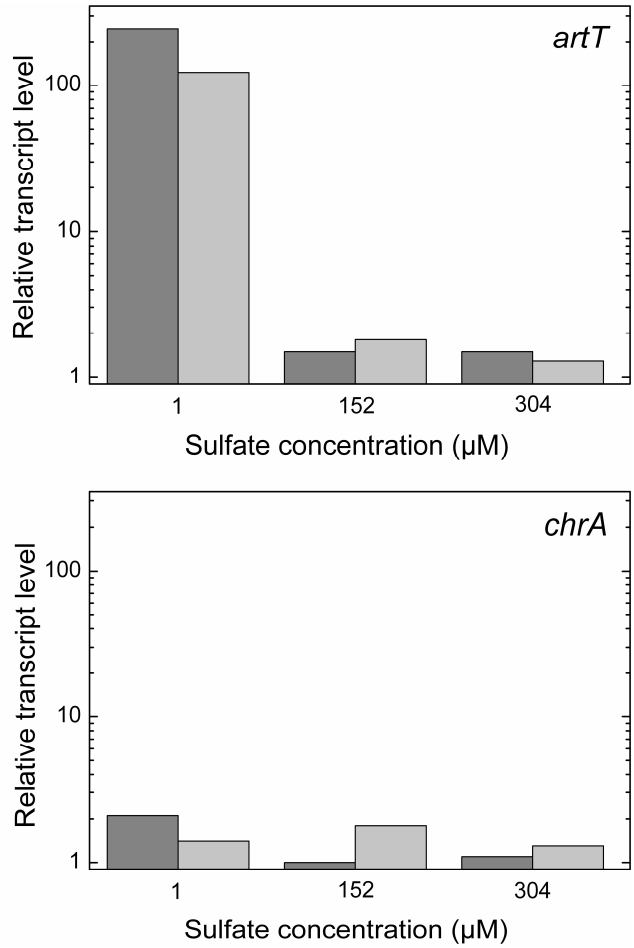

Figure 22. Chromate/sulfate-dependent inducibility of *artT* and *chrA* genes. *Synechocystis* cells were incubated in BG-11 medium containing the indicated sulfate concentrations and supplemented with 20 µM bichromate either for 15 min (dark gray columns) or 1h (light gray columns) and *artT* and *chrA* expression was assessed by qRT-PCR.

contains 304 µM sulfate ($BG\text{-}11_n$) until mid-log phase, then resuspended and incubated for 15 min in normal BG-11 medium (control) or modified BG-11 medium containing either 152 µM ($BG\text{-}11_{152\ SO4}$) or 1 µM sulfate ($BG\text{-}11_{1\ SO4}$). At this point each cell culture was supplemented with 20 µM bichromate and samples were collected for qRT-PCR analysis of *artT* and *chrA* expression after 15 min and 1h incubation. We found a very high increase in the transcript level of the *artT* gene in cells preincubated in $BG\text{-}11_{1\ SO4}$ for 15 min and exposed to chromate for 15 min or 1 h (245 and 122 fold increase, respectively; Fig. 22). The transcript levels for *artT* in the samples collected after 15 min incubation in $BG\text{-}11_n$, $BG\text{-}11_{152\ SO4}$ and $BG\text{-}11_{1\ SO4}$ media were very similar (data not shown). This is an indication that the *artT* transcript accumulation is not triggered by short-term sulfate limitation, but by the addition of bichromate on a sulfate-limited background. Additional experiments confirmed that the *artT* gene was not induced after 2 h of sulfate limitation (data not shown). The transcript level of *chrA* gene did not change substantially during the investigated conditions (Fig. 22). We have also detected strong increase in the transcript level of the *artT* gene upon exposure to As^{3+} (Fig. 13). This is the first reported CHR gene induced by As^{3+}. We wanted to know if the *artT* homologues from *Synechococcus* (*srpC*) and from *Anabaena* (*all1110*) are also induced by arsenite. *Synechococcus* and *Anabaena* cells were grown in $BG\text{-}11_n$ medium until mid-log phase and supplemented with As^{3+}. The transcript levels of *srpC* and *all1110* did not change upon 15 min incubation with 1mM As^{3+} (data not shown). Therefore As^{3+}-inducibility may be a specific function of the *artT* gene, not shared with related cyanobacterial genes.

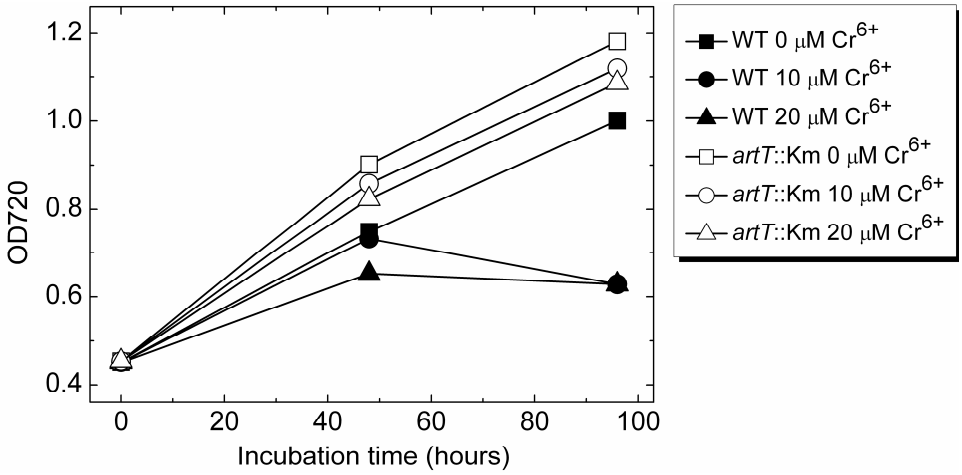

Figure 23. The influence of the sulfate and chromate content of the BG-11 medium on the growth rate of WT and *artT*::Km cells. The WT S*ynechocystis* and *artT*::Km cells were grown in low sulfate BG-11 (10 µM) medium supplemented with no, 10 µM or 20 µM $Cr_2(SO_4)_3$ and growth was monitored by measuring OD_{720}.

To elucidate the function of *artT*, a disruption mutant, *artT*::Km, was created in our laboratory (Fig. 27). We have investigated the growth rate of *artT*::Km in BG-11_n medium or low sulfate BG-$11_{1\ SO4}$ medium supplemented with none, 10 or 20 µM Cr^{6+}. The *artT::*Km mutant grew somewhat slower than the WT in BG-11_n, with or without added bichromate (data not shown). In BG-11 medium with low sulfate content (10 µM), the growth rate of *artT::*Km was moderately higher than the growth rate of WT, but appreciably higher when the medium was supplemented with 10 or 20 µM potassium bichromate (Fig. 23). Additionally, *artT*::Km cells showed higher resistance to Cr^{6+} when grown on solid BG-$11_{1\ SO4}$ medium supplemented with 40 µM chromate (Fig. 24). Therefore, since *artT*::Km is more resistant to chromate when the cells are grown in low sulfate medium, we can conclude that the *artT* gene is involved in chromate uptake when sulfate is low in the medium. Its protein product may work as a chromate/sulfate antiporter as suggested by Nies and co-workers (1990) for the CHR superfamily proteins. These proteins would export the erroneously accumulated chromate by exchanged for sulfate that is usually high in the extracellular medium compared to the chromate concentration. At low sulfate and high chromate concentrations in the extracellular medium, they work as chromate uptake systems, thereby explaining the chromate resistance phenotype of the *artT* disrupted mutant (see Section 2.8.3 for discussion on the function of CHR proteins). A similar phenotype was found in *Synechococcus* after interruption of the *srpC* gene (Nicholson and Laudenbach 1995), suggesting that SrpC may take up chromate, instead of exporting it (Díaz-Pérez et al. 2007).
Since the *artT* gene is induced by arsenite, we further investigated the growth of *artT*::Km in BG-11 medium supplemented with As^{3+}. Both the WT and the *artT*::Km strains were grown in BG-11 supplemented with 4.5 mM As^{3+} (starting at OD_{720} 0.03). Both WT and *artT*::Km strain started to grow after a lag period of about 3 and 5 days, respectively, with *artT*::Km growing at a substantially higher rate than the WT (Fig. 25). When grown on agar-solidified BG-11 supplemented with 3.5 mM As^{3+}, *artT*::Km showed a higher arsenite resistance, as well (Fig. 24). The arsenic resistance phenotype of the *artT*::Km mutant was observed both in liquid and on agar-solidified media. Therefore, we conclude that, in addition to chromate transport, *artT* may be involved in arsenite transport. The genomic context sugests that CHR proteins possess other physiological functions in addition to chromate transport (Díaz-Pérez et al. 2007).

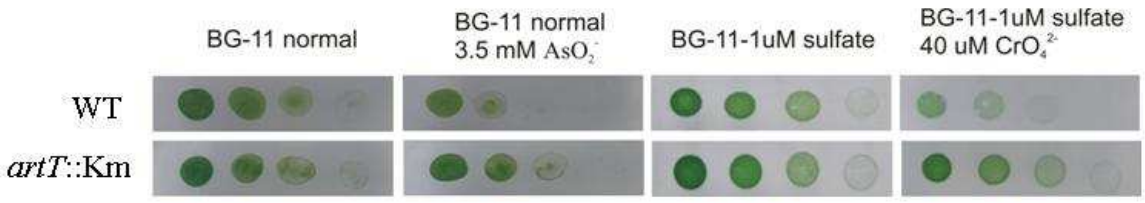

Figure 24. Tolerance of *Synechocystis* WT and *artT*::Km to arsenite and chromate ions. Tenfold serial dilutions of cell culture were spotted on BG-11_n or BG-11_1 $_{SO4}$ media supplemented with the indicated concentrations of $NaAsO_2$ or Na_2CrO_4 and photographed after 10 days of growth.

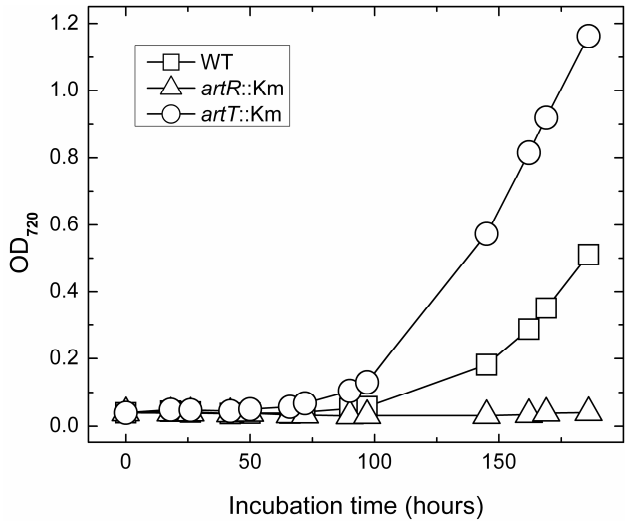

Figure 25. The growth of *Synechocystis* WT, *artT*::Km and *artR*::Km in BG-11_n supplemented with 4.5 mM As^{3+}. The cells were inoculated in BG-11_n medium supplemented with 4.5 mM $NaAsO_2$ and growth was monitored by measuring OD_{720}.

5.4.2. The *artC* and *artT* genes are cotranscribed

Situated at 39 bp upstream of *artT* and transcribed in the same direction is the *artC* gene (Fig. 26, panel A). The proximity and the direction of transcription suggest that the two genes are cotranscribed. Indeed, we found a ~300 fold induction of both *artC* and *artT* transcript levels after incubation with 400 µM As^{3+} for a period of 15 minutes (Fig. 26, panel B). To test if *artC* and *artT* are cotranscribed, we used cDNA from *Synechocystis* cells treated with 1 mM As^{3+} for 1 h as PCR template, and the primers *artC-F1* and *artT-R1* that anneal with the *artC* and *artT* gene sequences, respectively. The amplicon can only form if the two genes are situated on the same mRNA (hence, the same cDNA molecule). We obtained an amplicon of 420 bp, in both the control and the As^{3+} treated samples (Fig. 26, panel C),

indicating that the *artC* and *artT* genes are cotranscribed. The amplicon amount was much higher in the As^{3+} treated samples, in accordance with the previously described inducibility of *artT*.

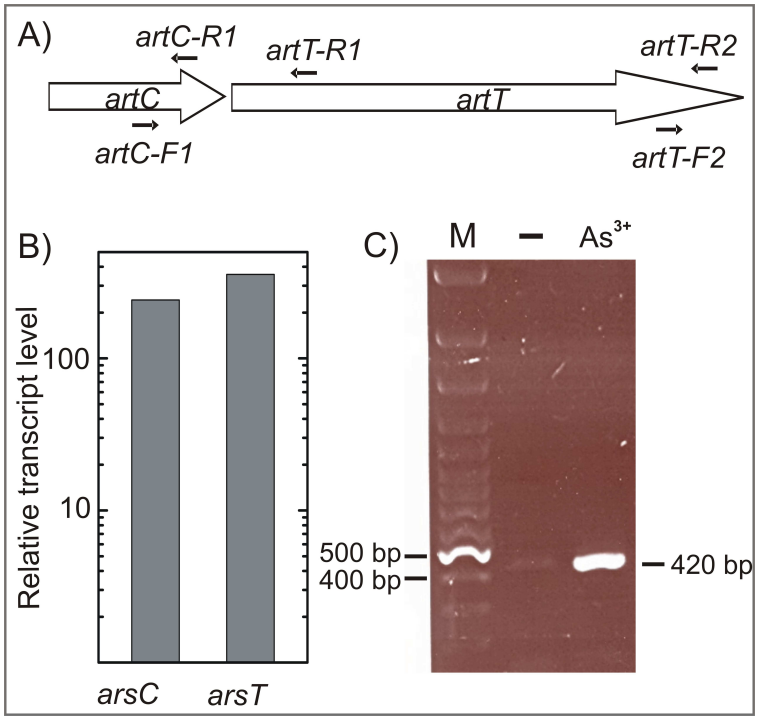

Figure 26. The *artC* and *artT* genes are cotranscribed. (A) The *artC* and *artT* genes (wide arrows) and the primers used for amplification (small black arrows). (B)The induction of *artC* and *artT* upon incubation with 400 µM As^{3+} for a period of 15 minutes as determined by qRT-PCR with the primer pairs *artC-F1/artC-R1* and *artT-R1/artT-F1*. (C) DNA gel electrophoresis of the PCR products obtained with *artC-F1/artT-R1* primer pair and cDNA from Synechocystis cells exposed to a concentration of 1 mM As^{3+} for 1h. Control cells were not exposed to As^{3+} (–).

5.4.3. ArtR is a repressor of the *artCT* operon

Upstream of the *artCT* operon, and transcribed in the opposite direction, there are two ORFs that we designated *artS* and *artR* (Fig. 27; see Table 3 for Cyanobase ORF ID), encoding a putative sulfide-quinone reductase and a transcriptional regulatory protein from the SmtB/ArsR family of prokaryotic metalloregulatory transcriptional repressors, respectively (Cyanobase annotation). The members of the SmtB/ArsR protein family repress the expression of operons involved in responses to stess-inducing concentratios of metal ions, such as: Zn^{2+}, As^{3+}, Cd^{2+}, Pb^{2+}, Bi^{2+}, Co^{2+}, and Ni^{2+}. Direct binding of metal ions by these homodimeric metal sensor proteins results in derepression of the respective promoter regions (Busenlehner 2003). Due to the involvement of this class of transcriptional repressors in metal ion sensing, the proximity of *artR* to the *artCT* operon and their opposite orientation,

we hypothesized that the *artR* gene encodes a repressor that regulates the expression of O/P$_{artCT}$. A disruption mutant created in our laboratory (Fig. 27) showed constitutive derepression of O/P$_{artCT}$ (Fig. 28), partially confirming our hypothesis. ArtC is annotated as a conserved hypothetical protein that belongs to a Domain of Unknown Function, DUF302, in Pfam database (Bateman et al. 2002). The coordinate regulation of the *artC* and *artT* genes suggests that they are functionally related.

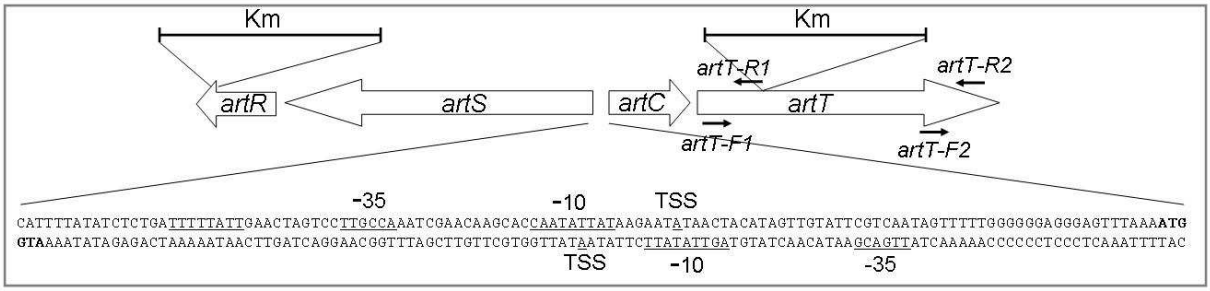

Figure 27. The chromosomal arrangement of the *art* genes and the *artS-artC* intergenic region. The start codons for *artS* and *artC* are shown in bold. Putative transcription start sites (TSS), -35, and -10 promoter elements are underlined. The insertion sites of the kanamycin cassette in the *artR*::Km and *artT*::Km disruption mutants are indicated. Two pairs of qRT-PCR primers used for investigating the phenotypes of the mutants are shown as thin arrows: *artT-F1/artT-R1* and *artT-F2/artT-R2* (see Table 1).

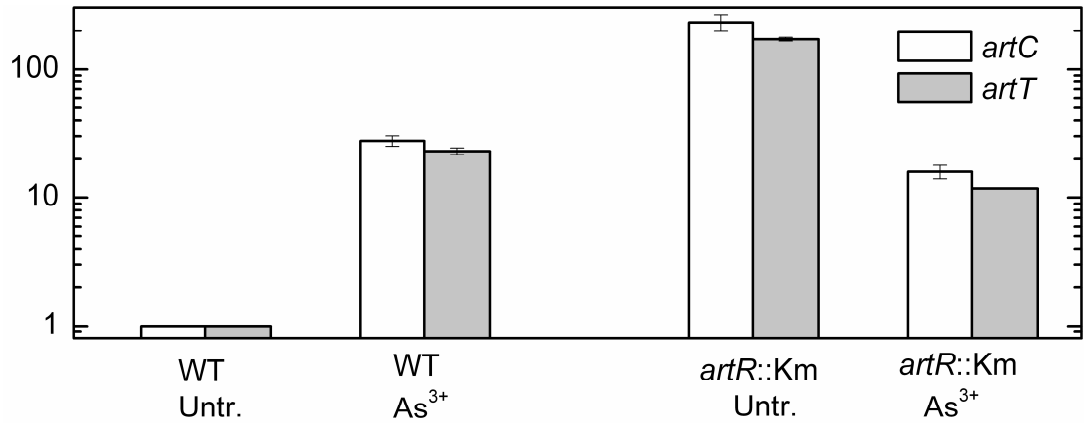

Figure 28. The expression of the *artC* and *artT* genes in WT and *artR*::Km cells following incubation with 4 mM As^{3+} for 24 h. The transcript levels relative to untreated cells (Untr.) of *artC* and *artT* genes were determined by qRT-PCR with the primers *arsC-F1/arsC-R1* and *artT-F1/artT-R1*.

5.5. Specific and generalized metal ion-induced responses

Even in bacteria that possess specific metal ion resistance mechanisms, excess concentrations of metal ions reach a "tilt" point beyond which homeostasis is perturbed and bacterial repair mechanisms cannot efficiently cope with the excess levels of ions within the cell and the secondary damage caused by them (Hobman et al. 2007). We aimed at detecting the border between the specific (primary) and the generalized (secondary) stress responses in *Synechocystis* for the following metal ions: Zn^{2+}, Cd^{2+}, Ni^{2+}, Co^{2+}, As^{3+}, and Cu^{2+}. To this end, we have selected specific inducible genes for each of these ions (except for Cu^{2+}, for which no specific upregulated gene was found; see Section 4.2.2.4.) and a set of general and oxidative stress-inducible genes (hereafter referred to as GO genes) from the literature (Table 5, Table 6), and their expression was tested in cells exposed for 2 h to increasing concentrations of metal salts. The highest tested concentration was close to IC_{max} (Table 2). A fixed threshold of 2.0 fold change was used for detecting substantial changes in gene expression. The results of this small scale investigation may prove valuable for those who study the specific metal ion-induced stress responses in *Synechocystis.*

Table 5. The response of GO genes upon exposure to oxidative stress (H_2O_2 or methyl viologen in the presence of light that facilitates the production of superoxide)

Gene: Function	Induction ratio
isiA: iron stress chlorophyll-binding protein	8.2 ± 5.4^{a}, 11.3^{b}
perR: transcription factor PerR	12 ± 2.2^{a}, 7^{b}, $2.63 \pm 0.24^{c^{o}}$, $4.29 \pm 0.19^{c^{*}}$
sigD: group2 RNA polymerase sigma factor	4.7 ± 0.5^{a}, 7.9^{b}
hspA: 16.6-kDa small Hsp	76.8 ± 17.4^{a}, 5.9^{b}
dnaJ: DnaJ-like protein	5.1^{b}
ahpC: AhpC-peroxiredoxin	13.4 ± 6.0^{a}, 13.1^{b}, $2.57 \pm 0.13^{c^{o}}$, $26.47 \pm 5.48^{c^{*}}$
lilA: light harvesting-like protein	131.3 ± 11.2^{a}, 9.1^{b}
nblA1: phycobilisome degradation protein NblA	18.1 ± 2.3^{a}, 4.2^{b}

a – 0.25 mM H_2O_2 for 20 min (Yu 2007)
b – 1.5 mM H_2O_2 for 30 min (Li 2004)
c – 10 μM methyl viologen for 15 min under conditions of normal light^{o} (50 μE m^{-2} s^{-1}) or high light* (200 μE m^{-2} s^{-1}) (Kobayashi 2004)

Note: the numbering of ORFs corresponding to the CyanoBase identifier is given in Table 3.

Table 6. The response of selected genes upon exposure to five types of stress factors in *Synechocystis*. Significant upregulation is marked by (+) (Los et al. 2008)

Gene	Stress factor				
	H_2O_2	Cold	Osmo	Salt	Heat
isiA	+				
perR	+				
sigD	+	+	+	+	
hspA	+		+	+	+
dnaJ	+				
ahpC	+				
lilA	+	+	+	+	
nblA1	+				

For investigating the specific response to Cd^{2+} we have chosen the *ziaA* gene that was previously shown to be specifically induced by Cd^{2+} and possibly involved in Cd^{2+} transport (see Section 4.2.2.1). After 2 h incubation with 2 µM Cd^{2+}, the *ziaA* transcript increased ~10 fold and remained at about the same level until 16 µM Cd^{2+} (Fig. 29, panel A). The GO gene transcripts were not upregulated by 2 µM Cd^{2+} (except the *isiA* transcript). Both *isiA* and *hspA* were moderately induced at 4 µM Cd^{2+}. At 8 µM Cd^{2+} four of the GO genes were induced, and 5 of them at 16 µM Cd^{2+}. We can say that the response to Cd^{2+} is specific until ~2 µM, and the general and oxidative stress response was triggered above 8 µM Cd^{2+} (Fig. 29, panel A). Similarly, the response to Ni^{2+} was specific at 5 µM, with *nrsB* being the only induced gene. At 10 µM and higher concentrations of Ni^{2+}, all GO genes except *ahpC* were upregulated (Fig. 29, panel B), indicating that the general stress response has already been induced in the cell. In the case of As^{3+}, the *arsB* gene was used as a marker of arsenite-specific response. We detected a specific response up to a concentration as high as 720 µM As^{3+}, and a generalized stress response (6 out of 8 GO genes induced) at 2 mM As^{3+} (Fig. 29, panel C). The expression of GO genes was below the significance threshold at 0.5 µM Cu^{2+}, and above it, at 1.25 µM Cu^{2+} and higher concentrations, for all GO genes except *isiA* (Fig. 29, panel D). Therefore, we can conclude that the general stress response already started at 1.25 µM Cu^{2+} and gradually increased in amplitude at higher concentrations of copper. Using *ziaA* and *coaT* as Zn^{2+}-specific indicators we have detected a specific response up to 8 µM Zn^{2+}, two of the GO genes moderately induced at 16 µM Zn^{2+}, and four of them highly

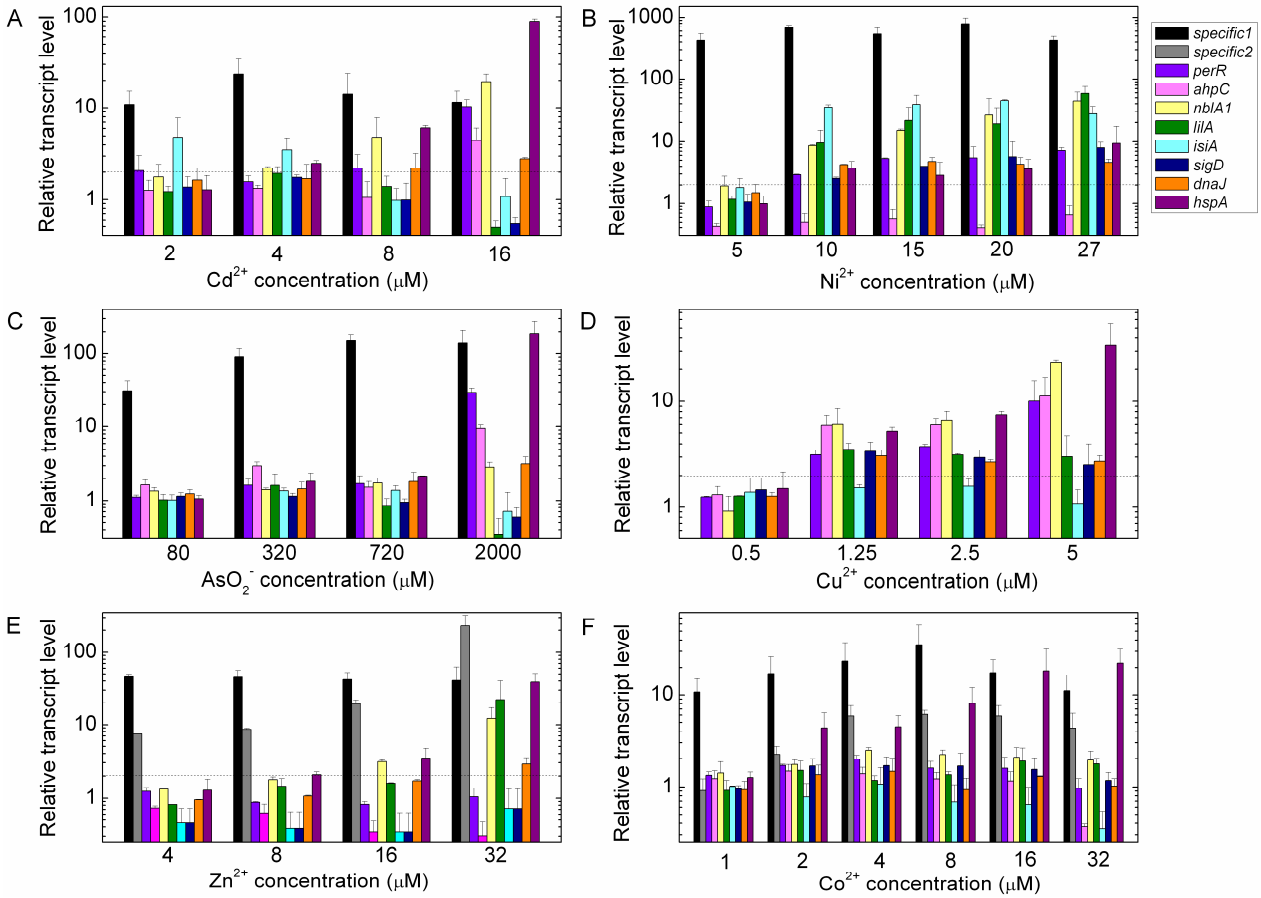

Figure 29. The metal ion-induced responses of selected oxidative stress-inducible genes. Specific inducible genes were chosen for each metal ion (except Cu^{2+}) and they are represented as black and gray columns as follows: A) *ziaA* (black), B) *nrsB* (black), C) *arsB* (black), E) *ziaA* (black) and *coaT* (gray), F) *coaT* (black) and *nrsB* (gray). Total RNA was isolated from mid-log-phase *Synechocystis* cells exposed for 2 h to the indicated concentrations of Cd^{2+} (A), Ni^{2+} (B), As^{3+} (C), Cu^{2+} (D), Zn^{2+} (E) and Co^{2+} (F). Control cells were not exposed to metal salts. One µg of total RNA was reverse transcribed and used as template for qRT-PCR with gene-specific primers (Table 1). The interrupted line indicates the fixed threshold of 2.0 for fold change that was used in this study to detect significant changes in gene expression. The experiments were performed on two independent occasions. Standard errors are indicated.

induced at 32 µM Zn^{2+} (Fig. 29, panel E). The Co^{2+}-specific response was investigated with *coaT* and *nrsB* as specific inducible genes. We found a specific response at 1 µM Co^{2+} where only the *coaT* gene is induced ~10 folds. At 2 µM Co^{2+}, *nrsB* is also slightly upregulated, together with *hspA* that is induced ~4 times. The *hspA* is the only GO gene whose expression was upregulated by the tested concentrations of Co^{2+} (Fig. 29, panel F). This is an indication that no serious general and oxidative stress response occurred even at the highest tested concentration of Co^{2+} of 32 µM.

An interesting finding of this study was that *hspA*, encoding a low molecular weight heat shock protein, was highly induced in response to all tested metal salts at concentrations close to IC_{max} (Fig. 29). Low molecular weight heat shock proteins (LMW-HSPs) are

molecular chaperones that bind and prevent aggregation of non-native proteins (Sakthivel et al. 2009). Like many prokaryotic LMW-HSPs, *hspA* is synthesized in response to a variety of stress factors (Section 1.8.). It was previously shown that the upregulation of chaperones is one of the earliest responses to $CdSO_4$ in *Synechocystis*, with *hspA* showing the highest transcript level (Houot et al. 2007). The HspA protein from *Synechococcus vulcanus*, that shows high homology in the N-terminal and internal amino acid sequences with *Synechocystis* HspA is also Cd^{2+}-inducible (Roy et al. 1999). The chloroplast homologs of the cyanobacterial LMW-HSPs were shown to protect photosynthesis during metal ion stress. Several experiments indicated that exposure to Cu^{2+}, Ni^{2+}, Pb^{2+}, and Zn^{2+} leads to increased chloroplast low molecular weight heat shock protein content in *Zea mays* (Heckathorn et al. 2004). In our experiments, As^{3+} and Cd^{2+} produced the highest induction of *hspA*, in accordance with their high sulphydryl reactivity and putative role in protein denaturation (Verbruggen et al. 2009).

The *nblA1* gene, whose induction was found to be necessary for phycobilisome degradation under nitrogen deprivation (Baier et al. 2001), was significantly induced in our experiments upon exposure to Ni^{2+} (~8 to 45-fold induction at 10 to 27 µM), Zn^{2+} (~3 to 12-fold induction at 16 and 32 µM, respectively) and Cu^{2+} (~6 to 22 fold induction at 1.25 to 5 µM). Using a *chlN* deletion mutant of *Synechocystis* as an experimental system for the study of the structure and function of PBSs in vivo, Liu and co-workers (2005) showed that H_2O_2 induced an obvious disassembly of the cores of PBSs, and also that among several tested metal salts ($AgNO_3$, $CaCl_2$, $CoCl_2$, $CrCl_2$, $CuSO_4$, $MnCl_2$, $NiSO_4$, or $ZnCl_2$) only silver ions induced disassembly of the cores of PBSs. Therefore, we are cautious in the interpretation of *nblA1* induction by Ni^{2+}, Zn^{2+} and Cu^{2+} as an indication of direct involvment in PBS degradation. Rather, we consider it an effect of intracellular oxidative stress triggered by these metal ions. There are studies in the literature that report the involvement of nickel, zinc and cadmium salts in oxidative stress generation (Drazkiewicz et al. 2004, Tripathi et al. 2006, Storni et al. 2007).

We also found a significant increase in the expression of the transcription regulator *perR*, upon incubation with As^{3+} (~30-fold induction at 2 µM), Cd^{2+} (~2 and 10-fold induction at 8 and 16 µM, respectively), Cu^{2+} (~3 to10-fold induction at 1.25 to 5 µM), and Ni^{2+} (~3 to 7-fold induction at 10 to 27 µM). PerR proteins function as the central regulators of the inducible peroxide stress response (see Section 1.8.). *Synechocystis* PerR is a Fur-type transcriptional regulator that is induced by H_2O_2 (Kobayashi et al. 2004) and was also shown to mediate Cd^{2+}-elicited toxic effects, such as the breakdown of the photosynthetic machinery (Houot et al. 2007). Here we show that besides Cd^{2+}, *perR* is induced by As^{3+}, Co^{2+}, and Ni^{2+}.

Wheather the response is directely induced by the metal ions or is a consequence of a secondary oxidative stress effect remains an open question. The homolog gene from *B. subtilis* is regulated by both peroxide and metal ions (manganese or iron; Herbig and Helmann 2001, Fuangthong et al. 2002).

The *ahpC* gene that encodes a peroxiredoxin from the AhpC/TSA family was induced by cadmium (~4-fold induction at 16 µM), arsenite (~10-fold induction at 2 mM), and copper salts (~6 to 10-fold induction at 1.25 to 5 µM Cu^{2+}). The *ahpC* gene is located next to *perR* in the genome and they share a divergent promoter that is thought to be regulated by the PerR repressor (Kobayashi et al. 2004). In our experiments the two genes are concomitantly induced by Cd^{2+}, As^{3+} and Cu^{2+}, but show different patterns of expression upon incubation with 10 to 27 µM Ni^{2+}, with *perR* being moderately induced (~3 to 7-fold induction), while *ahpC* is repressed. This finding suggests that additional transcriptional regulators, besides PerR, may play a role in the regulation of the *ahpC* and *perR* genes.

The *dnaJ* gene, encoding a putative chaperone, was moderately induced by all tested metal salt except Co^{2+}, as follows: ~3-fold induction by 8 µM and 16 µM Cd^{2+}, ~4-fold induction by Ni^{2+} at 10 µM to 27 µM, ~3-fold induction by 2 mM As^{3+}, ~3-fold induction by Cu^{2+} at 1.25 µM to 5 µM, ~3-fold induction by 32 µM Zn^{2+} (Fig. 29). The gene was previously shown to be moderately upregulated by the addition of iron to iron-deficient cells (Singh et al. 2003) and by cadmium ions (Huout et al. 2007).

An interesting finding was the strong induction of *isiA* following incubation with Ni^{2+} (~40-fold between 10 and 27 µM Ni^{2+}). Previously *isiA* was shown to be highly induced under iron deficiency (Singh et al. 2003, DeRuyter and Fromme 2008) but also in response to various other stress factors (see Section 1.8.). Using a DNA microarray, Singh and co-workers (2003) have shown that in *Synechocystis* cells grown in low-iron medium the *isiA* gene displayed the largest (22-fold) transcriptional increase increase. Complexes consisting of an 18-mer ring of chlorophyll-binding IsiA molecules around a PSI trimer were discoverd in such conditions (Bibby et al. 2001, Boekema et al. 2001). Here we show a higher Ni^{2+}-triggered direct or Ni^{2+}-elicited oxidative stress-mediated induction in the expression of *isiA*, but in the same order of magnitude as the induction produced by iron starvation. It is possible that IsiA rings form around the trimeric PSIs not only under iron-starvation, but also in the presence of excess of nickel ions. Moderate upregulation of *isiA* was also found at 2 µM and 4 µM Cd^{2+} (~4-fold induction), but surprisingly not at the higher concentrations tested (8 and 16 µM). Houot and co-workers (2007) also found that many of the high light-inducible genes were also upregulated by Cd^{2+}, including *isiA*, suggesting that Cd^{2+}-exposed cells become light sensitive and possibly more prone to oxidative stress.

The *sigD* gene that encodes a primary-like sigma factor (Pollari and Tyystjärvi 2007) was highly induced in our experiments upon exposure to Ni^{2+} (~2.5 to 10-fold induction at 10 to 27 µM) and moderately following incubation with Cu^{2+} (~3-fold induction at 1.25 to 5 µM Cu^{2+}). The transcription factor *sigD* is a non-essential primary-like sigma factor (Pollari and Tyystjärvi 2007) that was shown to be upregulated by high light (Hihara et al. 2001), inorganic carbon limitation (Wang et al. 2004) and H_2O_2 (Li et al. 2004, Yu et al. 2007). Here we show that it is also induced by Ni^{2+} and Cu^{2+}.

The expression of a light harvesting-like protein-encoding gene *lilA* (Kufryk et al. 2008) with the highest H_2O_2-induced expression in the microarray study of Yu and co-workers (2007), showed a high increase in the transcript level upon incubation with Ni^{2+} (~10 to 60-fold induction at 10 to 27 µM) and Zn^{2+} (~20 fold-induction by 32 µM), and moderately by exposure to Cu^{2+} (~3-fold at 1.25 to 5 µM). The *lilA* gene was previously shown to be induced by H_2O_2 (Li et al. 2004, Yu et al. 2007), cold (Suzuki et al. 2001), osmotic (Mikami et al. 2002) and salt stress (Marin et al. 2003).

Not much is known about the transcriptional responses elicited by excess amount of metal ions in cyanobacteria. For the model species *Synechocystis*, only a single DNA microarray study, investigating Cd^{2+}, Zn^{2+} and Fe^{2+}-induced modification in gene expression, was published to date (Houot et al. 2007). Here we show the transcriptional changes found in a set of selected stress-inducible genes, trying to find the border between specific and general stress responses for several metal ions. The data contain interesting findings, such as Ni^{2+}-inducibility of the gene encoding the chlorophyll-binding IsiA protein, or the upregulation of the chaperone gene *hspA* at high concentrations of all tested metal salts. And last, but not least, the similar pattern of induction found in GO genes at the highest concentrations of Cd^{2+} and As^{3+} indicates the possibility that *Synechocystis* employs similar mechanisms for coping with excess Cd^{2+} and As^{3+}. For all the other investigated metal ions, we encountered relatively different pattern of GO gene expression, suggesting that the cells handle their excess in different ways.

6. Conclusions

1) The *arsB, nrsB, coaT* and *ziaA* genes were induced by pairs of ions. We found that a pronounced gene induction generally occurred within 15 min of exposure, and the expression pattern did not change significantly for the next 45 min. The characteristics of *arsB, nrsB, coaT,* and *ziaA* genes induction following 2 h exposure to concentrations that belong to the (IC_{min}-IC_{max}) interval are summarized below: We found that besides the known

Gene name	Metal ion	Maximal level of induction (approximate fold induction)	Interval of concentration corresponding to maximal induction
arsB	As^{3+}	1000	500-3500 µM
	As^{5+}	80	2-47 mM
nrsB	Ni^{2+}	700	1-27 µM
	Co^{2+}	5	4-32 µM
coaT	Zn^{2+}	300	32 µM
	Co^{2+}	20	2-32 µM
ziaA	Zn^{2+}	45	2-16 µM
	Cd^{2+}	13	2-16 µM

Zn^{2+}-inducibility, Cd^{2+} is also a strong inducer of the *ziaA* gene and we propose that ZiaA ATP-ase transports Cd^{2+} as well, in addition to Zn^{2+}. The transcripts of the *ctaA, pacS* and *atx1,* all supposed to play a role in copper transport and chaperoning, did not significantly changed during short time incubation with concentrations of Cu^{2+} that belong to the interval (IC_{min}-IC_{max}). Therefore, the expression of *pacS* seems to be regulated differently than that of its homolog gene from *Synechococcus,* whose transcript and protein product levels were specifically increased upon addition of copper to the growth medium

2) We have characterized, optimized and shown the potential applications of two whole-cell bioluminescent reporters previously constructed in our laboratory, namely *coaLux* and *nrsLux*. The detection range of *coaLux* bioreporter was 0.3-6.4 µM for Co^{2+} and 1-3.2 µM for Zn^{2+}. In a soil-like mixture of different chemical and oil industry wastes, the *coaLux* reporter strain detected about 92 % of the AAS determined Zn^{2+} concentration of the sample. The second reporter strain, *nrsLux* had a detection range of 0.2-8 µM Ni^{2+} and is the first Ni^{2+}-specific whole cell reporter published to date with a clear dose-signal relationship. This reporter is potentially useful in the development of a bioreporter for Ni^{2+} detection in drinking

water. Aditionally, we created an As^{3+}/As^{5+}-responsive bioreporter, designated *arsLux*. It responded to As^{3+} and As^{5+} in very different concentration ranges. The bioluminescent response was linearly dependent of the amount of As^{3+} from 8 µM to 500 µM. With further optimization for improving its sensitivity, the *arsLux* bioreporter can be applied for arsenic detection in such waters.

3) We have shown that the *artT* gene that encodes a putative chromate transporter from the CHR superfamily is cotranscribed with the neigbouring *artC* gene and both are under the regulation of the ArtR repressor. We found that *artCT* is upregulated by long-term sulfate limitation, by chromate exposure in cells grown on low sulfate medium, as well as by As^{3+}. This is the first As^{3+}-inducible CHR gene described to date. The *artT*::Km strain was more resistant to As^{3+} than the WT strain, as well as to chromate when grown in low sulfate medium. The *artR*::Km strain was more sensitive than the WT when exposed to As^{3+}. Together these lines of evidence suggest that the protein encoded by *artT* may work as a chromate/sulfate antiporter. Wether ArtT transports As^{3+} as well, remains an open question.

4) We established the concentrations for several metal ions to which *Synechocystis* cells respond specifically to the ion excess, as well as the concentration to which general and oxidative stress responses occur. The results are summarized below. No substantial stress

Metal ion	Specific response	General and oxidative stress response
Cd^{2+}	2 µM	8 µM
Ni^{2+}	5 µM	10 µM
As^{3+}	80-720 µM	2 mM
Zn^{2+}	4 µM	16 µM
Co^{2+}	1 µM	–
Cu^{2+}	–	1.25 µM

response has occurred below the highest tested concentration of 32 µM Co^{2+}. The small heat shock protein-encoding hspA was highly induced by all tested metal ions at concentrations close to IC_{max}. The gene that encodes the chlorophyll-binding protein IsiA, previously shown to be activated by iron deficiency, was also induced by Ni^{2+}.

Acknoledgements

"I am a part of all that I have met"
Alfred, Lord Tennyson

First of all I want to thank my supervisor, Imre Vass, for his continuous support and patience. His task-oriented, rigorous and orderly work style had a great influence on me. I am also grateful to him for the opportunities to attend many conferences and workshops during my doctoral studies. Unlike most of the Ph.D. fellows, I've been fortunate to have a second supervisor, Péter Kós. Not only he did teach me laboratory work, he encouraged me to find the answers by myself and to believe in my own potential.

Many people brought their contributions to the present work. The strain of *Synechocystis* that constitutively express the bacterial luciferase substrate used in this study was generated by Zoltán Máté by inserting the *luxAB* genes in a vector backbone obtained from Susan Golden. He also constructed the pND6luxAB insertion vector, by using a vector backbone constructed by Mihály Kis (unpublished data). The *coaLux*, *nrsLux* and *ziaALux* bioreporters were generated by Zoltán Máté, as well. The *artT*::Km and *artR*::Km mutants were generated by Csaba Nagy and Péter Kós. The quantitative real-time data from Figure 33 were measured by Barbara Blasi. I would like to acknowledge all of them.

I am grateful to Zóltán Gombos and Miklós Szekeres for carefully reviewing the manuscript of my thesis and to Boglarka Csiszar, Istvan Vass and Csaba Nagy for translating the thesis abstract in Hungarian.

Many thanks goes to Éva Hideg for teaching me Eskrima, to Zsuzsanna Deák and Márta Dorogi for keeping the door of their office wide open for me, to Gabriella Fleit and Erzsébet Bárdosi, for all their affective and technical assistance in the lab, and to Mariann Károlyi for her help with all the difficulties I've been having as a non-Hungarian speaker.

Thanks to many ITC and Ph.D. students of various nationalities for making my stay at BRC enjoyable: Özge Sözer, Radek Kana, Boglarka Csiszar, Leyla Abasova, Otilia Cheregi, Oana and Cosmin Sicora, Ina Rus, Ana-Maria Pilbat, Kinga Klodawska, Engin Boynik, Zoltan Turoczy, Milan Szabo, Bhavyashree Suresh, András Fülöp, Sashka Krumova, Ibolya Stiller, Jan Rodewald, Emine Dinç, Ping Yu, Himabindu and Vamsi Krishna Gali, Mary and Badri Prashad, Giorgia Carletti, Hajnalka Laczko-Dobos, Enikő Molnár, János Kelemen, Erika Bereczki, Éva Korpos, Manuela Jurca, Hajnalka Viragh, Miroslava Zhiponova, Gabriela Ion, Szilvia Bajkán, Éva Kiss, Özge. Gündüz Çınar and Resat Cinar, Iva Šnyrychová

and Hongyan Wu. The multicultural atmosphere made me more aware of the constants of our nature, in spite of the many cultural differences.

My gratitude also goes to several people that helped me to find a “home away from home”: Maria Garvra and Stefan Gencărău from the Romanian Language and Literature Department of Juhász Gyula College, Katalin Bihari Kimpiánné, my French teacher from the University of Szeged, Radu Florea and Razvan Ciolcă from the Romanian Consulate and Zsuzsánna Máté and Ádám Lukács from the Romanian Cultural Institute.

Finally, but most importantly, I will like to thank to Chris and to my family for their unconditional support over all these years.

Summary of the PhD thesis

INTRODUCTION

Metal[1] pollution is a quickly growing problem for the aquatic and terrestrial ecosystems. Organisms must tightly control intracellular metal ion levels to avoid toxicity. Toxicity is a result of excessive accumulation of essential metal ions, or a consequence of over-accumulation of metal ions with no biological function.

All organisms possess resistance mechanisms for protection against the excess of metal ions, involving proteins encoded by chromosomal or plasmid-located genes. They are believed to have arisen soon after life began, in a biosphere polluted by volcanic activities and other natural geological sources [Silver and Phung (1996) *Annu Rev Microbiol* 50: 753]. The main mechanisms of resistance are: efflux 'pumping' of the toxic ions that enter the cell, enzymatic detoxification that converts more toxic to less toxic or less available metal ion species, and intracellular sequestration of the toxic metal ions. These processes are usually regulated by metalloregulatory proteins of either the MerR or ArsR/SmtB families.

Analysis of the fully sequenced *Synechocystis* genome [Kaneko et al. (1996) *DNA Res* 3: 10] led to the identification of 11 clustered chromosomal ORFs that encodes homologs of metal transport proteins. The region is organized into six putative transcriptional units: *(i*) the *nrsBACD* operon induced by Ni^{2+} and Co^{2+} and regulated by the upstream *nrsSR* operon products [García-Dominguez et al. (2000) *J Bacteriol* 182: 1507; López-Maury et al. (2002) *Mol Microbiol* 43: 247], (ii) *ziaA*, induced by Zn^{2+}, encoding a putative Zn^{2+} efflux P_1-type ATPases and regulated by the product of the preceding ORF, *ziaR* [Thelwell et al. (1998) *PNAS* 95: 10728], and (iii) *coaT*, induced by Co^{2+} and Zn^{2+}, encoding a putative Co^{2+} translocating P_1-type ATPase under the regulation of the upstream *coaR* product [Rutherford et al. (1999) *J Biol Chem* 274: 25827; García-Dominguez et al. (2000) *J Bacteriol* 182: 1507]. The resistance to arsenic salts in *Synechocystis* is exerted by the protein products of the *arsBHC* operon. The operon is induced by $As^{5+}/As^{3+}/Sb^{3+}$ and its expression is under the regulation of the ArsR repressor protein. Besides CoaT and ZiaA, *Synechocystis* has two more P_1-type ATPases, CtaA and PacS that are putative copper cation transporters localized in the plasma membrane and thylakoid membrane, respectively [Tottey et al. (2001) *J Biol Chem* 276: 19999]. Atx1 is a metallochaperone which interacts with the amino-terminal domains of CtaA and PacS and might play a role in chaperoning Cu^{2+} en route to the

[1] For simplicity, throughout this summary, the term metal refers to both metal and semimetal

thylakoid [Borelly et al. (2004) *Biochem J* 378: 293; Tottey et al. (2002) *J Biol Chem* 277: 5490].

In the *Synechocystis* genome there are two ORFs that encode members of the chromate ion transporter (CHR) superfamily [Díaz-Pérez et al. (2007) *FEBS J* 274: 6215]: *slr5038*, located on the pSYSM plasmid, and the chromosomally encoded *chrA*. The function has been elucidated only for two members of this superfamily. They are membrane proteins that pump out chromate from the cytoplasm using the proton motive force, conferring in this way chromate resistance [Alvarez et al. (1999) *J Bact* 181: 7398; Pimentel (2002) *FEMS Microbiol Lett* 212: 249]. Another member of this superfamily, SrpC from *Synechococcus* sp. PCC 7942, is encoded on the plasmid pANL that was shown to be involved in cell adaptation to sulfur starvation. The *srpC* disruption mutant showed an increase, rather than a decrease, in chromate resistance, when grown in low sulfate medium [Nicholson and Laudenbach (1995) *J Bact* 117: 2143]. A hypothesis was formulated that CHR proteins perform chromate/sulfate antiport: they change the intracellular accumulated chromate for sulfate from the growth environment; when the sulfate concentration in the growth environment is occasionally lower than the chromate concentration, the antiporter works as a chromate uptake system, therefore explaining the chromate resistance phenotype of the *srpC* disruption mutant [Nies (1998) *J Bact* 180: 5799].

In the last two decades, bacterial resistance mechanisms against various metal ions have been used to construct whole-cell bioreporters. These are genetically modified living bacteria, which express molecular fusions of regulatory circuits operated by metal ions with reporter genes encoding easily detectable proteins. Hence, they are able to sense the metal ions in their environment, representing an alternative to traditional analytical chemical methods. Their greatest advantage is the ability to detect the bioavailable fraction (rather than total concentration) of an analyte, allowing for more accurate assessment of polluted sites. Photoautotrophic cyanobacteria represent an advantage over the use of heterotrophic microorganisms because they can grow on low-cost media and require little maintenance. Because *Synechocystis* is naturally transformable and its full genomic sequence is available, it represents a suitable organism for whole-cell bioreporter construction.

OBJECTIVES

The main goals of our studies were to

I. Investigate the changes in transcript level for genes that were demonstrated, or suggested to be involved in metal ion transport in the cyanobacterium *Synechocystis*, following a short exposure to concentrations close to IC_{min} of the following metal ions: Co^{2+}, Zn^{2+}, Ni^{2+}, Cd^{2+}, Cr^{3+}, Cr^{6+}, As^{3+} and As^{5+}.

II. Characterize the activity of two whole-cell bioluminescent reporters that were previously generated in our laboratory by fusing the Co^{2+}/Zn^{2+} inducible $O/P_{\boldsymbol{coaT}}$ (the operator-promoter region of the *coaT*) or the Ni^{2+} /Co^{2+} inducible $O/P_{\boldsymbol{nrsBACD}}$, with the promotorless *luxAB* reporter genes, and to test their application to environmental samples. Generate an arsenic bioreporter on the same principle using the $As^{3+}/As^{5+}/Sb^{3+}$-inducible $O/P_{\boldsymbol{arsBHC}}$.

III. Investigate the function and regulation of the *slr5038* gene that encodes a putative chromate transporter, and was shown by us to be induced by As^{3+} and also by Cr^{6+} when the cells were grown in low sulfate medium.

IV. Find the concentration ranges for Cd^{2+}, Ni^{2+}, As^{3+}, Zn^{2+}, Co^{2+}, and Cu^{2+} in which *Synechocystis* cells respond specifically to the ion excess, as well as the concentration ranges in which general and oxidative stress responses occur.

METHODS

Growth conditions and metal salt treatment

The Synechocystis sp. PCC 6803 wild-type and its mutant derivatives were grown in BG-11 medium [Rippka et al. (1979) *J Gen Microbiol* 111: 1] supplemented with 20 mM HEPES (pH 7.5). The cell cultures were maintained in an incubator at: 30 °C, 120 rpm rotation speed, 3% CO_2, 40 µmol photons m^{-2} s^{-1}. When appropriate, antibiotics were included in the medium. The treatments were carried out in BG-11 medium supplemented with $ZnSO_4$, $CdCl_2$, $NiCl_2$, $CoCl_2$, $NaAsO_2$, KH_2AsO_4, $CuSO_4$, $Cr_2(SO_4)_3$ or Na_2CrO_4.

Growth inhibition caused by excess metal ions

The growth of cyanobacterial cultures was quantified by measuring the optical density at 720 nm for a period of 3 to 4 days. Two inhibition parameters were determined for each metal ion: minimal inhibitory concentration (IC_{min}) and maximal inhibitory concentration (IC_{max}). The IC_{min} refers to the lowest tested concentration leading to growth inhibition, whereas IC_{max} refers to the highest tested concentration where no further growth was observed.

Nucleic acid extraction and quantitative real-time PCR analysis

Total RNA was isolated from *Synechocystis* cultures by the hot phenol method [Mohamed and Jansson (1989) *Plant Mol Biol* 13: 693]. The reverse transcription and the quantitative real-time PCR were performed following the instructions provided by High Cappacity cDNA Reverse Transcription Kit and Power SYBR Green PCR Master Mix (Applied Biosystems). Oligonucleotides were designed using Primer Express 2.0 software (Applied Biosystems). The relative changes in gene expression were calculated using delta-delta C_T method [Applied Biosystems (2001) User Bulletin #2: 11] and were normalized to the expression of the RNase P subunit B-encoding *rnpB* gene as internal standard.

Generation of bioreporters

Two bioluminescent bioreporters, *nrsLux* and *coaLux* were previously generated in our laboratory [Peca et al. (2008) *FEMS Microbiol Lett* 289: 258]. For generation of the *arsLux* bioreporter, a sequence upstream of the *arsBHC* coding region containing the O/P_{arsBHC} and the 5' end of *sll0914* was ligated upstream of the promoterless *luxAB* luciferase genes, in the vector pND6luxAB. The constructs were used for the transformation of a *Synechocystis* strain harboring the *luxCDE* luciferase substrate genes along with a spectinomycin resistance

casette. The constructs were integrated into the chromosome, along with a chloramphenicol resistance cassette, via homologous recombination in the neutral site *ssl0410*.

Bioluminescence assay

Metal salt treatments were carried out in 96-well black microtiter plates in a volume of 300 µL per well. The plates were incubated for 3 h, or 18 h in the case of *arsLux* reporter strain, in light (40 photons µmol m^{-2} s^{-1}) or darkness. Luminescence intensity was determined with a Top Count NXT luminometer (Packard Instruments).

Acidic extraction of environmental sample

The soil-like material used for this study consists of a mixture of different chemical and oil industry wastes from a bauxite residue disposal area. Samples collected from the composting piles were dried and passed through a 2-mm sieve. To assess the exchangeable, acid-soluble fractions of Ni^{2+}, Co^{2+} and Zn^{2+}, one-step acetic acid extraction of the material was carried out according to [Bódog et al. (1996) *Int J Environ An Ch* 66:79]. The metal content was determined using an atomic absorption spectrometer (Perkin-Elmer model 3110).

RESULTS

I. Searching for potential promoters for bioreporter construction, we selected ORFs that encode for proteins which have been demonstrated or suggested to be involved in metal ion transport in the cyanobacterium *Synechocystis*, as follows: (i) genes encoding P_1-type ATPases that transport Zn^{2+} (*ziaA*), Co^{2+} (*coaT*) and Cu^{2+} (*ctaA, pacS*), (ii) *atx1* that encodes a copper chaperone, (iii) *slr5038* (designated by us as *artT*) and *chrA* that encode members of the chromate ion transporter (CHR) superfamily, (iv) *nrsB* whose protein product is a putative Ni^{2+} efflux transporter, and (v) *arsB,* encoding a putative As^{3+} exporter. We investigated the induction pattern for these genes by quantitative real-time PCR, upon incubation with concentrations falling between IC_{min} and IC_{max} of the following metal ions: Co^{2+}, Zn^{2+}, Ni^{2+}, Cd^{2+}, Cr^{3+}, Cr^{6+}, As^{3+} and As^{5+}. We found that a pronounced gene induction generally occurred within 15 min of exposure, and the expression pattern did not change significantly for the next 45 min. The characteristics of *arsB, nrsB, coaT* and *ziaA* gene induction are summarized below. We found that besides the known Zn^{2+}-

Gene name	Metal ion	Peak level of induction (approximate fold induction)	Interval of concentration corresponding to peak induction
arsB	As^{3+}	1000	500-3500 µM
	As^{5+}	80	2-47 mM
nrsB	Ni^{2+}	700	1-27 µM
	Co^{2+}	5	4-32 µM
coaT	Zn^{2+}	300	32 µM
	Co^{2+}	20	2-32 µM
ziaA	Zn^{2+}	45	2-16 µM
	Cd^{2+}	13	2-16 µM

inducibility, Cd^{2+} is also a strong inducer of the *ziaA* gene. Since P_1-type ATP-ases commonly have high specificity for metal ions which they transport [Liu et al. (2002) *J Bacteriol* 184: 5027], we think it is likely that ZiaA ATP-ase transports Cd^{2+} as well, in addition to Zn^{2+}.

The transcripts of the *ctaA*, *pacS* and *atx1,* all supposed to play a role in copper transport and chaperoning, did not significantly changed during short time incubation with concentrations of Cu^{2+} that belong to the interval (IC_{min}-IC_{max}). Therefore, the expression of *pacS* seems to be regulated differently than that of its homolog gene from *Synechococcus*,

whose transcript and protein product levels were specifically increased upon addition of copper to the growth medium [Kanamaru et al. (1994) *Mol Microbiol* 184: 5027].

II. We have characterized, optimized and shown the potential applications of two whole-cell bioluminescent reporters previously constructed in our laboratory, namely *coaLux* and *nrsLux*. Both the *coaLux* and *nrsLux* strains showed a dose-dependent response to the metal salts added to the culture medium. The detection range of *coaLux* bioreporter was 0.3–6.4 µM for Co^{2+} and 1–3.2 µM for Zn^{2+}. The shape of the concentration-dependent luminescence response for Zn^{2+} and the detection range are similar to those obtained with the cyanobacterial sensor based on *Synechococcus smt-luxCDABE* transcriptional fusion [Erbe et al. (1996) *J Ind Microbiol* 17: 80]. The application of the *coaLux* bioreporter for Zn^{2+} detection has been tested using a polluted soil-like sample material collected from a composted mixture of different chemical and oil industry wastes. The *coaLux* reporter strain detected about 92 % of the concentration of zinc determined by atomic absorption spectrometry.

The detection range of *nrsLux* bioreporter was 0.2–8 µM Ni^{2+}. Since zinc and nickel pollution coexist in many sites, the performance of the *nrsLux* reporter strain in mixed samples was tested using Ni^{2+} and Zn^{2+} salt standards. We found that the half maximal inhibitory concentration of Zn^{2+} (IC_{50}) on the Ni^{2+} induced bioluminescence response is about 6 µM. The detection range of *nrsLux* matches the upper nickel concentration limit admitted in the drinking water specified by WHO's Guidelines for Drinking-water Quality (0.07 mg/L = 1.19 µM). Therefore the *nrsLux* bioreporter presented here is potentially useful for Ni^{2+} detection in drinking water, with the limitation that the accompanying zinc concentration is relatively low. Since zinc concentration in tap water is seldom above 0.15 µM, i.e. about 70 times less than IC_{50} for Zn^{2+}, this is not a serious drawback. The luminescence response of the *coaLux* and *nrsLux* bioreporters was also evaluated in darkness. Under this condition the luminescence peak was shifted to about 4 times higher concentrations of Co^{2+} and Zn^{2+} in the *coaLux* bioreporter, accompanied by a reduction of the maximal extent of luminescence value to approximately 65% and 50% of the respective values obtained after incubation in light. On the contrary, the *nrsLux* reporter strain did not show any luminescence when incubated in darkness with the tested concentrations of Ni^{2+}. The cause remained elusive.

We created an As^{3+}/As^{5+}-responsive bioreporter, designated *arsLux*. It responded to As^{3+} and As^{5+} in very different concentration ranges. The bioluminescent response was linearly dependent of the amount of As^{3+} from 8 µM to 500 µM. In the case of As^{5+}, the bioluminescent signal increased slowly from 2.3 mM to 10 mM As^{5+} and then at a higher rate up to 150 mM As^{5+} (the highest concentration tested). Arsenic is a frequent contaminant of

the groundwater, sometimes at concentrations that greatly exceed the WHO drinking water quality limit for arsenic ions of 10 µg/l (0.13 µM). An example is the water from about 11 Hungarian settlements, that contains arsenic levels higher than 0.65 µM [Jones et al. (2008) *Rev Environ Contam Toxicol* 197: 163], up to 7.3 µM [Csalagovics (1999) *Annu Rep Geol Inst Hung II*: 85]. With further optimization for improving its sensitivity, the *arsLux* bioreporter could be applied for arsenic detection in such waters.

III. We have shown that the *artT* gene that encodes a putative chromate transporter from the CHR superfamily is cotranscribed with the neigbouring *slr5037* gene (designated by us as *artC*), which encodes a conserved, hypothetical protein. Upstream of the *artCT* operon and transcribed in the opposite direction, there are *sll5036* and *sll5035* genes (designated by us as *artS* and *artR*, respectively), encoding a putative sulfide-quinone reductase and a putative SmtB/ArsR family metalloregulatory transcriptional repressor, respectively. Due to the involvement of this class of transcriptional repressors in metal ion sensing, the proximity of *ArtR* to the *artCT* operon and their opposite orientation, we have hypothesized that the *artR* gene encodes a repressor that regulates the expression of the *artCT* operon. Disruption mutants were generated in our laboratory by cloning a kanamycin resistance marker into *artR* and *artT* genes. The *artR*::Kan strain showed a constitutive derepression of the O/P_{artCT}, partially confirming our hypothesis.

We found that the *artCT* operon was induced by chromate exposure when when grown in BG-11 that contains low levels of sulfate (10 µM), as well as by As^{3+}. The *artT*::Kan strain was more resistant to As^{3+} than the wild type, as well as to chromate when grown in BG-11_{-S} that contains 1µM sulfate (300 times less than normal BG-11). The *artR*::Kan disruption mutant was more sensitive than the wild type when exposed to As^{3+}. Taken together, these lines of evidence suggest that the protein encoded by *artT* works as a chromate/sulfate antiporter. At low sulfate concentrations the antiporter works as a chromate uptake system, therefore explaining the chromate resistance phenotype of the *artT* disrupted mutant. Weather ArtT is also able to transport As^{3+} remains an open question. The genomic context suggests that CHR proteins possess other physiological functions in addition to chromate transport (2007) [Díaz-Pérez et al. (2007) *FEBS J* 274: 6215].

IV. We established the concentration ranges for Cd^{2+}, Ni^{2+}, As^{3+}, Zn^{2+}, Co^{2+}, and Cu^{2+} in which *Synechocystis* cells respond specifically to the ion excess, as well as the concentration ranges in which general and oxidative stress responses occur. We investigated the transcriptional changes of specific inducible genes for each of these ions (except for Cu^{2+}, for which no specifically induced gene is known), and the following oxidative or general stress-inducible genes, chosen from the literature (as markers of general and oxidative stress): *isiA*

(iron stress chlorophyll binding protein), *perR* (transcription regulator Fur family), *sigD* (group2 RNA polymerase sigma factor), *hspA* (16.6-kDa small heat shock protein), *dnaJ* (DnaJ-like protein), *ahpC* (AhpC-peroxiredoxin), *lilA* (light harvesting-like protein), and *nblA1* (phycobilisome degradation protein). The results are summarized below. No

Metal ion	Specific response	General and oxidative stress response
Cd^{2+}	2 µM	8 µM
Ni^{2+}	5 µM	10 µM
As^{3+}	80-720 µM	2 mM
Zn^{2+}	4 µM	16 µM
Co^{2+}	1 µM	–
Cu^{2+}	–	1.25 µM

substantial stress response has occurred until the highest tested concentration of 32 µM Co^{2+}. The small heat shock protein-encoding hspA was highly induced by all tested metal ions at concentrations close to IC_{max}. The gene that encodes the chlorophyll-binding protein IsiA, previously shown to be activated by iron deficiency [Singh et al. (2003) *Plant Physiol* 132: 1825], was also induced by Ni^{2+}.

LIST OF PUBLICATIONS

Peca L, Kós PB, Vass I (2007) Characterization of the activity of heavy metal-responsive promoters in the cyanobacterium *Synechocystis* PCC 6803. *Acta Biol Hung* 58: 11-22.
IF: 0.688

Peca L, Kós PB, Máté Z, Farsang A, Vass I. (2008) Construction of bioluminescent cyanobacterial reporter strains for detection of nickel, cobalt and zinc. *FEMS Microbiol Lett* 289: 258-264.
IF: 2.021

(these publications are directly related to the subject of the thesis)

POSTER PRESENTATIONS

Peca L, Kós PB, Vass I (2006) Regulation of zinc, cobalt and chromium responsive genes in the cyanobacterium *Synechocystis* PCC 6803. 12th International Symposium on Phototrophic Prokaryotes. Pau, France, Aug. 27- Sept. 1st.

Peca L, Kós BP, Vass I (2008) Development and utilisation of two bioluminescent reporter strains of *Synechocystis* PCC 6803 for detection of Ni^{2+}, Co^{2+} and Zn^{2+} contaminants. ESF-EMBO Symposium - Molecular Bioenergetics of Cyanobacteria: Towards systems biology level of understanding, San Feliu de Guixols, Spain, March 29-April 3rd.

ORAL PRESENTATIONS

Peca L (2005) Quantitative analysis of *Synechocystis* sp. PCC 6803 gene expression in heavy metal stress. Genomics and Bioinformatics: Exploiting Microarrays in Plant Physiology, European Networking Summer School, Ljubljana, Slovenia, 22-31 August

Peca L (2005) Quantitative analysis of *Synechocystis* sp. PCC 6803 gene expression in heavy metal stress. EMBO Practical Course on Analysis and Informatics of Microarray Data, Cambridge, UK, 3-9 April

Phd tézis összefogalása

BEVEZETŐ

A fémszennyezés napjaink egyre növekvő problémája, mely mind a vízi, mind a szárazföldi ökoszisztémákat érinti. A fémionok toxikus hatása a sejten belüli, biológiailag inaktív, használhatatlan fémionok túlzott felhalmozódásának eredménye. Az élő szervezetek ezt a sejten belüli ionszintek szigorú szabályozása révén igyekszenek elkerülni.

Minden élő szervezet rendelkezik a fémionok felhalmozódása ellen védelmet nyújtó rezisztencia mechanizmusokkal. Ezen mechanizmusok feltehetőleg az élet megjelenését közvetlenül követően alakulhattak ki, a mainál sokkal élénkebb vulkanikus aktivitás és egyéb geológiai folyamatok mellett [Silver és Phung (1996) *Annu Rev Microbiol* 50: 753]. A fő rezisztencia mechanizmusok: a sejtbe jutó toxikus ionok efflux pumpák által történő kijuttatása illetve az enzimatikus detoxifikáció, melynek során a sejten belüli toxikus fémionok átalakulnak kevésbé toxikus változatokká. E folyamatok szabályzását általában a MerR vagy ArsR/SmtB családba tartozó, fémszabályzó (fémregulátor) fehérjék végzik.

A *Synechocystis* genomjának elemzése során [Kaneko et al. (1996) *DNA Res* 3: 10] tizenegy egymással szomszédos elhelyezkedésű gént azonosítottak, melyek fémtranszport fehérjék homlógjait kódolják. Ezek a régiók hat transzkripciós egységet alkotnak: (i) a Ni^{2+} és Co^{2+} által indukált *nrsBACD* operon, melynek a szabályzásában a tőlük 5' irányban elhelyezkedő *nrsSR* operon géntermékei vesznek részt [García-Dominguez et al. (2000) *J Bacteriol* 182: 1507; López-Maury et al. (2002) *Mol Microbiol* 43: 247], (ii) Zn^{2+} indukálta *ziaA,* mely egy P_1-tipusú ATP-áz Zn^{2+} efflux pumpát kódol, és az előtte elhelyezkedő gén terméke, a *ziaR,* [Thelwell et al. (1998) *PNAS* 95: 10728], valamint a (iii) Co^{2+} és Zn^{2+} indukálta *coaT,* ami egy P1-típusú ATP-ázt, a Co^{2+} transzlokátort kódolja, és a tőle 5' irányban található *coaR* gén termékének szabályzása alatt áll. [Rutherford et al. (1999) *J Biol Chem* 274: 25827; García-Dominguez et al. (2000) *J Bacteriol* 182: 1507]. A *Synechocystis* arzén rezisztenciáját az *arsBHC* operon kódolja. A *arsBHC* operon indukciójáért a $As^{5+}/As^{3+}/Sb^{3+}$ a felelős, míg expressziója az ArsR represszor protein szabályzása alatt áll. A CoaT és ZiaA mellett a *Synechocystis*-nek két másik P1-típusú ATP-áza is van, a CtaA és PacS, melyek valószínüleg réz kation transzporterek, és a plazma membránban vagy a thylakoid membránban helyezkednek el [Tottey et al. (2001) *J Biol Chem* 276: 19999]. Az Atx1 fémkötő fehérje kölcsönhatásban van a CtaA és PacS aminoterminális doménjeivel, és szerepe lehet a Cu^{2+} transzportban a tilakoid felé [Borelly et al. (2004) *Biochem J* 378: 293; Tottey et al. (2002) *J Biol Chem* 277: 5490].

A *Synechocystis* genomjában két gén található, melyek a kromát ion transzporter (CHR) szupercsaládot kódolják [Díaz-Pérez et al. (2007) *FEBS J* 274: 6215]: a *slr5038*, a pSYSM plazmidon található, és a kromoszomálisan kódolt *chrA*. A szupercsalád mindössze két tagjának szerepe tisztázott. Ezek a membrán proteinek kromátot pumpálnak ki a citoplazmából a proton-pumpák segítségével, ezáltal biztosítva a kromát rezisztenciát [Alvarez et al. (1999) *J Bact* 181: 7398; Pimentel (2002) *FEMS Microbiol Lett* 212: 249]. A *Synechococcus* sp. PCC 7942-ben a szupercsalád egy másik tagja, a pANL plasmid által kódolt SrpC. Ismeretes, hogy a pANL plazmidnak szerepe van a kén éhezéshez való alkalmazkodásban. A *srpC* inaktivált mutáns alacsony szulfáttartalmú médiumon tenyésztve magasabb kromát rezisztenciát mutatott [Nicholson és Laudenbach (1995) *J Bact* 117: 2143]. Az egyik hipotézis szerint a CHR proteinek kromát/kén antiport folyamatokat bonyolítanak le, és a sejten belül felhalmozódott kromátot a környezetből származó szulfáttal helyettesítik; ha alkalmanként a tenyésztő közegben a szulfát koncentráció alacsonyabb, mint a kromát koncentrációja, az antiporter kromát felvevő rendszerként működik, és ez a magyarázata az *srpC* mutáns kromát rezisztenciájának. [Nies (1998) *J Bact* 180: 5799].

Keveset tudunk a prokarióták fémion felhalmozódásra adott transzkripciós válaszreakcióiról. A modellünk, a *Synechocystis* sp. PCC 6803 esetében egyetlen DNS microarray tanulmány látott napvilágot, ami a Cd^{2+}, Zn^{2+} és Fe^{2+} által indukált génexpressziót vizsgálta [Houot et al. (2007) *BMC Genomics* 8: 350]. Vannak specifikus stressz gének, melyek egy specifikus stresszre adnak választ, és vannak általános stressz gének, melyek több, különböző stressz faktorra reagálnak. A shock proteinek (pl. *hspA*) és a proteázok génjei az általános stressz gének csoportjába tartóznak, indukáló tényezők: az oxidtív stressz, hiperozmózis, hő, só, UV-B, és fény, de a hideg stressz nem indukáló hatású.

Az elmúlt két évtizedben számos egész sejtes bioszenzort hoztak létre bakteriális fémion-rezisztencia géncsaládok alkalmazásával. Ezek genetikailag módosított baktériumok, melyekben fémionok jelenlétére érzékeny szabályzás alatt álló, jól detektálható fehérjék fejeződnek ki. Mivel ezek képesek érzékelni a környezetükben jelenlevő fémeket, a hagyományos analitikai kémiai módszerek mellett alternatív megoldást jelentenek. Legnagyobb előnyük mégis az, hogy jóval kisebb mennyiségű fém ionra is reagálnak, vagyis egy szennyezett környezet pontosabban kiértékelésre képesek.

A fotoautotróf cianobaktériumok nagy előnye a heterotróf mikroorganizmusokkal szemben, hogy sokkal olcsóbb az előállításuk, és tenyésztésük. A *Synechocystis* teljesn genomtérképe ismert, és természetes módon transzformálható, ezért megfelelő az egész sejtes bioszenzorként való alkalmazásra.

CÉLKITŰZÉSEK

A vizsgálataink fő céljai a következők voltak:

I. Biológiai szempontból jelentős koncentrációjú Co^{2+}, Zn^{2+}, Ni^{2+}, Cd^{2+}, Cr^{6+}, Cr^{3+}, As^{3+}, As^{5+}, és Cu^{2+} ionoknak, rövid ideig kitett *ziaA, coaT, nrsB, arsB, chrA, artT, pacS, atx1*, és *ctaA* gének transzkript szintjének elemzése. Ezek a gének bizonyítottan vagy vélhetőleg részt vesznek a fémionok transzportjában.

II. Két, teljes sejtes bioluminescens szenzor aktivításának és környezeti mintáknál való alkalmazhatóságának jellemzése. Ezek előzőleg, a Co^{2+}/Zn^{2+} által indukálható O/P_{coaT} (a *coaT* operátor-promóter régiója) vagy a Ni^{2+} /Co^{2+} által indukálható $O/P_{nrsBACD}$ és a promóter nélküli luxAB reporter gének egyesítésével lettek létrehozva a laborunkban. Ugyanezen elv alapján egy arzén bioszenzor létrehozása, amelyben az $As^{3+}/As^{5+}/Sb^{3+}$ által indukálható O/P_{arsBHC} és a promóter nélküli luxAB reporter gének kerülnek egyesítésre.

III. A feltételezetten egy kromát-transzportert kódoló *slr5038* gén működésének vizsgálata, amelyről kimutattuk, hogy As^{3+} által, vagy alacsony szulfát tartalmú tápközegben Cr^{6+} által indukálódik.

IV. Megtalálni a Cd^{2+}, Ni^{2+}, As^{3+}, Zn^{2+}, Co^{2+}, és Cu^{2+} koncentrációk azon tartományait, amelyekben a *Synechocystis* sejtekben ion-specifikus válaszreakció alakul ki, illetve amelyek általános és oxidatív stresszel jellemezhető állapotot hoznak létre.

MÓDSZEREK

Nevelési körülmények és fémsó kezelés

A *Synechocystis sp. PCC 6803* vad típus és mutáns változatai 20 mM HEPES-szel (pH 7.5) kiegészített BG-11 tápoldatban [Rippka et al. (1979) *J Gen Microbiol* 111: 1] neveltem, 40 µmol m^{-2} s^{-1} fényben, 30 °C hőmérsékleten és CO_2-dal dúsított (3%) légtérben, 120 rpm rázás mellett. Szükség esetén a tápoldat különböző antibiotikumokat is tartalmazott. A kezeléseket $ZnSO_4$, $CdCl_2$, $NiCl_2$, $CoCl_2$, $NaAsO_2$, KH_2AsO_4, $CuSO_4$, $Cr_2(SO_4)_3$ vagy Na_2CrO_4-tal kiegészített BG-11 tápoldatokban végeztem.

Fémionok többlete által okozott növekedési gátlás

A cianobaktérium tenyészetek növekedését a 720 nm-en, 3-4 napon keresztül mért optikai sűrűségük mérésével követtem. Mindegyik fémionra vonatkozóan meghatároztam kétféle gátlási paramétert: a minimális gátló koncentráció (IC_{min}) és a maximális gátló koncentráció (IC_{max}). A IC_{min} a legalacsonyabb, növekedést gátló koncentrációt jelöli, a IC_{max} pedig az a legmagasabb koncentrácó, amelynél már további növekedés nem figyelhető meg.

Nukleinsav-kivonás és kvantitatív real-time PCR vizsgálat

Az össz-RNS izolálására a forró fenolos módszert [Mohamed és Jansson (1989) *Plant Mol Biol* 13: 693] alkalmaztam, 20 ml, exponenciális növekedési fázisú *Synechocystis* tenyészetből. A reverz transzkripciók és a kvantitatív real-time PCR vizsgálatok a "High Cappacity cDNA Reverse Transcription Kit and Power SYBR Green PCR Master Mix (Applied Biosystems)" útmutatásainak megfelelően lettek végrehajtva. Az oligonukleotidok a "Primer Express 2.0 software (Applied Biosystems)" segítségével lettek megtervezve. A génexpresszió relatív változásait a delta-delta C_T módszer [Applied Biosystems (2001) User Bulletin #2: 11] segítségével számoltam ki, és az értékek az RNase P, B alegységét kódoló *rnpB* gén expressziós értékeihez normáltam.

Bioreporter sejtvonalak előállítása

A laborunkban két bioriporter már korábban elkészült: *nrsLux és coaLux* [Peca et al. (2008) *FEMS Microbiol Lett* 289: 258]. Az *arsLux* bioreporter kialakítása érdekében az *arsBHC* kódoló régiójától 5' irányban elhelyezkedő O/P_{arsBHC} és a *sll0914,* 5' vége került a pND6luxAB vektorban lévő, promóter nélküli *luxAB* luciferáz gén promóter régiójába. Az így keletkezett konstrukcióval olyan *Synechocystis* sejtvonalat transzformáltam, amely

tartalmazta a *luxCDE* luciferáz szubsztrát gént, valamint egy spektinomicin-rezisztencia kazettát. A fenti konstrukció egy kloramfenikol-rezisztencia kazettával együtt, homológ rekombináció útján, a kromoszóma semleges *ssl0410* helyére épült be.

Biolumineszcencia-elemzés

A fémsós kezeléseket 96 lukú, fekete mikrotiter lemezekben végeztem, egyenként 300 µL térfogatban. A *arsLux* reporter sejtvonal esetében a lemezeket, fényben (40 µmol foton m^{-2} s^{-1}) vagy sötétben, 3 vagy 18 órán keresztül inkubáltam. A lumineszcencia intenzitását Top Count NXT luminométer (Packard Instruments) segítségével határoztam meg.

A környezeti minták savas kivonása

A vizsgálathoz használt talajszerű anyagot különböző, kémiai és olajiparból származó hulladék alkotja. A minták egy bauxit-tározó telepről származnak. A komposztáló halmokból gyűjtött minták ki lettek szárítva, és egy 2 mm-es lyukátmérőjű szitán át lettek szitálva. Ahhoz, hogy fel lehessen mérni a cserélhető, savoldékony Ni^{2+}, Co^{2+} és Zn^{2+} részecskék mennyiségét, az anyag egy egylépéses sav-kivonásnak lett alávetve, a [Bódog et al. (1996) *Int J Environ An Ch* 66:79] által leírt módszer szerint. A fémkoncentrációt egy atomabszorbciós spektrofotométer segítségével határozták meg (Perkin-Elmer model 3110).

EREDMÉNYEK

I. Bioszenzorok előállításához olyan potenciális promoterrégiókat választottunk, amelyek bizonyítottan vagy feltételezhetően fémionok transzportjában vesznek részt a *Synechocystysis*-ben: (i) P_1-típusú ATPázokat kódoló géneket, amelyek Zn^{2+} (*ziaA*), Co^{2+} (*coaT*) és Cu^{2+} (*ctaA, pacS*) szállításában vesznek részt, (ii) *atx1*, ami egy Cu^{2+} chaperont kódol, (iii) *slr5038* (ezt *artT*-nek neveztük el) és *chrA*, aminek a króm szállításában van szerepe, (iv) *nrsB,* ami egy feltételezett Ni-transzportert kódol és (v) *arsB*, aminek As^{3+} szállításban lehet szerepe. Real-time PCR-rel követtem a fenti gének kifejeződésének mértékét. A génexpresszió kiváltásához az alabbi nehézfémek IC_{min} és IC_{max} közötti koncentrációját használtam: Co^{2+}, Zn^{2+}, Ni^{2+}, Cd^{2+}, Cr^{3+}, Cr^{6+}, As^{3+} és As^{5+}. Azt találtam, hogy a maximális génexpresszió már 15 perc kezelés után megfigyelhető és az expresszió szintje nem változott a következő 45 percen belül. Az *arsB, nrsB, coaT* gének expressziós mintázatát az alábbi táblázatban foglaltam össze:

Gén neve	Fémion	Az indukció csúcsértéke (átlag értek)	A maximalis indukciót kiváltó nehézfémkoncentráció intervalluma
arsB	As^{3+}	1000	500–3500 µM
	As^{5+}	80	2–47 mM
nrsB	Ni^{2+}	700	1–27 µM
	Co^{2+}	5	4–32 µM
coaT	Zn^{2+}	300	32 µM
	Co^{2+}	20	2–32 µM
ziaA	Zn^{2+}	45	2–16 µM
	Cd^{2+}	13	2–16 µM

Azt találtam, hogy a Zn^{2+} mellett a Cd^{2+}-kezelés hatására is erősen indukálódik a *ziaA* gén. Mivel a P_1-típusú ATP-ázok specifikusak azokra a fémekre amelyeket szállítanak [Liu et al. (2002) *J Bacteriol* 184: 5027], ugy tűnik a Cd^{2+} nem véletlenszerűen indukalja a gént, hanem a ZiaA ATP-áz ennek specifikus transzportere.

Annak ellenére, hogy a *ctaA, pacS* és *atx1*gének termékei mind a réz szállításában játszanak szerepet, a Cu^{2+} ionoknak IC_{min}-IC_{max} közötti koncentrációja nem okozott változást ezen transzkriptumok mennyiségében rövid inkubációs idő alatt. Ezért a *pacS* gén szabályozasának a *Synechococcus* homolog génjétől eltérő módon kell történnie, ugyanis az

útóbbinál a génkifejeződés és fehérjeszintézis mértéke a rézkoncentráció függvényében változott [Kanamaru et al. (1994) *Mol Microbiol* 184: 5027].

II. Jellemeztam a korábban a laborunkban előállított *coaLux* és *nrsLux* bioluminesz cens teljes sejt rendszerű bioriportereket, és optimalizáltam a felhasználásuk módját. Mind a *coaLux* mind pedig az *nrsLux* törzsek fiziológiás válasza a tápoldatba adagolt fémionok koncentrációjától függött. A *coaLux* 0.3–6.4 µM Co^{2+} illetve 1–3.2 µM Zn^{2+} koncentráció tartományban adott mérhető lumineszcenciát. A Zn^{2+}-függő lumineszcencia-görbe alakja és az adott koncentráció intervallum összhangban áll Erbe és munkatársai [(1996) *J Ind Microbiol* 17: 80]. *Synechococcus smt-luxCDABE* rendszerein végzett méréseivel. A *coaLux* bioreporter működését egy vegyi- és ipari hulladékokat tartalmazó szennyezett talaj mintában is megvizsgáltam: a *coaLux* törzs a Zn^{2+} atomabszorbcios spektrometriával meghatarozott koncentrációjának 92%-át mutatta ki.

Az *nrsLux* bioreporter 0.2–8 µM közötti Ni^{2+}-koncentrációban mutat mérhető lumineszcenciát. Mivel a cink és a nikkel gyakran együtt fordulnak elő szennyezett talajokban, az *nrsLux* bioreportert vegyesen (Zn^{2+} és Ni^{2+}) szennyezett minta esetében is kipróbáltam. A Zn^{2+} koncentráció-függő módon csökkentette a Ni^{2+}-indukált biolumineszcenciát; 8 µM Ni^{2+} koncentációnál 6 µM Zn^{2+} a felére csökkentette a mért jelet (IC_{50}). Minthogy az *nrsLux* bioszenzor érzékenysége az ivóvízekből kimutatható, az Egészségügyi Világszervezet (WHO) által előírt Ni^{2+} koncentráció (0.07 mg/L = 1.19 µM) értékével azonos nagyságrendbe esik, ez a bioszenzor felhasználható az ivóvizek nikkellel való szennyezettségének kimutatására azzal a feltétellel, hogy a kísérő cink koncentráció nem túl magas. Mivel a vezetékes ivóvíz cink tartalma ritkán haladja meg 0.15 µM-os koncentrációt – ami amúgy is 70-szer kisebb mint a Zn^{2+} IC_{50} – ez nem jelent komoly hátrányt. A *coaLux* és *nrsLux* bioreporterek lumineszcencia válaszát sötétben is megvizsgáltam. Fény hiányában a *coaLux* bioriporter lumineszcencia maximuma mindkét fémionnál mintegy négyszer magasabb koncentrációnál jelentkezett, és ez a Co^{2+} iónnál 65%-a, Zn^{2+} ionnál 50%-a volt a fényben mért értékeknek. A *nrsLux* bioreporter törzs az alkalmazott Zn^{2+}-koncentrációk mellett nem mutatott lumineszcenciát fény hiányában, amire mindeddig nem találtunk magyarázatot.

Létrehoztunk egy As^{3+}/As^{5+}-szenzitív *arsLux* bioreportert is, ami As^{3+} és As^{5+} ionokra egymástól nagyon eltérő koncentrációknál adott válaszreakciót. 8 µM és 500 µM As^{3+} koncentráció között a bioluminszcencia értéke az ionkoncentráció növekedésével lineárisan változott. As^{5+}-ionnál a biolumioneszcencia mértéke lassan nőtt 2.3mM és 10mM As^{5+} között, majd gyorsabban 150mM As^{5+}-ig, ami a legmagassabb tesztelt koncentrációérték volt. Az arzén igen gyakori szennyezőanyaga a talajvíznek; sokszor meghaladja az Egészségügyi

Világszervezet (WHO) által jóváhagyott 10 µg/l (0.13 µM) koncentrációt. Jó példa erre, hogy 11 magyarországi településen az arzénkoncentráció eléri az 50 µg/l (0.65 µM) átlagértéket [Jones és mtsi. (2008) *Rev Environ Contam Toxicol* 197: 163], sőt, esetenként akár 560 µg/l (7.3 µM) maximális értéket is [Csalagovics (1999) *Annu Rep Geol Inst Hung II*: 85]. Az *arsLux* bioreporter további optimalizációt igényel annak érdekében, hogy a fent említett esetekben közvetlenül felhasznalható legyen.

III. Kimutattam, hogy az *artT* gén a szomszédos *slr5037* (általunk *artC*-nek elnevezett) génnel együtt íródik át. Az *artT* egy feltételezett krómtranszportert kódoló gén a CHR géncsaládból, az *artC* pedig egy konzervált, hipotétikus feherje. Az *artCT* operon előtt talalhatóak az ellentétes irányban átírt *sll5036* és *sll5035* gének (ezeket *artS*-nek és *artR*nek neveztük el). Az előbbi egy feltételezett szulfid-kinon reduktázt kódoló gén míg az utóbbi az SmtB/ArsR családba tartozó transzkripciós represszorokkal mutat homológiát. Az a tény, hogy ezek a transzkripciós represszorok fémek érzékelésében vesznek részt valamint az, hogy az *artR* az *artCT* operon közelében helyezkedik el az ellenkező irányban, arra enged következtetni, hogy *artR* egy represszort kódoló gén, ami az *artCT* operon kifejeződését szabályozza. Az *artR* és *artT* génekbe kanamicin-rezisztenciát kiváltó marker gént klónoztunk, inszerciós mutánsokat hozva létre. Az *artR*::Kan mutáns az $O/P_{\boldsymbol{artCT}}$ konstitutív derepresszióját eredményezte, ami részben megerősítette feltételezéseinket. Azt találtuk, hogy az *artCT* operon As^{3+} ionok valamint kromát ionok hatására indukálódik. A vad típushoz viszonyítva az *artT*::Kan mutáns jóval rezisztensebbnek mutatkozott az As^{3+}-al szemben de króm jelenlétében is jobban nőtt, ha lecsökkentettem a tápoldat szulfát tartalmát 10 µM-ra (ami 30-szor kisebb, mint a normál BG-11 oldatban). Az *artR*::Kan mutáns a vad típusnál érzékenyebbnek bizonyult As^{3+}-jelenlétében. Mindezt egybevetve arra következtethetünk, hogy az ArtT króm/szulfát antiporterként működik. Alacsony szulfát koncentrációnál az antiporter krómot vesz fel, ez a magyarázata az *artT* mutáns krómmal szembeni rezisztenciájának. A genomban való elhelyezkedés alapján a CHR proteineknek a krómtranszport mellett egyéb élettani szerepe is valószínűsíthető [Díaz-Pérez és mtsai. (2007) *FEBS J* 274: 6215].

IV. Meghatároztuk a Cd^{2+}, Ni^{2+}, As^{3+}, Zn^{2+}, Co^{2+} és Cu^{2+} esetében azokat a koncentráció intervallumokat amire a sejtek specifikusan válaszolnak, valmint azokat a koncentrációkat, amelyeknél már általános- illetve oxidatív stresszválaszt tapsztalunk. Nyomon követtük ezen fémionok specifikusan indukálható génjének expresszióját (kivéve a Cu^{2+}-ét, amelynél nem ismert ilyen gén), és a szakirodalomból ismert általános- vagy oxidativ stressz-indukált, következő génekét: *isiA* (vas-stressz klorofill-kötő protein), *perR* (Fur család transzkripciós regulátor), *sigD* (2-es csoport RNS polimeráz szigma factor), *hspA* (16.6-kDa kis hősokk

fehérje), *dnaJ* (DnaJ-típusú fehérje), *ahpC* (AhpC-peroxiredoxin), *lilA* (fény-begyüjtőszerű fehérje) és *nblA1* (fikobiliszóma lebontó protein). Az eredményeket az alábbi táblázat összegezi :

Fém ion	Specifikus válasz	Általános és oxidatív stresszválasz
Cd^{2+}	2 µM	8 µM
Ni^{2+}	5 µM	10 µM
As^{3+}	80–720 µM	2 mM
Zn^{2+}	4 µM	16 µM
Co^{2+}	1 µM	–
Cu^{2+}	–	1.25 µM

A tesztelt maximális 32 µM Co^{2+}-ig semmilyen lényeges stresszválaszt nem tapasztaltunk. A kis hősokk proteint kódoló *hspA* gén mindegyik fém esetében erősen kiejeződött az IC_{max}-körüli koncentrációnál. A már előzőleg kimutatott [Singh et al. (2003) *Plant Physiol* 132: 1825], vas hiány esetében aktiválodó IsiA klorofill-kötő fehérje a Ni^{2+}-által is indukálódik.

PUBLIKÁCIÓK LISTÁJA

Peca L, Kós PB, Vass I (2007) Characterization of the activity of heavy metal-responsive promoters in the cyanobacterium *Synechocystis* PCC 6803. *Acta Biol Hung* 58: 11-22.
IF: 0.688

Peca L, Kós PB, Máté Z, Farsang A, Vass I. (2008) Construction of bioluminescent cyanobacterial reporter strains for detection of nickel, cobalt and zinc. *FEMS Microbiol Lett* 289: 258-264.
IF: 2.021

(ezek a publikációk közvetlenül kapcsolódnak a dolgozat témájához)

POSZTEREK

Peca L, Kós PB, Vass I (2006) Regulation of zinc, cobalt and chromium responsive genes in the cyanobacterium *Synechocystis* PCC 6803. 12th International Symposium on Phototrophic Prokaryotes. Pau, France, August 27- September 1st.

Peca L, Kós BP, Vass I (2008) Development and utilisation of two bioluminescent reporter strains of *Synechocystis* PCC 6803 for detection of Ni^{2+}, Co^{2+} and Zn^{2+} contaminants. ESF-EMBO Symposium-Molecular Bioenergetics of Cyanobacteria: Towards systems biology level of understanding, San Feliu de Guixols, Spain, March 29-April 3rd.

ELŐADÁSOK

Peca L (2005) Quantitative analysis of *Synechocystis* sp. PCC 6803 gene expression in heavy metal stress. Genomics and Bioinformatics: Exploiting Microarrays in Plant Physiology, European Networking Summer School, Ljubljana, Slovenia, 22-31 August

Peca L (2005) Quantitative analysis of *Synechocystis* sp. PCC 6803 gene expression in heavy metal stress. EMBO Practical Course on Analysis and Informatics of Microarray Data, Cambridge, UK, 3-9 April

References

Allen MM (1968) Ultrastructure of the cell wall and division of unicellular blue-green algae. *J Bacteriol* 96: 842-852.

Alvarez AH et al. (1999) Chromate efflux by means of the ChrA chromate resistance protein from *Pseudomonas aeruginosa*. *J Bacteriol* 181: 7398-7400.

Aoki S et al. (1995) Circadian expression of the *dnaK* gene in the cyanobacterium *Synechocystis* sp. strain PCC 6803. *J Bacteriol* 177: 5606-5611.

Bachmann T (2003) Transforming cyanobacteria into bioreporters of biological relevance. *Trends Biotechnol* 21: 247-249.

Baier K et al. (2001) Expression of two *nblA*-homologous genes is required for phycobilisome degradation in nitrogen-starved *Synechocystis* sp. PCC 6803. *FEMS Microbiol Lett* 195: 35-39.

Banci L et al.(2002) Solution structure of the N-terminal domain of a potential copper-translocating P-type ATPase from *Bacillus subtilis* in the apo and Cu (I) loaded states. *J Mol Biol* 317: 415-429.

Banci L et al. (2006) The delivery of copper for thylakoid import observed by NMR. *PNAS USA* 103: 8320-8325.

Bateman A et al. (2002) The Pfam protein families database. *Nucleic Acids Res* 30: 276-280.

Bednar AJ et al. (2009) Comparison of standard and reaction cell inductively coupled plasma mass spectrometry in the determination of chromium and selenium species by HPLC-ICP-MS. *Anal Chim Acta* 632: 27-34 .

Bhattacharjee H and Rosen BP (2007) Arsenic metabolism in prokaryotic and eukaryotic microbes. In: Nies DH, Simon S (eds) Molecular microbiology of heavy metals. Springer-Verlag, Berlin: 371-406.

Bibby TS et al. (2001) Iron deficiency induces the formation of an antenna ring around trimeric photosystem I in cyanobacteria. *Nature* 412: 743-745.

Bódog I et al. (1996) Determination of heavy metals in lake and river sediments by selective leaching. *Int J Environ An Ch* 66: 79-94.

Boekema EJ et al. (2001) A giant chlorophyll-protein complex induced by iron deficiency in cyanobacteria. *Nature* 412: 745-748.

Borrelly GPM et al. (2004b) A novel copper site in a cyanobacterial metallochaperone. *Biochem J* 378: 293-297.

Borrelly GPM et al. (2004a) Chimeras of P1-type ATPases and their transcriptional regulators: contributions of a cytosolic amino-terminal domain to metal specificity. *Mol Microbiol* 53: 217-227.

Braun V and Killmann H (1999) Bacterial solutions to the iron-supply problem. Trends Biochem Sci 24: 104-109.

Braun V and Hantke K (2007) Acquisition of iron by bacteria. In Nies DH, Silver S (eds) Molecular Microbiology of Heavy Metals. Springer-Verlag, Berlin: 190-212.

Busenlehner LS et al. (2003) The SmtB/ArsR family of metalloregulatory transcriptional repressors: structural insights into prokaryotic metal resistance. *FEMS Microbiol Rev* 27: 131-143.

Cai J and DuBow MM (1996) Expression of the *Escherichia coli* chromosomal *ars* operon. *Can J Microbiol:* 42662-671.

Castielli O et al. (2009) Proteomic analyses of the response of cyanobacteria to different stress conditions. *FEBS Lett* 583: 1753-1758.

Cavet JS et al. (2003) Zn, Cu and Co in cyanobacteria: selective control of metal availability. *FEMS Microbiol Rev* 27: 165-181.

Cervantes C et al. (1990) Cloning, nucleotide sequence, and expression of the chromate resistance determinant of *Pseudomonas aeruginosa* plasmid pUM505. *J Bacteriol* 172: 287-291.

Cervantes C et al. (2001) Interactions of chromium with microorganisms and plants. *FEMS Microbiol Rev* 25: 335-347.

Cervantes C and Campos-Garcia J (2007) Reduction and efflux of chromate by bacteria. In Nies DH, Silver S (eds) Molecular Microbiology of Heavy Metals. Springer-Verlag, Berlin: 407-420.

Chao Y and Fu D (2004) Kinetic study of the antiport mechanism of an *Escherichia coli* zinc transporter, ZitB. *J Biol Chem* 279: 12043-12050.

Cioni P et al. (2003) Active-site copper and zinc ions modulate the quaternary structure of prokaryotic Cu,Zn Superoxide Dismutase. *J Mol Biol* 326: 1351-1360.

Clifford M and McGeer JC (2009) Development of a biotic ligand model for the acute toxicity of zinc to Daphnia pulex in soft waters. *Aquat Toxicol* 91: 26-32.

Collier JL and Grossman AR (1994) A small polypeptide triggers complete degradation of light-harvesting phycobiliproteins in nutrient-deprived cyanobacteria. *EMBO J* 13: 1039-1047.

Cook WJ et al. (1998) Crystal structure of the cyanobacterial metallothionein repressor SmtB: a model for metalloregulatory proteins. *J Mol Biol* 275: 337-346.

Csalagovits I (1999) Arsenic-bearing artesian waters of Hungary. *Annual Rep Geol Inst Hung* 1992-1993/II: 85-92.

Da Re S et al. (1999) Phosphorylation-induced dimerization of the FixJ receiver domain. *Mol Microbiol 34*: 504-511.

Denkhausa E and Salnikowb K (2002) Nickel essentiality, toxicity, and carcinogenicity. *Crit Rev Oncol Hematol* 42: 35-56.

DeRuyter YA and Fromme P (2008) Molecular structure of the photosynthetic apparatus. In: Herrero A and Flores E (eds) The cyanobacteria: molecular biology, genomics and evolution. Caister Academic Press, Norfolk UK: 217-269.

Dey S and Rosen BP (1995) Dual mode of energy coupling by the oxyanion-translocating *ArsB* protein. *J Bacteriol* 177: 385-389.

Díaz-Pérez C et al. (2007) Phylogenetic analysis of the chromate ion transporter (CHR) superfamily. *FEBS J* 274: 6215-6227.

Dietz KJ et al. (2002) The function of the chloroplast 2-cysteine peroxiredoxin in peroxide detoxification and its regulation. *J Exp Bot* 53: 1321-1329.

Douglas SE (1998) Plastid evolution: origins, diversity, trends. *Curr Opin Genet Dev* 8: 655-661.

Drazkiewicz M et al. (2004) Copper-induced oxidative stress and antioxidant defence in *Arabidopsis thaliana*. *Biometals* 17: 379-387.

Duffus J H (2002) "Heavy metals"-a meaningless term? (IUPAC Technical Report). *Pure Appl Chem* 74: 793-807.

Ellison DW and McCleary WR (2000) The unphosphorylated receiver domain of PhoB silences the activity of its output domain. *J Bacteriol* 182: 6592-6597.

Endo G and Silver S (1995) CadC, the transcriptional regulatory protein of the cadmium resistance system of *Staphylococcus aureus* plasmid pI258. *J Bacteriol* 177: 4437-4441.

Engebrecht J et al. (1983) Bacterial bioluminescence: isolation and genetic analysis of functions from *Vibrio fischeri. Cell* 32:773-781.

Erbe JL et al. (1996) Cyanobacteria carrying an *smt-lux* transcriptional fusion as biosensors for the detection of heavy metal cations. *J Ind Microbiol* 17: 80-83.

Ermler U et al. (1997) Crystal structure of methyl-coenzyme M reductase: the key enzyme of biological methane formation. *Science* 278**:** 1457-1462.

Fang F and Barnum SR (2004) Expression of the heat shock gene *hsp16.6* and promoter analysis in the cyanobacterium, *Synechocystis* sp. PCC 6803. *Curr Microbiol* 49: 192-198.

Fatma H and Fatma T (2009) Screening of cyanobacteria for phycobiliproteins and effect of different environmental stress on its yield. Bull Environ Contam Toxicol DOI: 10.1007/s00128-009-9837-y.

Ferguson AD and Deisenhofer J (2004) Metal import through microbial membranes. *Cell* 116: 15–24.

Fiedler U and Weiss V (1995) A common switch in activation of the response regulators NtrC and PhoB: phosphorylation induces dimerization of the receiver modules. *EMBO* 14**:** 3696-3705.

Frank JK and Mudway IS (2007) Particle-mediated extracellular oxidative stress in the lung. In Donaldson K, Borm P (eds) Particle toxicology, CRC Press. 90-110.

Fraústo da Silva JJR and Williams RJP (2001) The biological chemistry of the elements: the inorganic chemistry of life. Clarendon Press, Oxford.

Fuangthong M et al. (2002) Regulation of the *Bacillus subtilis* fur and *perR* genes by PerR: not all members of the PerR regulon are peroxide inducible. *J Bacteriol* 184: 3276-3286.

Furumichi M et al. (2002) CYORF: Community annotation of cyanobacteria genes. *Genome Inform* 13: 402-403.

García-Domínguez M et al. (2000) A gene cluster involved in metal homeostasis in the cyanobacterium *Synechocystis* sp. strain PCC 6803. *J Bacteriol* 182: 1507-1514.

Glatz A et al. (1999) The *Synechocystis* model of stress: From molecular chaperones to membranes. *Plant Physiol Biochem* 37: 1-12

Golecki J R (1977) Studies on ultrastructure and composition of cell walls of the cyanobacterium Anacystis nidulans. *Arch Microbiol* 114: 35-41.

Grass G et al. (2001) NreB from *Achromobacter xylosoxidans* 31A is a nickel-induced transporter conferring nickel resistance. *J Bacteriol* 183**:** 2803-2807.

Grass G et al. (2005) The metal permease ZupT from *Escherichia coli* is a transporter with a broad substrate spectrum. *J Bacteriol* 187: 1604-1611.

Green LS and Grossman AR (1988) Changes in sulfate transport characteristics and protein composition of *Anacystis nidulans* R2 during sulfur deprivation. *J Bacteriol* 170: 583-587.

Hansen JM et al. (2006) Differential oxidation of thioredoxin-1, thioredoxin-2, and glutathione by metal ions. *Free Radical Biol Med* 40: 138-145.

Haraguchi H (2004) Metallomics as integrated biometal science. *J Anal At Spec* 19: 5-14.

Harms H (2007) Biosensing of heavy metals. In: Nies DH, Simon S (eds) Molecular microbiology of heavy metals. Springer-Verlag, Berlin: 143-157.

Harms H et al. (2006) Whole-cell living biosensors - are they ready for environmental application? *Appl Microbiol Biotechnol* 70: 273-280.

Harrison MD et al. (2000) Intracellular copper routing: the role of copper chaperones. *Trends Biochem Sci* 25: 29-32.

Heckathorn SA et al. (2004) Chloroplast small heat-shock proteins protect photosynthesis during heavy metal stress. *Am J Bot* 91:1312-1318.

Helmann JD et al. (2007) Metalloregulators: Arbiters of metal sufficiency. In Nies DH, Simon S (eds) Molecular microbiology of heavy metals. Springer-Verlag, Berlin: 38-63.

Herbig AF and Helmann JD (2001) Roles of metal ions and hydrogen peroxide in modulating the interaction of the *Bacillus subtilis* PerR peroxide regulon repressor with operator DNA. *Mol Microbiol* 41: 849-59.

Hihara Y et al. (2001) DNA Microarray Analysis of cyanobacterial gene expression during acclimation to high light**.** *Plant Cell* 13: 793-806.
Hobman JL, Wilkie J, Brown NL (2005) A design for life: prokaryotic metal-binding MerR family regulators. *Biometals* 18: 429-436.

Hobman JL et al. (2007) Transcriptomic Responses of Bacterial Cells to SublethalMetal Ion Stress. In: Nies DH, Simon S (eds) Molecular microbiology of heavy metals. Springer-Verlag, Berlin: 73-115.

Hoffman et al. (2002) Peroxiredoxins. *J Biol Chem* 383: 347-364.

Holm RH et al. (1996) Structural and functional aspects of metal sites in biology. *Chem Rev* 96: 2239-2314.

Hosoya-Matsuda N et al. (2005) Anti-oxidative stress system in cyanobacteria. Significance of type II peroxiredoxin and the role of 1-Cys peroxiredoxin in *Synechocystis* sp. strain PCC 6803. *J Biol Chem* 280: 840-846.

Houot L et al. (2007) Cadmium triggers an integrated reprogramming of the metabolism of *Synechocystis* PCC6803, under the control of the Slr1738 regulator. *BMC Genomics* 8**:** 350.

Huang L et al. (2002) Global gene expression profiles of the cyanobacterium *Synechocystis* sp. PCC 6803 in response to irradiation with UV-B and white light. *J Bact* 184: 6845-6858.

Huckle JW et al. (1993) Isolation of a prokaryotic metalothionein locus and analysis of transcriptional control by trace metal ions. *Mol Microbiol* 7:177-187.

Hughes MN and Poole RK (1989) Metals and microorganisms. Chapman and Hall, London.

Ikeuchi M and Tabata S (2001) *Synechocystis* sp. PCC 6803-a useful tool in the study of the genetics of cyanobacteria. *Photosynth Res* 70: 73-83.

Imlay JA (2006) Iron-sulphur clusters and the problem with oxygen. *Mol Microbiol* 59: 1073-1082.

Islam FS et al. (2004) Role of metal-reducing bacteria in arsenic release from Bengal delta sediments. *Nature* 430: 68-71.

Jones H et al. (2008) Case reports: Arsenic pollution in Thailand, Bangladesh, and Hungary. *Rev Environ Contam Toxicol* 197: 163-87.

Kanamaru K et al. (1994) A copper-transporting P-type ATPase found in the thylakoid membrane of the cyanobacterium *Synechococcus* species PCC 7942. *Mol Microbiol* 13: 369-377.

Kandegedara A et al. (2009) Role of bound Zn(II) in the CadC Cd(II)/Pb(II)/Zn(II)-responsive repressor. *J Biol Chem* 284: 14958-14965.

Kaneko T et al. (1996) Sequence analysis of the genome of the unicellular cyanobacterium *Synechocystis* sp. strain PCC6803. II. Sequence Determination of the Entire Genome and Assignment of Potential Protein-coding Regions. *DNA Res* 3: 10-136.

Kaneko T et al. (2003) Structural analysis of four large plasmids harboring in a unicellular cyanobacterium, *Synechocystis* sp. PCC 6803. *DNA Res* 10: 221-228.

Kanesaki Y et al. (2002) Salt stress and hyperosmotic stress regulate the expression of different sets of genes in *Synechocystis* sp. PCC 6803. *Biochem Biophys Res Commun* 290: 339-348.

Kasprzak KS (2002) Oxidative DNA and protein damage in metal-induced toxicity and carcinogenesis. *Free Radical Biol Med* 32: 958-967.

Kobayashi M et al. (2004) Response to oxidative stress involves a novel peroxiredoxin gene in the unicellular cyanobacterium *Synechocystis* sp. PCC 6803. *Plant Cell Physiol* 45: 290 - 299.

Kopp RE et al. (2005) The Paleoproterozoic snowball Earth: A climate disaster triggered by the evolution of oxygenic photosynthesis. *PNAS* 102: 11131-11136.

Kozlova T et al. (2009) The effect of water chemistry on the acute toxicity of nickel to the cladoceran *Daphnia pulex* and the development of a biotic ligand model. *Aquat Toxicol* 91: 221-228.

Krishna SS et al. (2003) Survey and summary: Structural classification of zinc fingers. *Nucleic Acids Res* 31: 532-550.

Kufryk GI et al. (2002) Transformation of the cyanobacterium *Synechocystis* sp. PCC 6803 as a tool for genetic mapping: optimization of efficiency. *FEMS Microbiol Lett* 10: 215-219.

Kufryk G et al. (2008) Association of small CAB-like proteins (SCPs) of *Synechocystis* sp. PCC 6803 with Photosystem II. *Photosynth Res* 95:135-145.

Kühlbrandt W (2004) Biology, structure and mechanism of P-type ATPases. *Nat Rev Mol Cell Biol* 5: 282-295.

Kulp TR et al. (2008) Arsenic(III) fuels anoxygenic photosynthesis in hot spring biofilms from Mono Lake, California. *Science* 321*:* 967-970.

Kunert A et al. (2000) Construction of promoter probe vectors for *Synechocystis* sp. PCC 6803 using the light-emitting reporter systems Gfp and LuxAB. *J Microbiol Meth* 41: 185-194.

Lee S et al. (1998) A 16.6-kilodalton protein in the cyanobacterium *Synechocystis* sp. PCC 6803 plays a role in the heat shock response. *Curr Microbiol* 37: 403-407.

Lemeille S et al. (2005) Inferring the connectivity of a regulatory network from mRNA quantification in *Synechocystis* PCC 6803. *Nucleic Acids Res* 33: 3381-3389.

Leonard SS et al. (2004) Metal-induced oxidative stress and signal transduction *Free Radic Biol Med* 37: 1921-1942.

Li H and Sherman LA (2000) A Redox-responsive regulator of photosynthesis gene expression in the cyanobacterium *Synechocystis* sp. Strain PCC 6803. *J Bacteriol* 182: 4268-4277.

Li H et al. (2004) Differential gene expression in response to hydrogen peroxide and the putative PerR regulon of *Synechocystis* sp. strain PCC 6803. *J Bacteriol* 186: 3331-3345.

Li R et al. (2003) An arsenate reductase from *Synechocystis* sp. strain PCC 6803 exhibits a novel combination of catalytic characteristics *J Bact* 185: 6780-6789.

Liao VHC and Ou KL (2005) Development and testing of a green fluorescent protein-based bacterial biosensor for measuring bioavailable arsenic in contaminated groundwater samples. *Environ Toxicol Chem* 24: 1624-1631.

Lin Y-F et al. (2006) An arsenic metallochaperone for an arsenic detoxification pump. *PNAS* 103: 15617-15622.

Lippard SJ and Berg JM (1994) Overview of bioinorganic chemistry. In: Principles of bioinorganic chemistry. University Science Books, Mill Valley, California, 1-19.

Liu T et al. (2002) A novel histidine-rich CPx-ATPase from the filamentous cyanobacterium *Oscillatoria brevis* related to multiple-heavy-metal cotolerance. *J Bacteriol* 184: 5027–5035.

Liu X-G et al. (2005) Oxidative stress and metal ions effects on the cores of phycobilisomes in *Synechocystis* sp. PCC 6803. *FEBS Lett* 579: 4571-4576.

Liu Z et al. (2003) Structural proteomics of arsenic transport and detoxification. In Chappell WR, Abernathy CO, Calderon RL, Thomas DJ (eds) Arsenic exposure and health effects V, Elsevier B.V., Amsterdam. 241-255.

López-Maury L et al. (2002) A two-component signal transduction system involved in nickel sensing in the cyanobacterium *Synechocystis* sp. PCC 6803. *Mol Microbiol* 43: 247-256.

López-Maury L et al. (2003) Arsenic sensing and resistance system in the cyanobacterium *Synechocystis* sp. strain PCC 6803. *J Bacteriol* 185: 5363-5371.

López-Maury L et al. (2009) The glutathione/glutaredoxin system is essential for arsenate reduction in *Synechocystis* sp. Strain PCC 6803. *J Bact* 191: 3534-3543.

Los DA et al. (2008) Stress responses in *Synechocystis*: Regulated genes and regulatory systems. In Herrero A, Flores E (eds) The Cyanobacteria. Molecular biology, Genomics and Evolution. 117-157.

Lovley DR (2003) Cleaning up with genomics: applying molecular biology to bioremediation. *Nat Rev Microbiol* 1: 35-44.

Marin K et al. (2003) Identification of histidine kinases that act as sensors in the perception of salt stress in *Synechocystis* sp. PCC 6803. *Proc Natl Acad Sci USA* 100: 9061-9066.

Mary I et al. (2004) Effects of high light on transcripts of stress-associated genes for the cyanobacteria *Synechocystis* sp. PCC 6803 and *Prochlorococcus* MED4 and MIT9313. *Microbiol* 150: 1271-1281.

Melkozernov AN et al. (2003) Time-resolved absorptionn and emission show that the CP43' antenna ring of iron-stressed *Synechocystis* sp. PCCC 6803 is efficiently coupled to the Photosystem I reaction center core. *Biochemistry* 42: 3893-3903.

Mereschkowski C (1905) Über Natur und Ursprung der Chromatophoren im Pflanzenreiche. *Biol Centralbl* 25: 593-604.

Messens J and Silver S (2006) Arsenate reduction: Thiol cascade chemistry with convergent evolution. *J Mol Biol* 362: 1-17.

Mikami K et al. (2002) The histidine kinase Hik33 perceives osmotic stress and cold stress in *Synechocystis* sp. PCC 6803. *Mol Microbiol* 46:905-915.

Milgram S et al. (2008) Cytotoxic and phenotypic effects of uranium and lead on osteoblastic cells are highly dependent on metal speciation. *Toxicology* 250: 62-69.

Mohamed A and Janson C (1989) Influence of light on accumulation of photosynthesis specific transcripts in the cyanobacterium *Synechocystis* 6803. *Plant Mol Biol* 13: 693-700.

Mongkolsuk S and Helmann JD (2002) Regulation of inducible peroxide stress responses. *Mol Microbiol* 45: 9-15.

Mounicou S et al. (2009) Metallomics: the concept and methodology. *Chem Soc Rev* 38: 1119-1138.

Navarro C et al. (1993) The *nik* operon of *Escherichia coli* encodes a periplasmic binding-protein-dependent transport system for nickel. *Mol. Microbiol* 9:1181-1191.

Neyt C et al. (1997) Virulence and arsenic resistance in yersiniae. *J Bacteriol* 179: 612-619.

Nicholson ML and Laudenbach DE (1995) Genes encoded on a cyanobacterial plasmid are transcriptionally regulated by sulfur availability and CysR. *J Bacteriol* 177: 2143-2150.

Nies A et al. (1990) Nucleotide sequence and expression of a plasmid-encoded chromate resistance determinant from *Alcaligenes eutrophus*. *J Biol Chem* 265: 5648-5653.

Nies DH (2003) Efflux-mediated heavy metal resistance in prokaryotes. *FEMS Microbiol Rev* 27: 313-339.

Nies DH (2007) Bacterial transition metal homeostasis. In Nies DH, Silver S (eds) Molecular Microbiology of Heavy Metals. Springer-Verlag, Berlin: 117-142.

Nies DH et al. (1998) CHR, a novel family of prokaryotic proton motive force-driven transporters probably containing chromate/sulfate antiporters. *J Bacteriol* 180: 5799-5802.

Nies DH et al. (1989) Expression and nucleotide sequence of a plasmid-determined divalent cation efflux system from *Alcaligenes eutrophus*. *PNAS* 86: 7351-7355.

Nikaido H and Vaara M (1985) Molecular basis of bacterial outer membrane permeability. *Microbiol Rev* 49: 1-32.

Okkeri J and Haltia T (1999) Expression and mutagenesis of ZntA, a zinc-transporting P-type ATPase from *Escherichia coli*. *Biochem* 38: 14109-14116.

Ogawa T et al. (2002) A Two-component Signal Transduction Pathway Regulates Manganese Homeostasis in *Synechocystis* 6803, a Photosynthetic Organism, *J Biol Chem* 277: 28981-28986.

Páez-Espino D et al. (2009) Microbial responses to environmental arsenic. *BioMetals* 22: 117-130.

Paithoonrangsarid K et al. (2004) Five histidine kinases perceive osmotic stress and regulate distinct sets of genes in *Synechocystis. J Biol Chem* 279: 53078-53086.

Pao SS et al. (1998) Major facilitator superfamily. *Microbiol Mol Biol Rev* 62: 1-34.

Papp-Wallace KM et al. (2007) Manganese: Uptake, biological function, and role in virulence. In: Nies DH, Simon S (eds) Molecular microbiology of heavy metals. Springer-Verlag, Berlin. 236-250.

Paquin PR et al. (2002) The biotic ligand model: a historical overview. *Comp Biochem Physiol C Toxicol Pharmacol* 133: 3-35.

Paulsen IT and Saier MH Jr (1997) A novel family of ubiquitous heavy metal ion transport proteins. *J Membr Biol* 156: 99-103.

Petsko GA and Ringe D (2004) From structure to function. In Protein structure and function, New science Press Ltd, Middlesex House, London, UK. 50-82.

Pimentel BE et al. (2002) Efflux of chromate by *Pseudomonas aeruginosa* cells expressing the ChrA protein. *FEMS Microbiol Lett* 212: 249-54.

Pollari M and Tyystjärvi T (2007) The Sig B sigma factor of the cyanobacterium *Synechocystis* sp. PCC 6803 is necessary for adaptation to high-salt stress. In: Allen JF, Gantt E, Golbeck JH, Osmond B (eds) Photosynthesis. Energy from the sun. 14th International Congress on Photosynthesis, Springer Netherlands: 1351-1358.

Pollari M et al. (2008) Characterization of single and double inactivation strains reveals new physiological roles for group 2 sigma factors in the cyanobacterium *Synechocystis* sp. PCC 6803. *Plant Physiol* 147: 1994-2005.

Postier B et al. (2003) The construction and use of bacterial DNA microarrays based on an optimized two-stage PCR strategy. *BMC Genomics* 4: 23-33.

Prassana R et al. (2004) Modulation of pigment profiles of *Calothrix elenkenii* in response to environmental changes. *J Plant Physiol* 161: 1125-1132.

Rasmussen LD et al. (1997) Cell-density-dependent sensitivity of a *mer-lux* bioassay. *Appl Environ Microbiol* 63: 3291-3293.

Ramanathan S et al. (1997) Sensing antimonite and arsenite at the subattomole level with genetically engineered bioluminescent bacteria. *Anal Chem* 69: 3380-3384.

Ramanathan S et al. (1998) Bacteria-based chemiluminescence sensing system using *β*-galactosidase under the control of the ArsR regulatory protein of the *ars* operon. *Anal Chim Acta* 369: 189-195.

Ravenscroft P et al. (2009) Arsenic Pollution: A Global Synthesis. John Wiley and Sons.

Rensing C et al. (1999) Families of soft-metal-ion-transporting ATPases. *J Bacteriol* 181: 5891-5897.

Rhee JE et al. (2008) Amino acids important for DNA recognition by the response regulator OmpR. *J Biol Chem* 283: 8664-8677.

Richaud C et al. (2001) Nitrogen or sulfur starvation differentially affects phycobilisome degradation and expression of the *nblA* gene in *Synechocystis* strain PCC 6803. *J Bacteriol* 183: 2989-2994.

Rippka R et al. (1979) Generic assignments, strain histories and properties of pure cultures of cyanobacteria. *J Gen Microbiol* 111: 1-61.

Robinson NJ et al. (1999) Metal metabolism and toxicity: Repetitive DNA. In Whitton BA, Potts M (eds) The ecology of cyanobacteria: their diversity in time and space. Kluwer Academic Publishers.

Rodionov DA et al. (2006) Comparative and functional genomic analysis of prokaryotic nickel and cobalt uptake transporters: evidence for a novel group of ATP-binding cassette transporters. *J Bacteriol* 188: 317-327.

Rosen BP (2002) Transport and detoxification systems for transition metals, heavy metals and metalloids in eukaryotic and prokaryotic microbes. *Comp Biochem Physiol Part A Mol Integr Physiol* 133: 689-693.

Rosenzweig AC (2002) Metallochaperones: bind and deliver. *Chem Biol* 9: 673-677.

Roy SK et al. (1999) Purification and characterization of the 16-kDa heat-shock-responsive protein from the thermophilic cyanobacterium *Synechococcus vulcanus*, which is an a-crystallin-related, small heat shock protein. *Eur J Biochem* 262: 406-416.

Rutherford JC et al. (1999) Cobalt-dependent transcriptional switching by a dual-effector MerR-like protein regulates a cobalt-exporting variant CPx-type ATPase. *J Biol Chem* 274: 25827-25832.

Sakthivel K et al. (2009) A small heat-shock protein confers stress tolerance and stabilizes thylakoid membrane proteins in cyanobacteria under oxidative stress. *Arch Microbiol* 191: 319-328.

Sandström S et al. (2001) CP43′, the *isiA* gene product, functions as an energy dissipator in the cyanobacterium *Synechococcus* sp. PCC 7942. *Photochem Photobiol* 74: 431-437.

Sarangi R et al. (2009) Geometric and electronic structures of the Ni(I) and methyl-Ni(III) intermediates of methyl-coenzyme M reductase. *Biochem* 48: 3146-56.

Schmidt T and Schlegel HG (1994) Combined nickel-cobalt-cadmium resistance encoded by the *ncc* locus of *Alcaligenes xylosoxidans* 31A. *J Bacteriol* 176: 7045-7054.

Schwarz R and Forchhammer K (2005) Acclimation of unicellular cyanobacteria to macronutrient deficiency: emergence of a complex network of cellular responses. *Microbiology* 151: 2503-2514.

Sebbane F et al. (2002) Genes Encoding Specific Nickel Transport Systems Flank the Chromosomal Urease Locus of Pathogenic Yersiniae. *J Bact* 184: 5706-5713.

Semple KT et al. (2004) Defining bioavailability and bioaccessibility of contaminated soil and sediment is complicated. Environ Sci Technol 38:228A-231A.

Sharma R et al. (2000) The ATP hydrolytic activity of purified ZntA, a Pb(II)/Cd(II)/Zn(II)-translocating ATPase from *Escherichia coli*. *JBiolChem* 275: 3873-3878.

Sharma VK and Sohn M (2009) Aquatic arsenic: Toxicity, speciation, transformations, and remediation. *Environ Int* 35: 743-759.

Shcolnick S and Keren N (2006) Metal homeostasis in cyanobacteria and chloroplasts: balancing benefits and risks to the photosynthetic apparatus. *Plant Physiol* 141: 805-810.

Shehata FHA and Whitton BA (1982) Zinc tolerances in strains of the blue-green alga *Anacystis nidulans*. *Br Phycol* 17: 5-12.

Shipman LW et al. (2001) Crystal structure of precorrin-8x methyl mutase. *Structure* 9: 587-596.

Silver S and Phung LT (1996) Bacterial heavy metal resistance: New surprises. *Annu Rev Microbiol* 50: 753-789.

Singh AK et al. (2003) Microarray analysis of the genome-wide response to iron deficiency and iron reconstitution in the cyanobacterium *Synechocystis* sp. PCC 6803. *Plant Physiol* 132: 1825-1839.

Smolders E et al. (2009) Toxicity of trace metals in soil as affected by soil type and aging after contamination: Using calibrated bioavailability models to set ecological soil standards. *Environ Toxicol Chem*: In Press.

Song LY et al. (2001) The integration and expression of ββ mutant gene of human liver metallothionein in *Synechocystis* sp. PCC 6803 by homology recombination. *Acta Bot Sin* 43: 399-404.

Stock AM et al. (2000) Two-component signal transduction. *Annu Rev Biochem* 69:183-215.

Stocker J et al. (2003) Development of a set of simple bacterial biosensors for quantitative and rapid field measurements of arsenite and arsenate in potable water. *Environ Sci Technol* 37: 4743-4750.

Stohs SJ and Bagchi D (1995) Oxidative mechanisms in the toxicity of metal ions. *Free Radical Biol Med* 18: 321-336.

Storni MM et al. (2007) *Tolypothrix tenuis* stress response to nickel. *World J Microbiol Biotechnol* 23: 833-836.

Straus NA (1994) Molecular Biology of Cyanobacteria. In Bryant DA (eds) Kluwer Acad Press Dordrecht: 731-750.

Summers AO (1992) Untwist and shout: a heavy metal-responsive transcriptional regulator. *J Bacteriol* 174: 3097-3101.

Sun Y et al. (2001) Role of cysteinyl residues in sensing Pb(II), Cd(II) and Zn(II) by the plasmid pI258 CadC repressor. *J Biol Chem* 276: 14955-14960.

Suzuki I et al. (2001) Cold-regulated genes under control of the cold sensor Hik33 in *Synechocystis*. *Mol Microbiol* 40: 235-244.

Suzuki S et al. (2004). The SphS-SphR two component system is the exclusive sensor for the induction of gene expression in response to phosphate limitation in *Synechocystis*. *J Biol Chem* 279: 13234-13240.

Suzuki I et al. (2006) The heat shock response of *Synechocystis* sp. PCC 6803 analysed by transcriptomics and proteomics. *J Exp Bot* 57: 1573-1578.

Szpunar J (2005) Advances in analytical methodology for bioinorganic speciation analysis: metallomics, metalloproteomics and heteroatom-tagged proteomics and metabolomics. *Analyst* 130: 442-465.

Theil EC and Raymond KN (1994) Transition-Metal Storage, Transport, and Biomineralization. In Bertini I, Gray HB, Lippard SJ, Selverstone VJ (eds) Bioinorganic chemistry. University Science Books, Mill Valley, CA.

Thelwell C et al. (1998) An SmtB-like repressor from *Synechocystis* PCC 6803 regulates a zinc exporter. *PNAS* 95: 10728-10733.

Tottey S et al. (2001) Two Menkes-type ATPases Supply Copper for Photosynthesis in *Synechocystis* PCC 6803. *J Biol Chem* 276: 19999-20004.

Tottey S et al. (2002) A copper metallochaperone for photosynthesis and respiration reveals metal-specific targets, interaction with an importer and alternative sites for copper acquisition. *J Biol Chem* 277: 5490-5497.

Trang PTK et al. (2005). Bacterial bioassay for rapid and accurate analysis of arsenic in in highly variable groundwater samples. *Environ Sci Technol* 39: 7625-7630.

Tripathi BN et al. (2006) Oxidative stress in *Scenedesmus* sp. during short- and long-term exposure to Cu^{2+} and Zn^{2+}. *Chemosfere* 62: 538-544.

Verbruggen N et al. (2009) Mechanisms to cope with arsenic or cadmium excess in plants. *Curr Opin Plant Biol* 12: 1-9.

Vermaas W (1996) Molecular genetics of the cyanobacterium *Synechocystis* sp. PCC 6803: Principles and possible biotechnology applications. *J App Phycol* 8: 263-273.

Virta M et al. (1998) Bioluminescence-based metal detectors. *Meth Mol Biol* 102: 219-229.

Waldron KJ and Robinson NJ (2009) How do bacterial cells ensure that metalloproteins get the correct metal? *Nat Rev Microbiol* 7: 25-35.

Wang HL et al. (2004) Alterations in global patterns of gene expression in *Synechocystis* sp. PCC 6803 in response to inorganic carbon limitation and the inactivation of *ndhR*, a LysR family regulator. *J Biol Chem* 279: 5739-5751.

Wang Y et al. (2009) Identification and bioinformatic analysis of the membrane proteins of *Synechocystis* sp. PCC 6803. *Proteome Sci* 7**:** 11.

Williams RJP (2007) A system's view of the evolution of life. *J R Soc Interface* 4: 1049-1070.

Wood ZA et al. (2003) Structure, mechanism and regulation of peroxiredoxins. *Trends Biochem Sci* 28: 32-40.

Wu J and Rosen BP. Metalloregulated expression of the *ars* operon. *J Biol Chem* 268: 52-58.

Yamaguchi K et al. (2002) A two-component Mn2+-sensing system negatively regulates expression of the *mntCAB* operon in *Synechocystis*. *Plant Cell* 14: 2901-2913.

Ye J et al. (2005) Crystal structure of the *Staphylococcus aureus* pI258 CadC Cd(II)/Pb(II)/ Zn(II)-responsive repressor. *J Bacteriol* 187:4214-4221.

Yu K et al. (2007) Histidine kinases play important roles in the perception and signal transduction of hydrogen peroxide in the cyanobacterium, *Synechocystis* sp. PCC 6803. *Plant J* 49: 313-24.

Zhang L et al. (1992) Copper-mediated regulation of cytochrome *c553* and plastocyanin in the cyanobacterium *Synechocystis* 6803. *J Biol Chem* 267: 19054-19059.

Zhou W et al. (2006) Growth and photosynthetic responses of the bloom-forming cyanobacterium *Microcystis aeruginosa* to elevated levels of cadmium. *Chemosphere* 65: 1738-1746.